Basic and translational studies on species B adenoviruses

Hongjie Wang

Cancer Gene Therapy Group

Molecular Cancer Biology Program &
Transplantation Laboratory &
Haartman Institute

University of Helsinki

Helsinki, Finland

ACADEMIC DISSERTATION

To be publicly discussed with the permission of
the Faculty of Medicine of the University of Helsinki,
in lecture hall 2, Biomedicum I, Helsinki
On March 2nd 2012 at 12 noon

Helsinki 2012

SUPERVISORS

Akseli Hemminki, MD, PhD
K. Albin Johansson Research Professor (Finnish Cancer Institute)
Cancer Gene Therapy Group
Molecular Cancer Biology Program & Transplantation Laboratory & Haartman Institute &
Finnish Institute for Molecular Medicine
University of Helsinki
Helsinki, Finland

Professor Andre Lieber MD, PhD
Department of Medicine
Adjunct Professor of Pathology
University of Washington
Seattle, Washington, USA

Lotta Kangasniemi, PhD
Research Director
Oncos Therapeutics
Helsinki, Finland

REVIEWERS

Professor Ari Hinkkanen, PhD
University of Eastern Finland
A. I. Virtanen Institute for Molecular Sciences
Department of Biotechnology and Molecular Medicine
Kuopio, Finland

Docent Tuomas Rissanen MD, PhD
University of Eastern Finland
A. I. Virtanen Institute for Molecular Sciences
Department of Molecular Medicine
Kuopio, Finland

ISBN 978-952-10-7338-0 (paperback)
ISBN 978-952-10-7339-7 (PDF)
http://ethesis.helsinki.fi

Helsinki 2012
Yliopistopaino

TABLE OF CONTENTS

PART A

i. List of original publications

This thesis is based on the following original publications, which are referred to in the text by their roman numerals.

I **Wang H**, Liaw YC, Stone D, Kalyuzhniy O, Amiraslanov I, Tuve S, Verlinde CL, Shayakhmetov D, Stehle T, Roffler S, Lieber A. (2007) Identification of CD46 Binding Sites within the Adenovirus Serotype 35 Fiber Knob. Journal of Virology, 81(23):12785-92.

II **Wang H**, Liu Y, Li Z, Tuve S, Stone D, Kalyushniy O, Shayakhmetov D, Verlinde CL, Stehle T, McVey J, Baker A, Peng KW, Roffler S, Lieber A. (2008) *In vitro* and in vivo properties of adenovirus vectors with increased affinity to CD46. Journal of Virology, 82(21):10567-79.

III **Wang H**, Tuve S, Erdman DD, Lieber A. (2009) Receptor usage of a newly emergent adenovirus type 14. Virology, 387(2):436-41.

IV **Wang H**, Liu Y, Li ZY, Fan X, Hemminki A., Lieber A. (2010) A recombinant adenovirus type 35 fiber knob protein sensitizes lymphoma cells to rituximab therapy. Blood, 115(3):592-600.

V **Wang H**, Li ZY, Liu Y, Persson J, Beyer, I, Möller T, Koyuncu D, Drescher MR, Strauss R, Zhang X, Wahl JK, Urban N, Drescher C, Hemminki A, Fender P, Lieber A. (2011) Desmoglein 2 is a receptor for adenovirus serotypes 3, 7, 11 and 14.Nature Medicine, 17(1):96-104.

VI **Wang H**, Li ZY, Lara S, Hemminki A, Lieber A. (2011) Multimerization of adenovirus serotype 3 fiber knob domains is required for efficient binding of virus to desmoglein 2 and subsequent opening of epithelial junctions. Journal of Virology, 85(13):6390-402.

ii. Abbreviations

aa	Amino acids
Ad	Adenovirus
Ad#	Adenovirus serotype #
Ad5/#	Chimeric adenovirus (Ad5 capsid with fiber protein of serotype #)
Ad#K	Adenovirus serotype # fiber knob
ATCC	American Type Tissue Culture Collection
bp	Base pair
CAR	Coxsackie-adenovirus receptor
CBB	*Coomassie* Brilliant Blue staining
CDC	Complement-dependent cytotoxicity
CMV	Cytomegalovirus
CPE	Cytopathic effect
DNA	Deoxyribonucleic acid
DSG2	Desmoglein 2
E.coli	Escherichia coli
EMT	Epithelial‐mesenchymal transition
FBS	Fetal bovine serum
Fig.	Figure
FITC	Fluorescein isothiocyanate
GFP	Green fluorescent protein
^{3}HAd	Adenovirus labeled with (methyl-^{3}H)thymidine
HRP	Horseradish peroxidase
IPTG	Isopropyl β-D-1-thiogalactopyranoside
ITR	Inverted terminal repeat
i.v.	Intravenous
Ka	Association rate constant
Kd	Dissociate rate constant
kD	Kilodalton
mAb	Monoclonal antibody
MOI	Multiplicity of infection
NHS	Normal human serum
Ni-NTA agarose	Ni-nitrilotriacetic acid agarose
PBS	Phosphate-buffered saline
PBS-T	Phosphate-buffered saline +0.5% Tween20
PE	Phycoerythrin
pfu	Plaque-forming unit
sCAR	Soluble CAR
sCD46	Soluble CD46
SCR	Short consensus repeat domains
SPR	Surface Plasmon Resonance
TAA	Tumor associated antigens
vp	Viral particle
wt	Wild type

iii. Abstract

Human adenoviruses (Ads) have been classified into six species (A to F) currently containing 55 serotypes. For almost 2 decades vectors derived from group C serotype Ad5 have been extensively used for gene transfer studies. These Ad5 based vectors are able to efficiently infect many mammalian cell types (including both mitotic and post-mitotic cells) through interaction with a primary attachment receptor, the coxsackie and adenovirus receptor (CAR). Despite the many advantages of Ad5 based vectors a number of limitations have affected their therapeutic application to many diseases. Although they can transduce many tissue types, Ad5 based vectors are unable to efficiently transduce several potential disease target cell types, including hematopoietic stem cells and malignant tumor cells. Therefore, newer vectors have been developed based on Ad serotypes other than Ad5. This thesis focuses on species B Ads. Species B Ads are comprised of three groups based on their receptor usage. Group 1 of species B Ads (Ad16, 21, 35, 50) nearly exclusively utilize CD46 as a receptor; Group 2 (Ad3, Ad7, 14) share a common, unidentified receptor/s, which is not CD46 and which was tentatively named receptor X; Group 3 (Ad11) preferentially interacts with CD46, but also utilizes receptor X if CD46 is blocked.

Species B group Ads are important human pathogens. Species B group 2 serotypes are isolated from patients with respiratory tract infections, whereas the Group 1 viruses are described as causing kidney and urinary tract infections. B-group Ad infections often occur in immunocompromised patients, including AIDS patients, recipients of bone marrow transplants, or chemotherapy patients. Recent studies performed in U.S. military training facilities indicate an emergence of diverse species B serotypes at the majority of sites. This included the group 1 serotype 21 and the group 2 serotypes 3, 7, and 14.

CD46-targeting vectors derived from Ad35 and Ad11 are important tools for *in vitro* gene transfer into human stem cells, including hematopoietic stem cells and induced pluripotent stem cells. Ad35 and Ad11 have been used as tools for cancer therapy, because CD46 appears to be uniformely overexpressed on many cancers. Furthermore, receptor X-targeting vectors, i.e vectors derived from Ad3 or vectors containing Ad3 fibers have shown superior in the transduction of tumor cells both *in vitro* and *in vivo* and are currently being used clinically in cancer patients.

While extensive basic virology studies have been done on Ad5, the information of species B group 1 interaction with CD46 is limited. Furthermore, the receptor for a major subgroup of species B Ads (receptor X) is unknown. The goal of this thesis was it therefore to better understand virological and translational aspects of species B Ads. The specific findings described in this thesis include *i)* the identification of CD46 binding sites within the Ad35 fiber knob, *ii)* the study of the *in vitro* and in vivo properties of Ad vectors with increased affinity to CD46. *iii)* the study of the receptor usage of a newly emergent Ad14a, *iv)* the identification of desmoglein 2 as the receptor for Ad3, Ad7, Ad11, and Ad14, *v)* the delineation of structural details of Ad3 virus interaction with DSG2, and *vi)* the analysis of functional consequences of Ad3-DSG2 interaction. As a result of these basic virology studies two Ad-derived recombinant proteins have been generated that can be used to enhance cancer therapy by monoclonal antibodies.

PART B

REVIEW OF THE LITERATURE

1 Introduction

Adenoviral vectors are currently one of the most commonly used viral vector systems in the field of gene therapy and have successfully been employed to transduce a wide variety of cell types. They are easy to manipulate, have a relatively large insertion capacity and can be purified to titres of up to 10^{13} infectious units (iu)/ml. They are able to transduce both dividing and non-dividing cells but are mostly incapable of genome integration into host cell chromosomes.

2 Adenovirus structure and life cycle

Ads were first discovered in 1953 as agents, which spontaneously caused degeneration of

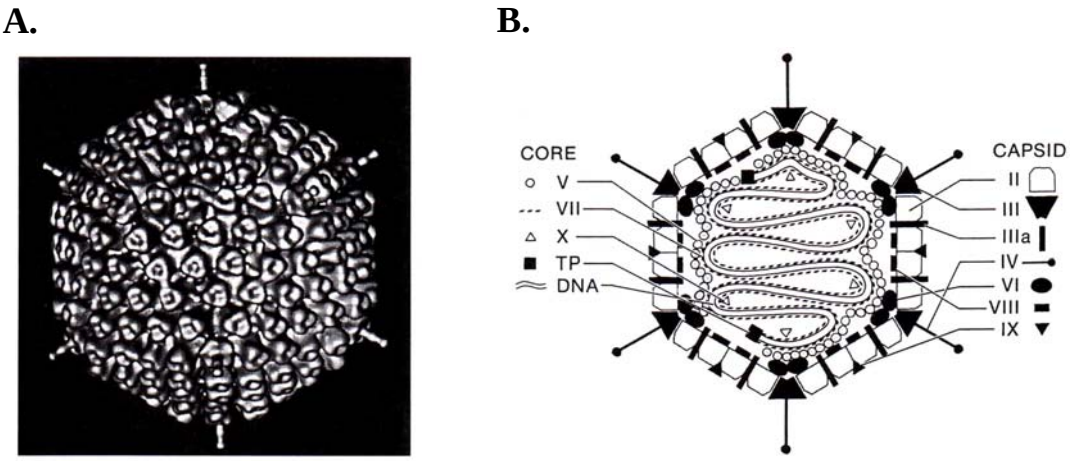

Figure 1 Three dimensional model of an Ad virion viewed along an icosahedral three-fold axis (**A**). Representative section of an Ad virion illustrating the current understanding of polypeptide component and DNA interactions (**B**). This figure was modified from Shenk (1996) Adenoviridae: The viruses and their replication. *Fundamental Virology*, 979-1016. Eds: Fields.B.N, Knipe.D.M & Howley.P.M. Lippincott-Raven Publishers, Philadelphia

primary cell cultures from human adenoid tissue (Rowe et al., 1953). Since then 55 human serotypes of the *adenoviridae* family have been identified and divided into 4 genera (aviadenovirus, atadenovirus, mastadenovirus, siadenovirus) and 6 species (A-F) (de Jong et al.,

2008). Ads have been shown to be responsible for a variety of illnesses including upper respiratory disease, epidemic conjunctivitis, and infantile gastroenteritis (Shenk, 1996).

Most studies analyzing the structure of Ads have been done with human serotypes 2 and 5, and have revealed that Ads have an icosahedral shape (20 triangular surfaces and 12 vertices) measuring about 90nm in diameter (Figure 1A). The virion has a protein shell (capsid) made up of 252 capsomere subunits composed of 240 hexons and 12 pentons. Each hexon is surrounded by 6 neighbouring subunits (Figure 2A) while each penton is surrounded by 5 neighbouring subunits and has a fiber projecting from its vertex (Figure 2B). Within the capsid are 4 polypeptides alongside a single copy of the double stranded DNA genome covalently attached at its 5' end to the terminal protein polypeptide (Figure 1B).

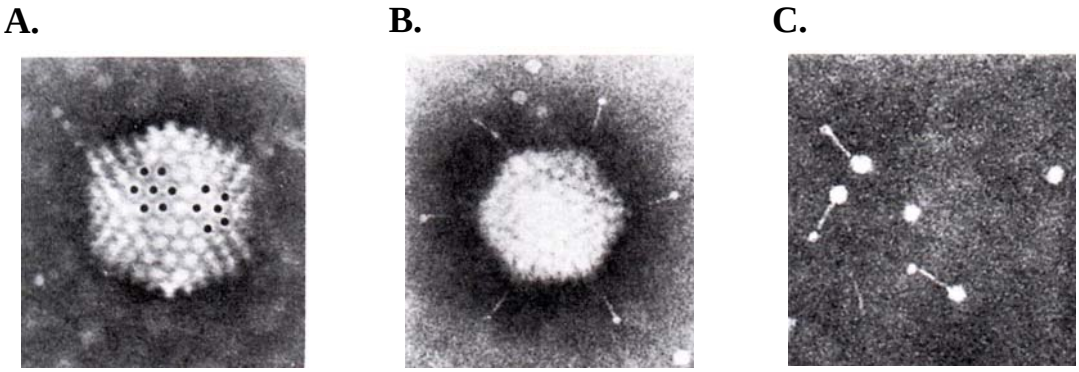

Figure 2 Electron microscopy images of Ad5. A hexon surrounded by six hexons and a penton surrounded by five hexons are marked by dots (**A**). Six fibers of twelve are visible projecting from penton capsomeres (**B**). Free penton capsomeres containing penton base and fiber are visible (**C**). Magnification is X 285 000. This figure was modified from Shenk.T (1996) Adenoviridae: The viruses and their replication. *Fundamental Virology*, 979-1016. Eds: Fields.B.N, Knipe.D.M & Howley.P.M. Lippincott-Raven Publishers, Philadelphia

The protruding fiber is the moiety within the Ad capsid that mediates a high affinity binding to the primary attachment receptor. Each Ad capsid has 12 fibers linked to penton bases. Each fiber consists of a tail domain that is anchored within the penton base, a shaft domain consisting of repeats of up to 14 aa that form β-sheets (with the number of repeats ranging from 6 to 23 in different serotypes), and the C-terminal homo-trimeric knob domain. For CAR- and CD46-interacting Ads, the knob domain binds with high affinity to the receptor and soluble fiber knobs completely block infection.

The genome of Ad (Figure 3) is typically around 36 kbp in length and has inverted terminal repeat (ITR) sequences of around 100-140 bp at each end which play important role in DNA

replication as they contain viral origins of replication. A *cis*-acting packaging sequence is present within several hundred base pairs of the left hand ITR and directs interaction of the genome with encapsidating proteins. Furthermore, the genome contains 5 early transcription units (E1A, E1B, E2, E3 and E4), two delayed early units (IX and IVa2) and one major late unit that is processed to generate 5 families of late RNAs (L1-L5). It has been demonstrated that, with the exception of E4 (Leppard, 1997), each early and late transcription unit encodes a series of polypeptides with related functions. Two E1A proteins are known to activate transcription and induce the cell to enter the S phase of the cell cycle (Shenk, 1996). Two E1B proteins are known to interact with E1A gene products (Shenk, 1996). Three E2 proteins are known to function in DNA replication. E3 proteins mostly play a role in modulation of the anti-viral host response to Ads and are therefore dispensable for *in vitro* replication (Wold et al., 1999). Late proteins are either capsid components, or proteins involved in capsid assembly (Shenk, 1996).

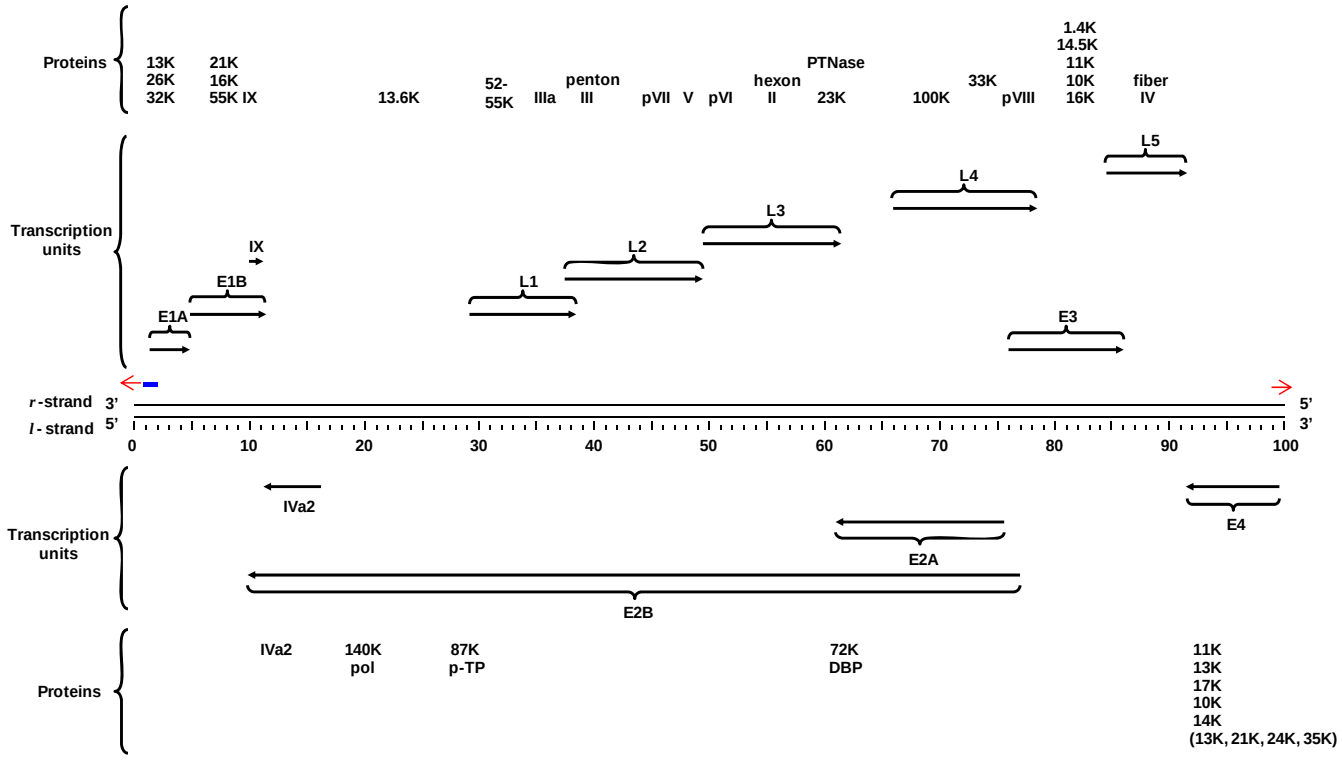

Figure 3 Linear representation of the Ad5 genome. The genome is divided into 100 relative map units and the *r* and *l* strands are transcribed in a rightward and leftward direction respectively. The ITRs are shown in red (←) and the packaging signal in blue (-) whilst early (**E**), delayed early (**IX** and **IVa2**) and late (**L**) transcription units are shown along with the viral proteins produced from each region.

The Ad life cycle (Figure 4) begins when the Ad fiber knob binds to a high affinity cell surface receptor. Most Ad species, except those belonging to subspecies B and some from subspecies D, are able to use the coxsackievirus-Ad receptor (CAR) on the cell surface for primary Ad attachment (Bergelson et al., 1997b; Roelvink et al., 1998). The Ad then undergoes receptor-mediated endocytosis and this is mediated by interactions between an Arg-Gly-Asp (RGD) motif within the viral penton base and cell surface $\alpha_v\beta_3$ and $\alpha_v\beta_5$ integrins (Wickham et al., 1993). Once internalized, a drop in pH within the endosome results in a conformational change in capsid structure, endosome disruption and release into the cytoplasm (Svensson, 1985). Hereafter, viral capsids become localized to the nucleus through a process that involves microtubules and dynein (Leopold et al., 2000). To enable this, a stepwise disassembly of Ad particles is necessary which involves fiber release, penton base dissociaton, DNA capsid scaffold protein degradation or shed, and elimination of the capsid stabilizing minor protein (Greber et al., 1993). When the capsid reaches the nuclear membrane the viral genome is injected into the nucleus, and associates with the nuclear matrix through interaction with the terminal protein (Fredman and Engler, 1993) and the process of early gene transcription begins.

The process of early gene transcription is initiated with the production of the viral E1A transactivator from a constitutive E1 promoter and has 3 main consequences. First, affected cells enter the S phase of the cell cycle to replicate the DNA. This is achieved through a number of processes including inhibition of the retinoblastoma tumour suppressor (pRb) by E1A, inhibition of the p53 tumour suppressor by E1B-55K and direct inhibition of apoptosis by the Bcl-2 homologue E1B-19K. The second consequence is the inhibition of host anti-viral responses and this is done by inhibition of α and β interferon responses by E1A proteins and VA RNAs, retention of MHC I molecules in the endoplasmic reticulum by E3-gp19K, inhibition of tumour necrosis factor alpha (TNF-α) mediated cytolysis by the E3 14.5K/10.4K complex or E3 14.7K, down regulation of Fas cell surface expression by the E3 14.5K/10.4K complex, which inhibits Fas mediated apoptosis of virus infected cells, and inhibition of FLICE (caspase 8) which plays a role in TNF and Fas mediated apoptosis (Chen et al., 1998). The third consequence is the synthesis of gene products needed for viral DNA replication.

Following synthesis of the early gene products, the processes required for virus production

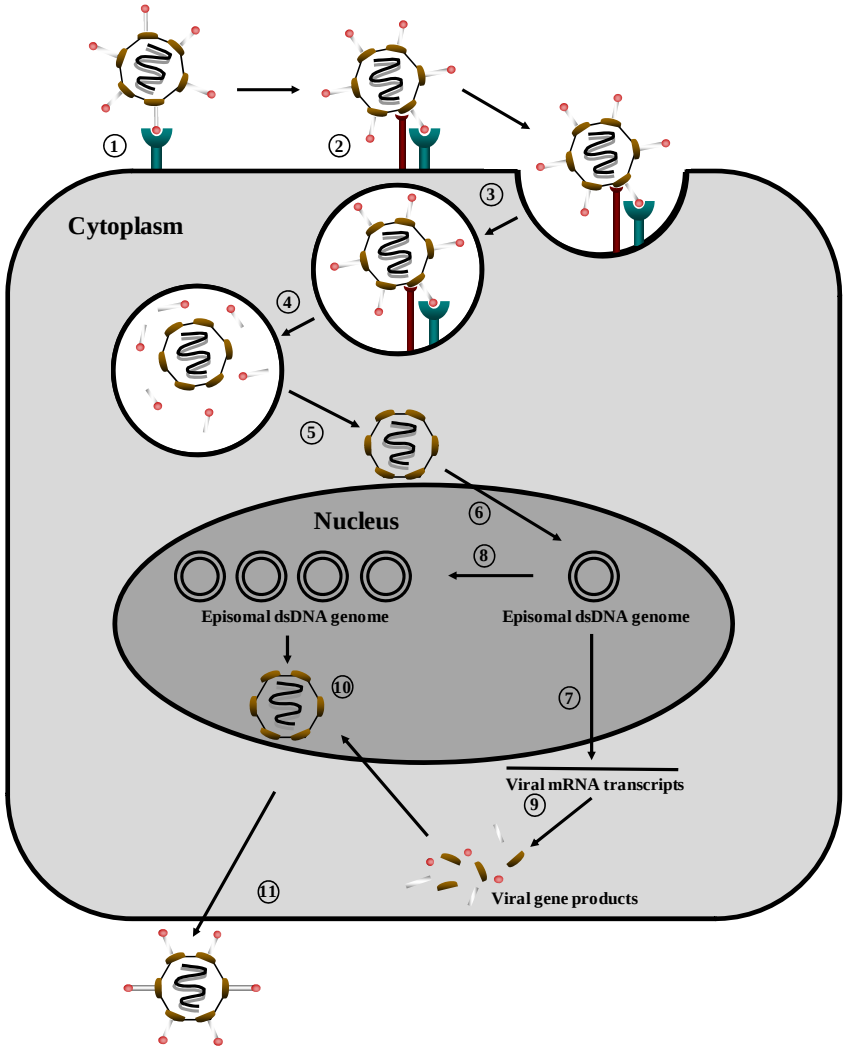

Figure 4 Ad life cycle. The Ad knob binds to its primary receptor (CAR) ① after which the penton base interacts with the secondary receptors (αvβ3/αvβ5 integrins) ② that in turn trigger the process of endocytosis ③. Once endocytosed acidification of the endosome triggers a conformational change in the viral capsid ④ that is then released into the cytoplasm and translocates to the nucleus ⑤. The viral genome then enters the nucleus ⑥ and from its episomal location undergoes transcription ⑦ and then replication ⑧. Viral gene products are then produced in the cytoplasm following translation ⑨ and capsid proteins localize to the nucleus where virus assembly occurs ⑩. Virus can then be released from the cell following lysis. Modified from Stone *et al.* 2000 (Stone et al., 2000).

are able to begin. DNA replication occurs within the nucleus and after transcription of the delayed early IX and IVa2 transcripts the major late promoter becomes activated by the IVa2 gene product and promotes production of late RNA species. The late RNA species are translated to produce capsid proteins within the cytoplasm but capsid assembly does not occur until these proteins are translocated to the nucleus. Virus assembly and genome packaging then occurs in the nucleus and Ad cannot be released from the cell until it is lysed. This cell lysis requires disruption of intermediate filaments (which are components of the cytoskeleton) such as vimentin and

cytokeratin K18, and results in the collapse of the cell and lysis (Belin and Boulanger, 1987; Chen et al., 1993).

3 Species B adenoviruses

Of the currently identified human Ads, 9 serotypes belong to species B and they have been further divided into subgroups B:1 (Ads 3, 7, 16, 21 and 50) and B:2 (Ads 11, 14, 34 and 35) based on DNA homology. Typically B:1 serotypes are isolated from patients with respiratory tract infections, whereas the B:2 viruses, with the exception of Ad11a and 14 (Mei et al., 1998), are described as causing kidney and urinary tract infections (Shindo et al., 1986) (Shields et al., 1985) (Hierholzer et al., 1975), while both B:1 and B:2 Ads have been associated with conjunctivitis (Sawada et al., 1987) (Saitoh-Inagawa et al., 2001). B-species Ad infections often occur in immunocompromised patients, including AIDS patients, recipients of bone marrow transplants, or chemotherapy patients. In general, B-species Ad infections (with the exception of Ad3 and Ad7) are relatively rare as reflected by the low percentage (<10%) of humans with neutralizing antibodies against B-species Ads that have been found in Europe, USA, Asia, and Africa (Vogels et al., 2003) (D'Ambrosio et al., 1982) (Nwanegbo et al., 2004).

Table 1 Ad disease table (Modified from Stone et al., 2006)

Disease	Most affected groups	Principle serotype
Acute febrile pharyngitis	Infants/young children	1, 2, **3**, 5, 6, **7**
Pharyngoconjunctival fever	School children	**3**, **7**, **14**
Acute respiratory disease	Military recruits	**3**, 4, **7**, **14**, **21**
Pneumonia	Infants/young children	1, 2, **3**, **7**
Pneumonia	Military recruits	4, **7**
Epidemic keratoconjunctivitis	Any age group	8, **11**, 19, 37
Pertussis-like syndrome	Infants/young children	5
Acute hemorrhagic cystitis	Infants/young children	**11**, **21**
Gastroenteritis	Infants/young children	40, 41
Hepatitis	Infants/children with liver transplants	1, 2, 5
Persistence of virus in urinary tract	Immunosupressed patients	**11**, **34**, **35**
Myocarditis	Infants/young children	5, **3**

(Serotype 3, 7, 11, 14, 21, 34 and 35 belongs to species B Ad)

Unlike species A, C, D, E and F Ads, the B species Ads are not able to utilize CAR as a primary attachment receptor (Roelvink et al., 1998), and this reflects their different tissue tropism and subsequent disease pathogenesis. Our lab (Gaggar et al., 2003b), and others (Segerman et al., 2003b) (Sirena et al., 2004) demonstrated that B species Ads are able to use the complement regulatory protein CD46 as a primary attachment receptor. CD46 is a membrane protein that is expressed on all nucleated human cells, and is also used as a receptor by keratoconjunctivitis causing D species Ads (Wu et al., 2004), measles virus laboratory strains (Dorig et al., 1993), human herpes virus 6 (Santoro et al., 1999), pathogenic *Neisseria* (including *Neisseria meningitidis, Neisseria gonorrhoeae*) and *Streptococcus pyogenes* (Johansson et al., 2003). In humans, there are four major isoforms of CD46 (BC1, BC2, C1 and C2), depending on the alternative splicing of a region encoding an extracellular domain and the choice between one or two cytoplasmic tails, Cyt-1 and Cyt2 (Purcell et al., 1991). CD46 expression is greatly upregulated in malignant tumor cells (Hara et al., 1992b) (Kinugasa et al., 1999b) (Murray et al., 2000a) (Thorsteinsson et al., 1998) and hematopoietic stem cells (Cho et al., 1991) (Manchester et al., 2002).

In addition to CD46, recently we had found the existence of an unknown receptor (receptor X) (Tuve et al., 2006) for several B species Ads. Receptor X is an abundantly expressed glycoprotein that interacts with Ads in a Ca^{2+}-dependent manner. This receptor is expressed at high levels on human mesenchymal and undifferentiated embryonic stem cells, as well as on human cancer cell lines. Competition studies with unlabeled and labeled Ads, recombinant Ad fiber knobs, and soluble CD46 and CD46 antibodies revealed three different subgroups of species B Ads, in terms of their receptor usage. Group I (Ad16, -21, -35, and -50) nearly exclusively uses CD46. Group II (Ad3, -7p, and -14) utilizes receptor X and not CD46. Group III (Ad11p) preferentially interacts with CD46, but also utilizes receptor X if CD46 is blocked. Interaction of group II and III Ads with receptor X occurs via the fiber knob. Collectively, we will refer to all receptor X-utilizing serotypes (Ad3, Ad7, Ad14 and Ad11) as AdB-2/3.

The first attempts to identify receptor X date back to 1995. These initial studies indicated the interaction of Ad3 with a ~130 kDa HeLa cell protein (Di Guilmi et al., 1995). In recent years, several candidates for receptor X such as CD46, CD80 and/or CD86 were suggested (Fleischli et al., 2007; Short et al., 2004; Short et al., 2006; Sirena et al., 2004). However, we and others have

thus far been unable to verify that these proteins can serve as the high affinity receptor for AdB-2/3 (Gaggar et al., 2003b; Gustafsson et al., 2006; Marttila et al., 2005; Persson et al., 2008; Segerman et al., 2003a; Tuve et al., 2006). Studies by us and others actually provide evidence that CD46, CD80 and CD86 are not receptor X. One possibility that could reconcile these controversial findings would be that Ad3 indeed interacts with CD46, CD86 and/or CD80 but only with a low affinity, so that only when very high ectopic receptor expression levels are used in re-expression models, through an avidity effect, virus entry could be triggered. Indeed, in the studies on CD46 by Fleischli et al. and on CD80/86 by Short et al., very high (and arguable non-physiologic) expression levels of these molecules were used on rodent CHO or BHK cells (Fleischli et al., 2007; Short et al., 2004). This hypothesis received experimental support by a recent study from Thilo Stehle's group. They found that Ad7 and 14 knobs bind to CD46 with low affinity (which was about 2000 fold lower than that of Ad35 or Ad11 binding to CD46). The binding was not stable and quickly dissociated. The authors concluded that, unlike Ad11 and Ad35, Ad7 and Ad14 cannot induce conformational changes within the fiber knob that transform this interaction into a stable contact with high affinity (Persson et al., 2008).

AdB-2/3 are common human pathogens. Since 2005, a simultaneous emergence of diverse species B serotypes at the majority of US military training facilities was observed. This included the group 1 serotype 21 and the group 2 serotypes 3, 7 and 14 (Metzgar et al., 2007). Ad14 outbreaks also occurred in the civil population. During March-June 2007, a total of 140 cases of confirmed Ad14 respiratory illness were identified in clusters of patients in Oregon, Washington and Texas. Thirty eight percent of these patients were hospitalized, including 17% who were admitted to intensive care units; 5% of patients died (Louie et al., 2008). Similar outbreaks were reported in 2008 from Alaska and from China. Independent isolates of this new virus (designated Ad14a) from multiple locations were identical by genome restriction analysis and sequencing of the complete hexon and fiber genes, and were similar to but distinct from the Ad14 reference strain from 1955 (de Wit) (Louie et al., 2008). Compared to the Ad14 (de Wit), this new virus had a deletion of two aa residues in the fiber protein knob.

One distinctive feature of AdB-2/3 is their ability to produce subviral dodecahedral particles during their replication, consisting of Ad fiber and penton base (Norrby et al., 1967). During Ad infection, free pentons and fibers are produced in excess and released with the virus progeny. For

a number of serotypes, pentons and fibers self-assemble in dodecahedra (PtDd) formed through interaction of 12 penton bases with protruding fibers. Published records for the formation of dodecahedra exist for Ad3, 9, 11, 13, 15, and 19 (Norrby et al., 1967). We found that Ad7 and 14 also form PtDd. Detailed studies have been done for Ad3 PtDd. Ad3 PtDd are assembled in the nucleus of Ad3 infected cells starting at 16 h post-infection and are arranged inside the nucleus along the nuclear membrane at 24 hours post-infection. PtDd are formed at an excess of 5.5×10^6 PtDd per infectious virus (Fender et al., 2005). The massive production of PtDd strongly suggests that they have a role in virus infection. It is thought that PtDd enhance infectivity by disturbing tight junctions and thus favoring virus spreading (Walters et al., 2002). Furthermore, PtDd competition with virus for its receptor during secondary infection can contribute to virus escape and spreading. Finally, because PtDd localize with the nuclear pore complex, a role in regulation of nuclear import and export is possible.

4 Development of species B adenoviruses as gene transfer vectors

One of the major limitations to gene therapy is the need for effective gene delivery vehicles. Due to their natural high efficiency of exogenous gene transfer, viral vectors have been widely studied. The tropism of each virus is a major determinant of its therapeutic use and due to their ability to efficiently infect multiple therapeutic target cell population's Ad vectors have shown considerable potential as vectors for delivery of therapeutic genes. For almost 2 decades vectors derived from species C serotype Ad5 have been extensively used for gene transfer studies. These Ad5 based vectors are able to efficiently infect many mammalian cell types (including both mitotic and post-mitotic cells) through interaction with the coxsackie and adenovirus receptor (CAR, (Bergelson et al., 1997b)), can be easily propagated to high titers, are replication deficient, are oncolytic, can accommodate relatively large inserts and are non-integrating.

Despite the many advantages of Ad5 based vectors a number of limitations have affected their therapeutic application to many diseases. Although they can transduce many tissue types, Ad5 based vectors are unable to efficiently transduce several potential disease target cell types, including hematopoietic stem cells HSCs (Neering et al., 1996) (Watanabe et al., 1996) and dendritic cells (DCs) (Arthur et al., 1997), without using high multiplicities of infection (MOI) and causing cytotoxicity or loss of cell function. This is primarily due to low expression of primary attachment receptor (CAR) and secondary internalizing receptor (integrins, (Wickham et

al., 1993)) on target cells. Additionally, following systemic *in vivo* delivery of Ad5 vectors, acute vector-mediated toxicity is seen (due to uptake by cells of the reticuloendothelial system and subsequent production of pro-inflammatory cytokines/chemokines) and immune responses to adenoviral proteins promote clearance of virus and limit duration of transgene expression that induce Ad specific immune responses and the release of pro-inflammatory cytokines. Also, Ad5 is an endemic virus and pre-existing humoral immunity to Ad5 is widespread among humans (Vogels et al., 2003) (D'Ambrosio et al., 1982) (Nwanegbo et al., 2004). The presence of anti-Ad5 neutralizing antibodies will inhibit systemic vector application and repeated administration of the same serotype . Furthermore, upon systemic delivery, Ad5 based vectors are directed to the liver through pathways thought to involve binding to blood factors (Shayakhmetov et al., 2005). This liver sequestration is detrimental to therapeutic strategies that involve *in vivo* targeting of Ad vectors to other organs or even tumors.

Many published reports have been focused on studying CD46 interacting (group 1) species B Ads, particularly Ad35 and its derivatives. Vectors based on Ad35 or Ad5 vectors containing Ad35 fibers have shown great promise as vehicles for gene transfer into multiple human cell types, including hematopoietic, embryonic, and mesenchymal stem cells (Stone and Lieber, 2006). Ad35-derived vectors also efficiently transduced cell lines derived from solid and liquid tumors. However, it was found that cancer cells that were cultured under conditions that maintained epithelial features (similar to the tumor in situ), were refractory to infection by CD46-targeting Ads (Strauss et al., 2009a). Overall, epithelial cells are characterized by two key features, *i)* polarized basolateral and apical membranes that differ in density of surface molecules and *ii)* intercellular tight and adherens junctions that are affiliated with the underlying apical actin-myosin ring. Tight and adherens junctions seal intercellular spaces and form permeability barriers, which prevent the flow of molecules across the epithelial layer and restrict the lateral diffusion of the apical and basolateral plasma membranes. Both CAR and CD46 are trapped in intercellular junctions of epithelial cancer cells and are not accessible to Ads that use these attachment receptors (Coyne and Bergelson, 2005; Strauss et al., 2009a). In contrast to group 1 Ads, AdB-2/3 efficiently infect epithelial cancer cells, which is accomplished in part through induction of processes that are reminiscent of Epithelial-to-Mesenchymal Transition (EMT)(Strauss et al., 2009a), a cellular transdifferentiation program where epithelial cells lose characteristics such as intercellular junctions and gain properties of mesenchymal cells (Thiery and Sleeman, 2006).

This feature makes AdB-2/3 important tools for gene transfer into epithelial cancer, which represents the bulk of solid cancers, and into normal epithelial cells (Yamamoto and Curiel, 2010).

4.1 Vectors utilizing species B adenovirus

Over the last decade several groups have attempted to overcome the disadvantages of Ad5 based vectors by developing Ad vectors that utilize elements of species B serotypes. These new Ad vectors show great promise for use in therapies where Ad5 based vectors have been unsuccessful. The cell binding characteristics of species B Ads were investigated for several therapeutic target cell populations. Studies have demonstrated efficient binding of species B Ads to human CD34 positive cells (Shayakhmetov et al., 2000; Stecher et al., 2001), to various epithelial cell lines (Mei et al., 1998), to cells of hematopoietic origin (Segerman et al., 2000), to neural cell lines (Skog et al., 2002), to primary neural tumor cells (Skog et al., 2004) and to endothelial and carcinoma cells (Zhang et al., 2003). Overall, the cell binding efficiency of these Ad serotypes demonstrates the potential of B species Ads as gene transfer vectors. More importantly, as species B Ad infections are relatively rare, the resulting low levels of pre-existing immunity in humans would enable B species vectors to be used more readily than Ad5 based vectors. This is relevant to both *ex vivo* and *in vivo* vector applications as both humoral and cellular elements of pre-existing immunity can be detrimental to genetic therapies through inhibition of vector transduction and elimination of transgene expression. The CAR-independent tropism of B species Ads would also be beneficial for certain therapeutic applications. By using different receptors as CD46 or receptor X, for cell entry B species Ads can infect target cell populations that Ad5 based vectors cannot. Taken together the lack of pre-existing immunity and enhanced tropism of species B Ads make them suitable candidate viruses for development of improved gene transfer vectors. Notably, it is unlikely that species B-Ad vectors can be re-administered.

4.1.1 Chimeric species B adenovirus vectors

As a means to improve gene transfer vectors, several groups have attempted to harness the unique properties of B species Ads in the context of Ad 5 based vectors. The first example of this by Stevenson et al. demonstrated that fiber knob domains could be swapped between Ad

serotypes (Stevenson et al., 1995). An Ad5 vector possessing the fiber knob domain of Ad7 (Ad5/7) was shown to bind to a different receptor than an Ad5 vector, demonstrating the feasibility of developing fiber chimeric Ad vectors. Around the same time Krasnykh and colleagues also developed a chimeric Ad5/3 virus possessing the fiber knob domain of Ad3 (Krasnykh et al., 1996). Subsequently, chimeric Ad5 vectors possessing the fiber knob or fiber knob and shaft domains of the other species B serotypes including Ad11 (Goossens et al., 2001) (Stecher et al., 2001), Ad14 (Havenga et al., 2002), Ad16 (Havenga et al., 2001), Ad21 (Havenga et al., 2002), Ad34 (Havenga et al., 2002), Ad35 (Shayakhmetov et al., 2000) and Ad50 (Knaan-Shanzer et al., 2001) were also developed, and data suggesting that these vectors are extremely efficient at infecting a variety of human target cell types has been generated. Human cells that can be readily transduced by species B fiber chimeric Ads include DCs (Rea et al., 2001), CD34 positive HSCs (Shayakhmetov et al., 2000) (Knaan-Shanzer et al., 2001), mesenchymal stem cells (Olmsted-Davis et al., 2002), immortalized and primary tumor cells (Havenga et al., 2002) (Kanerva et al., 2002b) (Shayakhmetov et al., 2002b), synoviocytes (Goossens et al., 2001), retinal cells (Mallam et al., 2004), endothelial cells (Havenga et al., 2002), cardiovascular cells (Havenga et al., 2001), fibroblasts (Havenga et al., 2002), amniocytes (Havenga et al., 2002) and chondrocytes (Havenga et al., 2002). This is highly encouraging as it suggests species B Ad vectors may be useful for treating a variety of diseases.

In an additional approach, aimed at avoiding pre-existing anti-adenovirus immunity, 2 studies demonstrated that the hexon of Ad5 could be substituted with that of another serotype. In the first study it was demonstrated that hexons from Ad3, Ad4 and Ad9 could be incorporated into infectious Ad5 virions (Ostapchuk and Hearing, 2001). Consequently this observation led the way to development of a species B chimeric Ad5/H3 vector based on Ad5, but containing the Ad3 hexon (Wu et al., 2002). Sera from mice pre-immunized with Ad5 could not inhibit *in vitro* infection by Ad5/H3. Furthermore, Ad5/H3 infection was not inhibited in vivo by pre-immunization of animals with Ad5. Although it has been suggested that T-cells specific to Ad5 may cross react with B species Ads *in vitro* (Smith et al., 1998) (Heemskerk et al., 2003), the data from Wu *et al* support the theory that B species Ad vectors may avoid pre-existing anti-Ad5 immunity generated *in vivo*, as hexon is the major determinant of Ad neutralizing immunity.

4.1.2 Species B adenovirus vectors

As a result of previous studies demonstrating that species B fiber/knob containing Ad vectors show improved infection of certain cell types, several groups have attempted to generate Ad vectors derived entirely from a species B Ad serotype. The first such species B Ad vector was based on serotype Ad7, was deleted in E1A, and contained a chloramphenicol acetyltransferase (CAT) expression cassette in the E1A region (Abrahamsen et al., 1997). This vector was constructed with DNA fragments from Ad7a and an Ad7a recombination reporter plasmid in 293 cells. Efficient expression of CAT was seen after *in vitro* infection of A549 cells, while systemic delivery to BALB/C mice resulted in CAT expression in liver, spleen, kidney and lung at 3 days post injection. Subsequently, another method of generating E1/E3 deleted Ad7 vectors in cosmids was reported (Nan et al., 2003). An Ad7 HIV env expressing vector was generated for vaccination studies and shown to infect cell lines and CD4(+) T lymphocytes.

The second serotype to be used in development of a B species Ad vector was Ad35 with 4 groups recently publishing methods for generating E1/E3 deleted Ad35 vectors. The first group at Crucell in the Netherlands has developed system for generating Ad35 vectors by homologous recombination of 2 shuttle plasmids in PER.C6 cells expressing the Ad35 E1B-55K protein (Vogels et al., 2003). This vector system was not hampered by pre-existing Ad5 immunity and could efficiently infect DCs, SMCs and synoviocytes. The second group at Genetic Therapy Inc were the first to publish a sequence for the Ad35 genome (Seshidhar Reddy et al., 2003). In the same study they also introduced a system of making E1A deleted Ad35 vectors in PER.C6 cells or E1A/E1B deleted Ad35 vectors in 293 cells expressing Ad5 E1, E2A and E4 proteins. Ad35 vectors did not efficiently transduce mouse cells and biodistribution studies in C57BL/6 mice revealed low levels of Ad35 in all organs evaluated, including liver, lung, spleen, and bone marrow, compared to Ad5. Minimal hepatotoxicity was seen with Ad35 and its half-life in mouse blood was found to be two to three times longer than that of Ad5. The third group developed E1A/E1B deleted Ad35 vectors and was able to grow them in 293 cells expressing Ad5 E1 and E4 (Sakurai et al., 2003a). In experiments with human CD34(+) cells Ad35, Ad5, and Ad5/35 infected 53%, 5%, and 52% of cells at MOI 300 PFU/ml. The mean of fluorescence intensity in the CD34(+) cells transduced with the Ad35 vectors was 12-76 and 1.4-3 times higher than that in the cells transduced with the Ad5 and Ad5/35 vectors, respectively. In another study the same group showed that an Ad35 vector efficiently transduced CAR-positive and CAR-negative cells (Sakurai et al., 2003b). Biodistribution studies in C57BL/6 mice showed that Ad5 and Ad35

vectors were rapidly cleared from the bloodstream with a half-life of approximately 3 minutes. When compared to an Ad5 vector, Ad35 showed lower levels of gene transfer 48 hours after infection in all organs tested and vector genomes were almost completely cleared from liver between 1 and 48 hours post injection. PCR analysis showed that more Ad35 localized with non-parenchymal liver cells, while Ad5 was localized with parenchymal and non-parenchymal liver cells at 1 and 48 hours. The fourth group reported both the sequence of Ad35 Holden strain and a system for making E1, E3 or E1/E3 deleted Ad35 vectors (Gao et al., 2003). Production of Ad35 vectors was achieved by transient transduction of a plasmid encoding the Ad35 E1B gene in HEK293 cells. Testing showed that the Ad35-based vector efficiently infected both human and rhesus macaque DCs.

As an alternative to Ad7 and Ad35 our lab sequenced the species B Ad serotype Ad11p (Stone et al., 2003) and developed an Ad11 vector system Ad11p. E1 deleted Ad11 vectors can be generated by homologous recombination in *E.coli* or homologous recombination in a 293 based complementing cell line that expresses Ad11-E1B55K. We found that like fiber chimeric Ad5/11 vectors, Ad11 vectors infect cells in a CAR-independent/CD46 dependent manner. Similarly Ad11 vectors can also efficiently infect tumor cell lines, human dendritic cells and PBMC derived CD34(+) cells. Compared to Ad 5 and Ad5/11 vectors Ad11 vectors are cleared from blood plasma more rapidly 3 minutes after systemic administration to CD46 transgenic mice, although clearance over time was comparable. Analysis of blood cell fractions for genomes showed that more Ad11 genomes are associated with blood cells than Ad 5 or Ad5/11 genomes. Analysis of tissues for Ad genomes revealed that, unlike Ad5 and Ad5/11, Ad11 vector genomes are cleared from liver between 30 minutes and 72 hours post administration. Another group has also proposed developing Ad11 vectors and recently sequenced the Ad11 genome to this purpose (Mei et al., 2003).

Most recently, Hemminki et al. reported the generation of the first selectively oncolytic Ad fully based on serotype 3 (Hemminki et al., 2011). Ad3-hTERT-E1A contains the promoter of the catalytic domain of human telomerase upstream of the E1A transcription site for tumor specific replication. *In vitro* experiment showed that this virus can kill cancer cell lines representing seven different major tumor types, although low toxicity was seen in non-malignant cells. *In vivo* data showed that the virus had anti-tumor efficacy in three different animal models. Compared to Ad5

or Ad5/3 based virus, the *in vitro* oncolysis mediated by Ad3-hTERT-E1A and wt Ad3 occurred more slowly, but *in vivo* data proved that these Ad3 based viruses are as potent as controls. Anti-tumor efficacy was retained in presence of neutralizing anti-Ad5 antibodies whereas Ad5 based controls were blocked.

4.2 Applications of vectors utilizing species B adenovirus

4.2.1 Animal models

Before CD46 was identified as a receptor for B species Ads an appropriate small animal model for testing B species fiber chimeric or B species Ad vectors was not available. Previously it was known that B species Ads could infect human and primate, but not rodent, cells although the reason for this was unclear. While all human nucleated cells express CD46, the expression of the murine CD46 homologue is restricted to the testis, which would seem to explain the specificity of infection towards human and primate cells. The identification of CD46 as the B species Ad receptor has enabled the use of existing CD46 transgenic mouse strains with widespread CD46 expression for gene transfer studies. The most representative strain of CD46 transgenic mice was developed using a ~400 kb yeast artificial chromosome (YAC) clone carrying the complete human CD46 gene (Kemper et al., 2001). The CD46 expression profile of these mice closely mimic's that observed in humans, including the same pattern of isoform expression as the donor. Tissue-specific isoform expression in the kidney, salivary gland and brain, parallel to that seen in man, is also seen. Our lab have utilized this strain for *in vivo* biodistributiion studies of a fiber chimeric Ad5/35 vector (Gaggar et al., 2003b). After intravenous injection, viral genomes were found in the liver, spleen, bone marrow, and lung. However, compared to mice injected with Ad5, the levels of Ad5/35 genomes were more than 20-fold lower in the liver (Shayakhmetov et al., 2002b). Ad5/35-mediated transgene expression in livers was seen only in sparse hepatocytes in the periportal region (in cells that are theoretically exposed to the highest dose of incoming virus). Transduced cells were also found in the spleen, specifically in the marginal zone of the red pulpa and appear to represent progenitors for dendritic cells (CD11c-positive). A study with Cy-3 labeled virus revealed that Ad5/35 uptake into Kupffer cells of CD46 transgenic mice was inefficient.

As an alternative to CD46 transgenic mice, large animal models are potentially available for species B Ad vector studies. Non-human primates could potentially be used since, unlike mice, they require CD46 expression for complement regulation. In baboons the CD46 expression profile is similar to humans (Hsu et al., 1997) and this would enable their use in gene transfer studies. As macaques have previously been used as host pathogens in measles (which also uses CD46 as a receptor) vaccine studies (Combredet et al., 2003), they could also be used in gene transfer studies.

With the identification of CD46 and receptor X new animal models for testing chimeric B species or B species Ad vectors will be obtained. Each new model will give a more appropriate representation of likely vector characteristics and host responses in humans. It is important that future experiments use these new models to thoroughly test the safety profiles of these vectors following *in vivo* delivery.

4.2.2 Cancer: Tumor targeting

A major challenge in the field of cancer virotherapy is to achieve targeted infection of metastatic tumors following the intravenous administration of Ad vectors. In the past, vectors based on Ad5 have been used for *in vivo* gene transfer. However, because Ad5 vectors predominantly transduce hepatocytes after intravenous injection, and because tumor cells often do not express CAR, these vectors are unsuitable for tumor targeting (Bergelson et al., 1997a; Li et al., 1999; Miller et al., 1998; Okegawa et al., 2000). Several strategies have been pursued with the aim of achieving tumor-targeted infection with Ad5 vectors, including the genetic modification of Ad5 by the incorporation of peptide motifs into specific sites within viral capsids, the complete substitution of the Ad5 fiber with heterologous targeting moieties, and chemical modification of the Ad5 capsid (for a review see reference (Campos and Barry, 2007)). These approaches have succeeded in changing the tropism of Ad5 to receptors that are predominantly expressed on tumor cells, such as EGFR, FGF receptor, HER2/neu and specific integrins. Another strategy for redirecting Ad5 vectors to tumor cells exploits the natural diversity present within the *Adenoviridae* family. While most Ad serotypes use CAR as the primary attachment receptor, species B Ads use CD46 or receptor x. Although in humans CD46 is expressed on all nucleated cells at a low level, RNA and protein studies with biopsy samples have demonstrated that CD46 expression is significantly upregulated in malignant tumor cells, including cells from

breast, colon, liver and endometrial cancers (Fishelson et al., 2003; Kinugasa et al., 1999a; Murray et al., 2000b). The implication of this observation is that Ad5 vectors containing fibers or fiber knobs derived from species B Ads are of interest for tumor gene therapy. Studies in non-human primates and CD46-transgenic mice that express CD46 in a pattern and at a level similar to that observed in humans demonstrated that hepatocyte transduction was significantly less pronounced with chimeric Ad5-based vectors that contained the B-species Ad35 fiber (Ad5/F35) compared with Ad5 vectors (Ni et al., 2005; Ni et al., 2006). In mouse models with pre-established liver metastases, intravenously injected Ad5/F35 vectors achieved tumor-localized transgene expression; however, the transduction efficiency of tumor cells was generally < 5% (Ni et al., 2006). In addition, several studies with Ad5 vectors containing Ad3 fibers or fiber knobs have demonstrated superior tumor cell transduction (Kanerva et al., 2002a; Kangasniemi et al., 2006).

Approximately 85 to 90% of all cancers arise from epithelial tissue, and epithelial tumor cells are therefore the main target for Ads used in antitumor therapies. Epithelial cells are defined by an apical-basal polarity that divides the plasma membrane into two specialized domains; the apical side that faces the lumen and the basolateral surface that connects to adjacent epithelial cells or to connective tissue. The apical-basal polarity of epithelial cells is reflected in the asymmetrical distribution of lipids and proteins, which is achieved by polarized trafficking and the establishment of intercellular junctional complexes (Turksen and Troy, 2004). A network of proteins in tight junctions seals the paracellular space near the apical surface, resulting in the epithelial cell layers assuming a barrier function (Madara, 1998). This permselective barrier function is based on occludins and claudins, two types of transmembrane proteins that have been identified among more than 40 proteins present within tight junctions (Furuse et al., 1993; Turksen and Troy, 2004). Cell adhesion between neighboring cells is initiated and maintained by components of adherens junctions, which are located just underneath tight junctions. In addition to these extracellular adhesive features, tight and adherens junctions are closely linked to the intracellular cytoskeleton and play important roles in cell signaling and in the regulation of gene transcription. Although cell membrane polarization in malignant epithelial cancer cells is often lost in multilayered tumors, other epithelial features, such as the presence of intercellular junctions, are maintained. Therefore, the epithelial phenotype of cancer cells and their ability to form a physical barrier represent mechanisms that restrict the access of drugs, antibodies, or immune cells to the tumor sites (Christiansen and Rajasekaran, 2004). Importantly, during the

progression toward metastatic competence, epithelial cells undergo an epithelial-mesenchymal transition (EMT), a cellular trans-differentiation program in which epithelial cells lose some of their characteristic features, such as tight and adherens junctions, and gain mesenchymal cell properties (Christiansen and Rajasekaran, 2006).

A recent study identified a new obstacle for the Ad transduction of tumors that had not been previously observed. Using an epithelial ovarian cancer model, the targeted cancer cell itself, while being restricted to an epithelial phenotype, did not efficiently support the infection and replication of commonly used oncolytic Ads (targeted to CAR or CD46) (Strauss et al., 2009a) (Figure 5). It is worth noting that the majority of cells in xenograft tumors and in patient biopsies exhibit an epithelial phenotype. In this study, a variety of claudins and other epithelial intercellular junction proteins were demonstrated to exclude viral particles from the paracellular space and restrict the access of the particles to the primary Ad attachment receptors (CAR and CD46) or to cellular integrins. Viral receptors also colocalized with the tight junction protein claudin 7 in xenograft tumors and patient biopsies. Consequently, Ad spread was restricted to areas surrounding the injection needle track and to blood vessels in the tumor periphery following intratumoral and intravenous application, respectively. However, only a small proportion of xenograft tumor cells was able to adapt to tissue culture. Cells from tumor xenografts that were exclusively in an epithelial/mesenchymal hybrid stage, underwent EMT rapidly and generated a mesenchymal cell culture during passaging. This mesenchymal phenotype supported viral infection and resulted in efficient oncolysis (Strauss et al., 2011). Overall, these results demonstrated that even early passage, primary *in vitro* cultures do not adequately model the phenotype of epithelial cells in solid tumors. Moreover, these observations were reproduced using other epithelial cell lines, including cervical and colon cancer, where a similar discrepancy between *in vivo* and *in vitro* phenotypes was identified (Strauss et al., 2011). Given that the majority of the targeted Ad vectors have been selected and assessed in cultured tumor cells, it is unclear whether these vectors have been developed to target the correct phenotype, and, subsequently, whether they can infect and lyse the majority of cancer cells in a given epithelial tumor. Another important conclusion from this study was that mesenchymal tumors, such as sarcomas, may be a better target for the available oncolytic Ads than epithelial tumors. Notably, a recent study indicated that Ad5 vectors can also infect tumor cells via FX and cellular HSPGs (Gimenez-Alejandre et al., 2008). This pathway, however, is also a major mechanism for non-

specific Ad5 sequestration to the liver, and research is underway to generate Ad5 vectors that are ablated for FX binding (Alba et al., 2009). However, it remains unclear whether avoiding FX-mediated sequestration would compensate for the potential loss of tumor cell transduction through this pathway.

The inaccessibility of Ad receptors in epithelial tumors is consistent with data from several earlier studies that used CAR-targeted Ad2 and Ad5 on human airway epithelial cells. Specifically, CAR was previously demonstrated to be an integral tight junction protein (Cohen et al., 2001), and apical Ad5 infection efficiency was limited on polarized epithelial cells (Walters et al., 1999). Similar to other tight junction proteins (e.g., claudins), CAR was demonstrated to form transcellular homodimers between neighboring cells (van Raaij et al., 2000), and overexpression of CAR led to increased transepithelial resistance (Cohen et al., 2001). The fiber protein of Ad2 also exhibited a higher affinity for CAR than CAR displayed for itself and triggered CAR homodimer disruption (Freimuth et al., 1999). Walters *et al* demonstrated that following the initial infection of polarized airway epithelial layers with Ad2, the first-progeny virus were released to the basolateral surfaces, subsequently traveling through the paracellular space toward the apical side (Walters et al., 2002). The production of high levels of soluble Ad fiber protein and the release of defective viral particles resulted in disruption of CAR homodimers and a concomitant decrease in transepithelial resistance. This effect was also accompanied by a breakdown of tight junctions in general, which ultimately led to the release of functional viral particles to the apical surface. Although the investigators interpreted this effect as a consequence of the CAR-CAR disruption, the contribution of an intracellular signal triggered by fiber binding to CAR to the increased epithelial permeability could not be excluded. The possibility that the binding of viral pentons to integrins might have facilitated Ad movement across epithelial barriers was also suggested. However, the study left unclear how Ad2 can initiate an efficient infection on polarized airway epithelial layers (Goosney and Nemerow, 2003).

Importantly, the loss of tight junctions is a hallmark of EMT, and EMT could be efficiently induced only by Ads targeting receptors other than CAR and CD46 when applied to the apical side of polarized epithelial ovarian cancer cell layers (Strauss et al., 2009a). This result suggested superior infectious abilities for species AdB-2/3 that were targeted to receptor X on epithelial cells (i.e., Ad3, Ad7, Ad11 and Ad14). Experimental support that these Ad serotypes can induce

EMT-like processes (e.g., the removal of E-cadherin from the cell surface) (Strauss et al., 2011), provides a rationale for the construction of oncolytic viruses in the future based on these serotypes. It is expected that oncolytic viruses derived from AdB-2/3 are able to initially transduce more tumor cells and disseminate better in epithelial tumors than conventional Ad5-based vectors. In the light of the concept of cancer stem cells, it might not be necessary to transduce 100% of tumor cells. It rather seems to be important to target the subfraction of malignant cells that drive tumor growth.

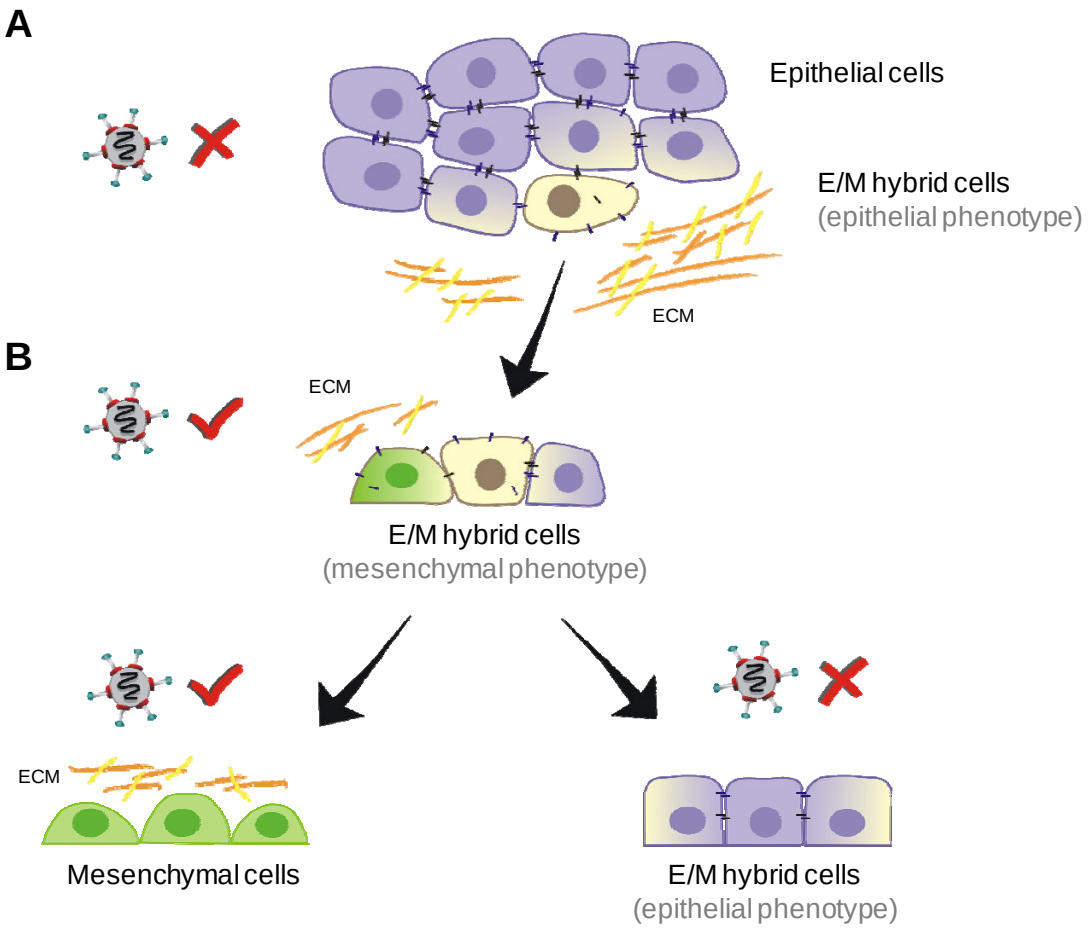

Figure 5 Phenotypes of ovarian cancer cells and their susceptibility to oncolytic adenoviruses. (A) *In situ*, tumors or tumor xenografts consist almost exclusively of epithelial and epithelial/mesenchymal (E/M) hybrid cells, which are restricted to an epithelial phenotype. These cells are resistant to adenovirus (Ad) infection and oncolysis (shown by the red cross). (B) *In vitro*, E/M hybrid cells that adapt to tissue culture mostly exhibit a mesenchymal phenotype and generate mesenchymal cells during passaging. These cultures comprise cells susceptible to Ad infection and oncolysis (shown by the red tick). A minority of the E/M hybrid cells are epithelial-restricted and can be isolated and propagated by clonal cell expansion *in vitro*. (ECM extracellular matrix)

4.2.3 Cancer: Immunotherapy

For many cancer gene therapists the concept of using the hosts own immune system to induce tumor specific immune responses in patients, by breaking tolerance, is very appealing but in order to achieve success an efficient method for delivery of tumor associated antigens (TAA) to antigen presenting cells (APCs) will be needed. Notably, the expression of TAAs in APCs ensures presentation in complex with MHCI molecules and efficient priming of CD8 T-cell responses. Previously, approaches that deliver TAAs to APCs, either *ex vivo* or *in vivo* have been utilized but to date no efficient TAA delivery system has been developed. Although Ad5 based vectors have been used as TAA delivery vehicles in cancer immunotherapy approaches the efficiency of gene transfer in human DCs has been poor. Several studies utilizing species B fiber chimeric Ads suggest they may be better vectors for delivery of TAAs in cancer immunotherapy treatments. The first study to investigate this tested a panel of chimeric Ads with alternate serotype fibers for infectivity of human DCs (Rea et al., 2001). Rea et al found that the most efficient vector was the Ad5/35 fiber chimera, which was 100-fold more potent than Ad5 for gene transfer and expression, and that Ad5/35 showed enhanced synergistic effects with other activation signals to trigger DC maturation. They also showed that DCs infected with an Ad5/35 vector expressing the melanoma associated TAA gp100 were able to generate gp100-specific CTL, and that in vivo delivery of the Ad5/35 vector enabled *in vivo* targeting of DCs. A subsequent study by the same group demonstrated that Ad5/35 was the best species B fiber chimeric Ad for infecting human DCs (Havenga et al., 2002). Further experiments from the same group then demonstrated that an Ad35 vector was extremely efficient at infecting DCs without being hampered by pre-existing Ad5 immunity. In an attempt to utilize Ad5/35 vectors for tumor immunotherapy vectors expressing the TAAs latent membrane antigens (LMP) 1 and 2 and CAMEL/NY-ESO-ORF2 have also been generated. In one study using LMP-2 as a TAA the vector Ad5/35-LMP-2 generated strong LMP-specific CTL responses in mice, a human CTL response to LMP antigens with expanded T cells lysing autologous target cells sensitized with LMP-2 CTL epitopes, and was also successfully used to reverse the outgrowth of LMP-1-expressing tumors in mice (Duraiswamy et al., 2004). It is important to note however that the mouse studies should be repeated in CD46 transgenic animal. In another study the author's show how peripheral blood can be used to produce DCs expressing LMP-2 after Ad5F35 transduction, and how an initial reactivation of LMP-2-specific CTLs can be followed by stimulation with lymphoblastoid cell lines overexpressing LMP-2 from

the same vector. Large numbers of LMP-2-specific cytotoxic lymphocytes are produced that contain both CD4+ and CD8+ T cells and recognize multiple LMP-2 epitopes (Bollard et al., 2004). In further studies efficient generation of CAMEL/NY-ESO-ORF2 specific immune responses were seen following infection of human peripheral blood mononuclear cells (PBMCs) or DCs with an Ad5/35-CAMEL/NY-ESO-ORF2 vector (Slager et al., 2003) (Slager et al., 2004).

The preliminary data suggests that species B fiber chimeric and species B Ad vectors will be useful vectors for tumor immunotherapy as TAA specific immune responses can be generated *in vitro* upon infection of human DCs. Until recently it was not possible to find out if anti tumor immune responses *in vitro* translate to anti tumor immune responses *in vivo* due to lack of a relevant mouse tumor model. Since CD46 transgenic mice can now be used for *in vivo* animal studies of species B fiber chimeric and species B Ad vectors it should be possible to test the immunotherapy potential of these vectors in a relevant mouse tumor model.

4.2.4 Vaccination

Ad5 based vectors have been extensively studied for use in vaccination against disease (For review see Tatsis and Ertl 2004). Although protective immunity can be conferred by Ad5 based vectors the ability of species B fiber chimeric Ads to infect APCs more efficiently has led to investigations into their use in vaccine development. Since Ad5/35 vectors showed the most efficient DC transduction studies have concentrated on their use as vaccines. In one report a fiber chimeric Ad5/35 vector was shown to infect cultured human DCs and circulating myeloid derived DCs with greater efficiency than Ad5, which resulted in increased T-cell activation *ex vivo* (Ophorst et al., 2004). In contrast Ad5/35 was less immunogenic in monkeys than Ad5. Also, mice with pre-existing Ad5-specific immunity showed no increase in anti-transgene immunity over Ad5. The investigators concluded that Ad5/35 is unable to circumvent anti-Ad5 immunity limiting its in vivo utility. In another study the efficacy of Ad5 and Ad35 vaccines expressing simian immunodeficiency virus (SIV) gag was assessed in mice with pre-existing anti-Ad5 immunity (Barouch et al., 2004). Levels of anti-Ad5 immunity similar to those found in humans inhibited the immunogenicity of an Ad5-gag vector but not the cellular immune responses elicited by an Ad35-gag vector. Cross-reactive Ad5/Ad35-specific CD4(+) T lymphocytes were found, but they were unable to suppress vaccine immunogenicity. A further study investigated an Ad35 vector for use in HIV vaccination (Kostense et al., 2004). Analysis of serum from European or

African patients revealed that seroprevalence to Ad35 was much lower than for Ad5, indicating Ad35 might be used as a vaccine vehicle. Overall these studies support the observations discussed in the cancer: immunotherapy section of this review and suggest that species B fiber chimeric and species B Ad vectors will be useful in the development of vaccines.

4.2.5 Hematopoietic gene transfer

Hematopoietic stem cells (HSCs) are an important target for gene therapy of diseases including sickle cell anemia and thalassemia. As efficient and stable transduction of HSCs is an important prerequisite for hematopoietic gene therapy, Ad5 based vectors are not considered good vectors for this purpose since they are unable to infect HSCs efficiently, due to low levels of CAR and integrin expression. In order to circumvent this problem studies have investigated the potential of utilizing B species Ad fibers to target Ad infection of HSCs. Following initial studies showing wild type B species Ad11p and Ad35 are able to bind human hematopoietic cells with high efficiency (Shayakhmetov et al., 2000) (Segerman et al., 2000; Stecher et al., 2001), the utility of species B fiber chimeric Ads for hematopoietic gene transfer was subsequently tested. In a pilot study Shayakhmetov et al demonstrated that a fiber chimeric Ad5/35 vector was able to infect umbilical cord blood (UCB) derived cells with potential stem cell capacity more efficiently than an Ad5 vector (Shayakhmetov et al., 2000). Both CD34(+) and CD34(+) c-Kit(+) cells were infected more readily with the Ad5/35 vector. In a subsequent study the same authors were able to demonstrate delivery of γ-globin to hematopoietic cells with an integrating Ad5/35 vector deleted of all viral genes (Shayakhmetov et al., 2002a). In another study the transduction of undifferentiated human hematopoietic cells by species B fiber chimeric Ads was analyzed (Knaan-Shanzer et al., 2001). Efficient transduction of UCB derived monocytes, granulocytes, and undifferentiated CD34(+) CD33(-) CD38(-) CD71(-) cells was seen with Ad5/35 and Ad5/50 chimeras showing the best levels of infection. In a study by Stecher et al efficient infection of PBMC derived CD34(+) cells was seen with an Ad5/11 vector (Stecher et al., 2001). A study by Yotnda et al demonstrated efficient infection of CD34(+) and CD34(-)lin(-) hematopoietic progenitor cells and Hoechst negative 'side population' (SP) cells of bone marrow with Ad5/35 but not Ad5 based vectors (Yotnda et al., 2001). In an analysis of transplantation efficiency one study demonstrated that CD34(+) cells infected with an Ad5/35 vector and sorted for GFP expression were able to consistently reconstitute bone marrow in the NOD/SCID mouse with

multilineage differentiation (Nilsson et al., 2004a). The same group was also able to demonstrate highly efficient infection of primary chronic myeloid leukemic (CML) cells and chronic lymphocytic leukemia (CLL) B cells with an Ad5/35 vector (Nilsson et al., 2004b). More recently a helper-dependent (HD) fiber chimeric Ad5/35 vector was developed which showed enhanced infection of erythroid K562 cells (Balamotis et al., 2004). Finally, a study utilizing an Ad35 vector was able to demonstrate that CD34(+) cells were as infectable with an Ad35 vector as with an Ad5/35 vector (Sakurai et al., 2003a). When these observations are looked at together it suggests that Ad vectors targeted through B species fibers are good candidates for delivery of therapeutic genes in hematopoietic gene therapy, particularly if these vectors are harnessed with an integration mechanism (for example by using phage integrases or transposons).

4.2.6 Other therapies

In addition to the studies mentioned above species B fiber chimeric Ads have shown the ability to infect other cell types and organs implicated in disease. One such example is synoviocytes which have previously been utilized for local delivery of anti-inflammatory proteins in therapies for arthritis, and are infected inefficiently by Ad5 vectors. In a study utilizing several fiber chimeric Ads an Ad5/16 vector was able to transduce synoviocytes more efficiently than any other Ad vector (Goossens et al., 2001). Another area of interest is cardiovascular disease where 2 studies have investigated the ability of fiber chimeric Ads to infect cell types targeted in vascular gene therapy. In the first study an Ad5/16 vector was found to infect primate cardiovascular cells and tissues more efficiently than other Ad vectors tested (Havenga et al., 2001). Similarly efficient infection was seen in the second study using an Ad5/3 vector to infect human smooth muscle cells from the aorta, coronary, renal, popliteal and pulmonary arteries (Su et al., 2001). Ad5/3 was also able to transduce fresh human arterial tissues. Such a vector might be of use in treating patients with cardiovascular disease - such as coronary artery restenosis following angioplasty. A further area of interest is osteogenesis where studies have investigated the use of B species fiber chimeric Ads to induce bone formation. In one study an Ad5/35 vector was used to deliver the human bone morphogenetic 2 (BMP2) gene to human bone marrow derived mesenchymal stem cells (hBM-MSCs) (Olmsted-Davis et al., 2002). These transduced cells were then used in an *in vivo* heterotopic bone formation assay and mineralized bone was only radiologically identified in muscle that received hBM-MSCs infected with the Ad5/35

vector. In a second study the same group was able to demonstrate heterotopic bone formation in the same assay using hBM-MSCs, primary human skin fibroblasts (SFs), or a human diploid fetal lung cell line (MRC-5), infected with an Ad5/35-BMP2, but not Ad5-BMP2, vector (Gugala et al., 2003). Considering recent reports that MSC home to tumors upon re-transplantation (Studeny et al., 2002) an application of B-species fiber containing vectors in a combined gene/cell tumor therapy approach could also be envisioned. An additional organ of interest has been the eye where Ad5/3 and Ad5/35 vectors have been used for transduction experiments. A study by Von Seggern et al showed that an Ad5/3 vector selectively transduced cilary bodies after intraocular injection of mice, which is of interest for treating diseases like glaucoma (Von Seggern et al., 2003). A study by Mallam et al showed that human retinoblastoma cells could be efficiently infected by an Ad5/35 vector *in vitro* (Mallam et al., 2004). The same study showed that mice given a single subretinal injection of Ad5/35-GFP showed transduction of cells in all layers of the retina especially photoreceptors and occasional neuronal cells, and Muller cells as well as retinal pigment epithelial cells. Mice given Ad5-GFP only showed transduction of retinal pigment epithelial cells and occasional photoreceptors and Muller cells. These studies demonstrate how species B fiber chimeric or species B Ad vectors will be useful tools in developing treatment of many diseases.

4.2.7 Clinical use of species B Ads

A number of publications report the clinical use of species B Ads or Ads containing species B Ad fibers. One groups of studies performed at Baylor Medical Center used Ad5/35 vectors to modify patient T-cells ex vivo to express CMV and EBV antigens. The authors showed that adoptive immunotherapy with these peripheral blood-derived T lymphocytes effectively prevented viral disease after conventional stem cell transplantation (Hanley et al., 2009; Knippertz et al., 2009; Leen et al., 2009; Leen et al., 2006; Micklethwaite et al., 2010). Another group of studies performed at the University of Helsinki used Ad3-derived viruses or Ad5 viruses containing Ad3 fiber for tumor therapy. These preliminary phase I studies showed that intratumoral, intracavitary and intravenous injection of Ad5/3 or Ad3 oncolytic vectors into humans was safe and might have exerted anti-tumor efficacy (Escutenaire et al., 2011; Hemminki et al., 2010; Koski et al., 2010; Pesonen et al., 2010).

5 Obstacles in mAb therapy of cancer

5.1 Obstacles in rituximab therapy

Monoclonal antibodies (mAbs) has emerged as a class of novel oncology therapeutics. To date, there are 27 marketed therapeutic mAbs, including 10 specific for malignant disease, and there are hundreds of mAbs currently in clinical development. Among the FDA-approved mAbs for hematological malignancies, rituximab (Mabthera, Rituxan) is regarded as one the first successful targeted treatments for cancer. Rituximab is a humanized unconjugated IgG1 mAb against CD20. CD20 is expressed on the surface of normal B-lymphocytes and B-cell lymphoma but not on hematopoietic stem cells, pro-B cells, and plasma cells. Rituximab is currently used for the treatment of B-cell non-Hodgkins lymphoma (NHL), mantle cell lymphoma, hairy cell leukemia, chronic lymphocytic leukemia. The most common B-cell lymphoid cancer is NHL, with an estimated 66,120 new cases of B-cell NHL diagnosed in 2008 and an estimated 19,160 deaths from this disease occurred last year in the United States (http://www.cancer.org/downloads/STT/2008CAFFfinalsecured.pdf). Notably, since the introduction of rituximab therapy for B-cell NHL, the 5-year survival rate increased only 16%, from 48% (1975-1977) to 64% (1996-2003), indicating that many patients are or become resistant to rituximab treatment.

Therapeutic mAbs confer killing of tumor cells by one or more mechanisms, including blocking and/or deregulating vital survival pathways and stimulating immune effector mechanisms, i.e., antibody-dependent cell mediated cytotoxicity (ADCC) and complement-dependent cytotoxicity (CDC). A series of studies have shown that rituximab is very effective in inducing CDC on B-cell lymphoma cells (Bellosillo et al., 2001; Di Gaetano et al., 2003; Golay et al., 2006; Harjunpaa et al., 2000; Reff et al., 1994; van der Kolk et al., 2001). The therapeutic potential of rituximab is significantly limited due to the ability of hematopoietic malignancies to block CDC by the over-expression of membrane complement regulatory proteins, such as CD46, CD55, and CD59 (Fishelson et al., 2003; Hara et al., 1992a; Ong et al., 2006). Several preclinical studies have shown that tumor cells can be sensitized to rituxmab induced CDC by CD55 and/or CD59 blocking antibodies (Guo et al., 2008; Ziller et al., 2005). A similar effect was seen with anti-sense oligonucleotides against CD55 and CD46, whereby these studies showed a predominant role of CD46 in protection of tumor cells against CDC (Zell et al., 2007). In addition

to blocking complement activation, CD55 and CD59 are also involved in T-cell activation (Deckert et al., 1992; Hamann et al., 1998). This might give tumor cells that lost these two proteins a selective advantage in escaping immune-mediated destruction and might explain why CD55 and CD59 are often absent on tumors (Hara et al., 1992a). Therefore, it is generally thought that CD46 alone can protect tumor cells from complement lysis (Madjd et al., 2005). Because of this as well as the observation that CD46 is uniformly expressed at high levels on many malignancies (Rushmere et al., 2004; Surowiak et al., 2006; Varela et al., 2008) (Hara et al., 1992b; Kinugasa et al., 1999b; Murray et al., 2000a; Thorsteinsson et al., 1998), including hematological malignancies (Hara et al., 1992a) (Ong et al., 2006), our strategy to sensitize tumor cells to mAbs is centered around CD46.

CD46, a membrane-linked glycoprotein that is expressed on all cells except red blood cells, attaches to complement fragments C3b and C4b that are bound to host cells and then serves as a cofactor for their targeted destruction by the plasma serine protease Factor I [reviewed in (Liszewski et al., 1996)]. CD46 is also a receptor for a number of pathogens, including measles virus, *Neisseria gonorrhea* and *N. meningitides*, group A streptococcus, and human herpes virus 6. Our lab and others reported that CD46 is a high-affinity receptor for a series of human Ad serotypes including Ad35 (Gaggar et al., 2003a; Sirena et al., 2004; Tuve et al., 2006). Ad35 engages CD46 via residues in the C-terminal trimeric fiber knob domain (Gaggar et al., 2003a). Binding of Measles virus (MV) or Ad35 to CD46 will lead to the downregulation of CD46 expression on the cell surface (Gill et al., 2003; Gill et al., 2005; Russell, 2004; Sakurai et al., 2007). It has been suggested that CD46 maybe internalized with virus without degradation after Ad35 infection, because of surface expression levels of CD46 are reduced but the total cellular protein levels of CD46 are not significantly decreased (Sakurai et al., 2007).

5.2 Obstacles in trastuzumab and cetuximab therapy

Trastuzumab targets the human epidermal growth factor receptor 2 (Her2/ ErbB-2). The receptor for cetuximab is the human epidermal growth factor receptor 1 (Her1/ErbB-1). Both receptors belong to the family of tyrosine kinase receptors and initiate signaling through several pathways which promote cell survival and proliferation (Harari et al., 2007). Trastuzumab is used as a first line therapy in Her2/*neu* positive breast cancer patients and has also been approved for metastatic Her2/*neu* positive gastric cancer. Current FDA-approved indications for cetuximab

include colorectal, head and neck, lung, and pancreatic cancer (Wheeler et al., 2010). Most patients with early stage breast or colon cancer have a measurable tumor response to trastuzumab and cetuximab therapy (in combination with chemotherapy). However, in patients with advanced or recurrent disease, the response rate to these mAbs is only 8% to 10% (Adams and Weiner, 2005).

The mechanisms of trastuzumab and cetuximab action include the activation of antibody-dependent or complement-dependent cytotoxicity, and interference with tyrosine kinase receptor signaling that is required for tumor cell survival (Wheeler et al., 2010). A unifying aspect among these mechanisms is that tumor cell growth inhibition is dependent on the binding of mAbs to their corresponding receptors. Therefore, molecules that prevent access and binding to the receptor, either by physically inhibiting intratumoral transport from blood vessels to malignant cells or masking of receptors, are predicted to block trastuzumab and cetuximab activity (Lesniak et al., 2009). Among these molecules are tumor stroma proteins such as collagen or laminin (Li et al., 2004). In a recent study, we demonstrated that transient degradation of these stroma proteins significantly improved trastuzumab therapy (Beyer et al., 2010).

In addition to obstacles formed by tumor stroma proteins, the epithelial phenotype of cancer cells also creates physical barriers to cancer therapy (Strauss and Lieber, 2009; Strauss et al., 2009b). Several studies demonstrated that the expression or upregulation of epithelial proteins correlated with increased resistance to trastuzumab (Fessler et al., 2009) and cetuximab (Oliveras-Ferraros et al., 2011) therapy of breast and colorectal cancer, respectively. Epithelial cells maintain several intercellular junctions (tight junctions, adherens junctions, gap junctions, and desmosomes), a feature which is often conserved in epithelial cancers *in situ* and in cancer cell lines (Turley et al., 2008). Epithelial junctions are composed of adhesive dimers consisting of cadherin molecules derived from two neighboring cells (Koeser et al., 2003). Desmogleins 1, 2, and 3 (DSG1-3) and desmocollins 1, 2, and 3 (DSC1-3) are subclasses of cadherins. DSC2 and DSG2 are widely expressed and are found together in desmosomes of the basal layer of epithelial cells. The cytoplasmic tails of the desmosomal cadherins link the plasma membrane to the cytoskeleton through a complex of proteins, which include plakoglobin, desmoplakin, and plakophilins. Desmoglein 2 (DSG2) is overexpressed in a series of epithelial malignancies, including breast cancer (Wang et al., 2011), ovarian cancer (Wang et al., 2011), lung cancer

(Wang et al., 2011), gastric cancer (Biedermann et al., 2005), squamous cell carcinomas (Harada et al., 1996), melanoma (Schmitt et al., 2007), metastatic prostate cancer (Trojan et al., 2005), and bladder cancer (Abbod et al., 2009). In contrast to normal epithelial tissues, epithelial tumors lack strict cell polarization, implying that a fraction of DSG2 molecules are not trapped in tight junctions (Ines Beyer, manuscript submitted). We speculate that this allows for initial entry of DSG2-binding viruses into the tumors. The production of PdDd and progeny virus then triggers further junction opening in a positive feed-forward manner, and lateral spread of virus.

AIMS OF THE STUDY

1. To identify the CD46 binding sites within the Ad35 fiber knob using an expression library of Ad35 knobs with random mutations. Additional methods to accomplish this aim include SPR and competition binding analysis, as well as X-ray crystallography (I).

2. To study the *in vitro* and *in vivo* properties of Ad vectors with increased affinity to CD46. This involves the construction of Ad vectors containing Ad35 knob mutants with higher affinity to CD46 and testing them on cell lines and in mouse models with pre-established $CD46^{high}$ liver metastases (II).

3. To study the receptor usage of a newly emergent Ad14a by competition analysis with radio-labeled viruses (III).

4. To study whether a high affinity Ad35 fiber knob can enhance the anticancer efficacy of monoclonal antibodies. Methods to address this aim include complement assays *in vitro* on lymphoma cell lines and safety and efficacy studies in preclinical models of lymphoma (IV).

5. To identify the receptor for Ad3, Ad7, Ad11, and Ad14. Potential receptor candidates will be identified using a new Western blot technique with Ad3 particles as a probe and subsequent mass-spectrometry. The role of the identified proteins as Ad3 receptor(s) will be validated by gain-of-function studies using ectopic expression of corresponding cDNAs in cells that do not bind Ad3, and by loss-of-function studies using siRNA (V).

6. To study structural details of Ad3 virus interaction with DSG2 (VI).

7. To study the functional consequences of Ad3-DSG2 interaction (V, VI).

MATERIALS AND METHODS

1 Cultured Cells and culture media

The listed cells (Table 2) were used throughout this thesis. All media and tissue culture supplements were obtained from Gibco BRL, Gaithersburg, MD unless indicated. All cell lines were cultured in the recommended growth medium supplemented with 10% FCS, 2mM L-glutamine, and penicillin-streptomycin solution. All cells were cultured at 37℃, 5% CO_2, and 95% humidity in cell culture incubators (Thermo Scientific).

Table2 : Cells used in this study

Cell line	Origin	Source	Study
HEK-293	Transformed embryonic kidney cells	Microbix[1]	I, II, III, V, VI
HeLa	Human cervical adenocarcinoma	ATCC [2] CCL-2	I, II, III, IV, V, VI
A549	Human lung adenocarcinoma	ATCC CCL-185	III,
K562	Human leukemia	ATCC CCL-243	II, V
Ramos	Burkitt's lymphoma	ATCC CRL-1596	II, V
CHO-CD46	CHO cells expressing human CD46	Prof. J. Atkinson[3]	II,
MO7e	Human erythroleukemia	Prof. L. Pegoraro[4]	II,
Raji	Burkitt's lymphoma	ATCC CCL-86	IV, V
Mino	B cell non-Hodgkin's lymphoma	ATCC CRL-3000	IV,
Farage	Non-Hodgkin's B cell lymphoma	ATCC CRL-2630	IV,
BJAB	EBV-negative B cell lymphoma	Prof. E. A. Clark[5]	IV, V
U937	Histiocytic lymphoma	ATCC CRL-1593.2	V
Karpas-299	Human T cell lymphoma	DSMZ ACC31	IV,
BT474	Ductal mammary carcinoma	ATCC HTB-20	V
T84	Human colon carcinoma	ATCC CCL-248	V, VI
CaCO-2	Human epithelial colorectal adenocarcinoma	ATCC HTB-37	V

[1]Microbix (Toronto, Canada)
[2]American type culture collection (Manassas, VA, USA)
[3]Washington University, St.Louis
[4] Istituto di Medicina Interna, Università de Torino, Italy.
[5]University of Washinton, Seattle

2 Proteins and antibodies

Recombinant human Desmoglein-1 (DSG1) (**V**) and Desmoglein-2 (DSG2) (**V, VI**) protein were from Leinco Technologies, Inc. (St. Louis, MO). Recombinant Ad3 penton-dodecahedra (PtDd) (**V, VI**) and base dodecahedra (BsDd) (**V**) were produced in insect cells and purified as described previously (Fender et al., 1997). Rituximab (**IV**) was from Genentech Inc. Daclizumab (**IV**) was from Roche Pharmaceuticals. Polyclonal rabbit antibodies against purified recombinant Ad3K and Ad35K++ knob (**V**) were produced by pickCell Laboratories. Anti-DSG2 mAbs 20G1, 7H9, 13B11, 10D2 and 8E5 (**V**) were purified from hybridoma culture supernatant using HiTrap protein G (GE Healthcare, Piscataway, NJ) following the manufacturer's protocol. Table 3 listed some antibodies used in this thesis.

Table 3 : Antibodies used in this study

Antibody name/clone	Source	Study
Mouse anti-human CD46 antibody (clone J 4.48)	Fitzgerald	I, II, III
Goat anti –mouse IgG HRP	BD Pharmingen	I, II, III, V, VI
Rabbit polyclonal anti-His_6 HRP	Abcam	I, II
Anti-human CD46 (clone MEM-258)	Serotec	II, III, IV
PE-conjugated anti-human CD46 (clone E4.3)	Santa Cruz Biotech.	II, IV
Rabbit polyclonal anti-cathepsin B antibody	Oncogene	II
PE-mouse anti-human CD20(clone 2H7)	BD Pharmingen	IV
FITC-mouse mAb anti-CD46 antibody	BD Pharmingen	IV, V
FITC-Rabbit anti-E-cadherin	BD Biosciences	V
Polyclonal goat anti-DSG2	R&D systems	V, VI
Mouse anti-DSG2 (clone 6D8)	Hycult Biotechnology	V, VI
Mouse anti –DSG2 (clone AH12.2)	Santa Cruz Biotech.	V
Rabbit anti-Claudin 7	Abcam	V, VI
FITC-Goat anti-adenovirus	Millipore	V, VI
Monoclonal anti-6xHis(MCA1396)	Serotec	VI

3 Oligonucleotides

All Oligonucleotides were purchased as lyophilized, salt-free stocks from Integrated DNA Technologies (IDT). The following table (Table 4) lists oligonucleotides used for generating recombinant Ad fiber proteins. The PCR products were then cloned into the *E.coli* expression vector pQE30 or pQE100.

Table 4: Oligonucleotides for Ad fiber proteins

Primer	**Direction**	**Sequence**	**Study**
Ad35 knob	Forward	5'CATCACGGATCCGGTGACATTTGTATAAAGGATAGT3'	I, II, IV
Ad35 knob	Reverse	5'AGCTAATTAAGCTTAGTTGTCGTCTTCTGTA3'	I, II, IV
Ad14/Ad14a knob	Forward	5'CAGACTGGATCCAATTCAAACAACATTTGCATTGATGACAA TATTAACACC3'	III
Ad14/Ad14a knob	Reverse	5'AGACTAAGCTTTCAGTCGTCTTCTCTGATGTAGTAAAAGGT AAATGGGGAGGTAACTAGG3'	III
Ad3 S6/Kn	Forward	5'CTGATGAATTCTTGATCAGGGGTTTTAAGTCTTAAATGTGTT AATCC3'	VI
Ad3 S6/Kn	Reverse	5'AGCTAATTAAGCTTAGTCATCTTCTCTAATATAGG3'	VI
Ad3 S5/Kn	Forward	5' TTACTGATGAATTCTTGATCA GGCTCCCTCCAACTTAAAGTGGGAAGTGGT3'	VI
Ad3 S5/Kn	Reverse	5'AGCTAATTAAGCTTAGTCATCTTCTCTAATATAGG3'	VI
Ad3 S4/Kn	Forward	5'TTACTGATGAATTCTGGATCC TTAGAAGAAAACATCAAAGTTAACAC3'	VI
Ad3 S4/Kn	Reverse	5'AGCTAATTAAGCTTAGTCATCTTCTCTAATATAGG3'	VI
Ad3 S3/Kn	Forward	5'TTACTGATGAATTCTGGATCC CATTCTATAAATTTACCAATAGGAAACGGT3'	VI
Ad3 S3/Kn	Reverse	5'AGCTAATTAAGCTTAGTCATCTTCTCTAATATAGG3'	VI
Ad3 S2/Kn	Forward	5'TTACTGATGAATTCTGGATCC AACAAACTTTGCAGTAAACTCGGAAATGG3'	VI
Ad3 S2/Kn	Reverse	5'AGCTAATTAAGCTTAGTCATCTTCTCTAATATAGG3'	VI
Ad3knob (S/Kn)	Forward	5'ACCATCACGGATCCAATTCTATTGCACTGAA3'	V, VI
Ad3 knob (S/Kn)	Reverse	5'AGCTAATTAAGCTTAGTCATCTTCTCTAATATAGG3'	V, VI
Ad3 K(E)/S2/Kn	Forward	5'ATCTAGGATCCGGTGGCGGTTCTGGCGGTGGCTCCGGTGGC GGTTCTAACAAACTTTGCAGTAAACTCGGAAATGGTCTTACA TTTGACT3'	VI
Ad3 K(E)/S2/Kn	Reverse	5'AGCTAATTAAGCTTAGTCATCTTCTCTAATATAGG3'	VI
Ad3 K(E)/S/Kn	Forward	5'TTATTGCTACTGGATCCGGTGGCGGTTCTGGCGGTGGCTCC GGTGGCGGTTCTAATTCTATTGCACTGAAAAATAACAC3'	VI
Ad3 K(E)/S/Kn	Reverse	5'AGCTAATTAAGCTTAGTCATCTTCTCTAATATAGG3'	VI
pQE30-Kcoil	Forward	5'GATCAAAGGTAAGCGCTTTAAAGGAGAAAGTTTCAGCACTT AAAGAAAAGGTATCCGCTTTAAAGGAGAAAGTTTCAGCACTT AAAGAAAAAGTGTCCGCTCTGAAAGAAG3'	VI
pQE30-Kcoil	Reverse	5'GATCCTTCTTTCAGAGCGGACACTTTTTCTTTAAGTGCTGAA ACTTTCTCCTTTAAAGCGGATACCTTTTCTTTAAGTGCTGAAA CTTTCTCCTTTAAAGCGCTTACCTTT3'	VI
pQE30-Ecoil	Forward	5'GATCAGAGGTAAGCGCTTTAGAGAAAGAAGTTTCAGCACTT GAGAAGGAGGTATCCGCTTTAGAGAAAGAAGTTTCAGCACTT GAGAAGGAAGTGTCCGCTCTGGAAAAAG3'	VI
pQE30-Ecoil	Reverse	5'GATCCTTTTTCCAGAGCGGACACTTCCTTCTCAAGTGCTGAA ACTTCTTTCTCTAAAGCGGATACCTCCTTCTCAAGTGCTGAAA CTTCTTTCTCTAAAGCGCTTACCTCT3'	VI

4 Adenoviruses

Wt Ad3 (GB strain) (IV, **V, VI**), Ad7p (Gomen strain) (**V**), Ad11p (Slobitski strain) (**V**), Ad14 (DeWit strain) (**IV, V**) and Ad35 (Holden strain) (**I, II, III, V**) were obtained from the American Type Culture Collection (ATCC). Ad14a (**IV, V**) is a new genomic variant of Ad14, provided by the Center for Disease Control and Prevention (Atlanta, GA). wtAd were propagated in HeLa cells or A549 cells, and purified by standard CsCl gradient methods.

All Ad5-based GFP vectors contained a 2.3-kb, cytomegalovirus (CMV) promoter-driven enhanced green fluorescent protein (EGFP) gene (derived from pEGFP-1 (Clontech, Palo Alto, CA) inserted into the E3 region of Ad genome. Chimeric Ad5/35 vector was generated earlier and described elsewhere (Shayakhmetov et al., 2000). To generate Ad5/35+ and Ad5/35++ (**II**), the corresponding wt Ad35 fiber knob of Ad5/35 was replaced by knob mutant (Asn217Asp, Thr245Pro, and Ile256Leu) and knob mutant (Asp207Gly and Thr245Ala) respectively. Ad5/3L-GFP and Ad5/3S-GFP (VI) vectors were constructed in this study. These Ad5-based vectors are deleted for E1/E3 and contain the Ad3 fiber knob (Ad5/3L-GFP) or the Ad3 fiber shaft and fiber knob (Ad5/3S-GFP).

Ad3-GFP (**V, VI**) is a wt Ad3-based vector, the region from nucleotide 29892 to 30947 of Ad3 genome (Genbank accession no. DQ086466) was replaced by a ~2kb CMV-GFP-pA transgene cassette, which was in the E3 region in front of the fiber gene. The recombinant Ad3-GFP viral genome was released by specific restriction enzyme digestion and transfected into 293 cells using a standard calcium phosphate method. After a first round of rescuing on 293 cells, HeLa cells were infected with the cell lysate containing Ad3-GFP virus for further virus propagation.

5 *In vitro* studies with adenoviruses

5.1 Production of recombinant fiber protein (I - VI)

To produce recombinant Ad fiber proteins, the *E.coli* expression vectors pQE30 or pQE100 from Qiagen were used. Protein expression was induced for 5 hours by addition of IPTG to a final concentration of 1mM. Cells were harvested and cell pellets were re-suspended in lysis buffer (50 mM NaH_2PO_4, 300 mM NaCl, 10 mM imidazole), followed by incubation with

1mg/ml lysozyme for 30 minutes on ice and subsequent sonication. Cellular debris was removed by centrifugation and the supernatant was incubated with Ni-NTA agarose at 4°C for 3 hours. Beads were washed with 50 mM NaH_2PO_4, 300 mM NaCl, 60 mM imidazole and 20% glycerol, and recombinant knob protein was eluted with 50 mM NaH_2PO_4, 300 mM NaCl, 250 mM imidazole and 20% glycerol. The fiber knob proteins were dialyzed against 20mM Hepes, 200 mM NaCl, 17% glycerol, and stored at - 80℃ after aliquoting.

5.2 Ad labeling with [*methyl*-^{3}H] thymidine (I, II, III, V)

To label Ads with [*methyl*-^{3}H]thymidine, 5×10^7 HeLa or 293 cells were grown in 175-cm^2 flasks with 15 ml of DMEM-10% FCS and infected with wt Ad at an MOI of 50 or higher, 1 mCi of [*methyl*-^{3}H]thymidine (Amersham, Arlington Heights, Ill.) was added to the medium, and cells were further incubated at 37°C until complete cytopathic effect was observed. Then cells were harvested, pelleted, washed once with cold phosphate-buffered saline (PBS), and resuspended in 5 ml of PBS. Virus was released from the cells by four freeze-thaw cycles. Cell debris was removed by centrifugation, and viral material was subjected to ultracentrifugation in CsCl gradients and subsequent dialysis as previously described. Virus purification and dialysis removed unincorporated radioactivity. Ad particle concentrations were determined spectrophotometrically by measuring the optical density at 260 nm (OD_{260}), using the extinction coefficient for wt Ad5, $\varepsilon_{260} = 9.09 \times 10^{-13}$ OD ml cm virion^{-1}. The virion-specific radioactivity was measured by a liquid scintillation counter and was always in the range of 10^{-5} to 10^{-4} cpm per virion.

5.3 Competition attachment studies (I, II, III, V)

Adherent cells were detached from culture dishes by incubation with Versene and washed with PBS. A total of $1.8x10^5$ cells / tube were resuspended in 100 µl of ice-cold adhesion buffer (DMEM supplemented with 2 mM $MgCl_2$, 1%FCS, and 20 mM HEPES) containing ^{3}H-labeled Ad at an MOI of 8,000 VP per cell. After 1 h of incubation at 4°C, cells were pelleted and washed twice with 0.5 ml of ice-cold wash-buffer (PBS, 1%FBS). After the last wash, the supernatant was removed and the cell-associated radioactivity was determined with a scintillation counter. The number of viral particles (VP) bound per cell was calculated by using the virion specific radioactivity and the number of cells. For competition studies, the competitors (fiber knobs or antibodies) were allowed to attach for 60 min at 4°C in attachment buffer and non-

bound knob removed by washing cells twice with PBS before cells were resuspended in attachment buffer containing ^{3}H-labeled Ad.

5.4 Ad labeling with Cy3 (II, IV, V, VI)

To label Ad capsids with Cy3 (red) fluorochrome (Cy3 Bifunctional Reactive Dyes; Amersham Pharmacia Biotech, United Kingdom), we used the manufacturer's protocol without modifications. The ratio between the volumes of Ad and labeling reagent was 1/9. Labeled viruses were dialyzed against 10 mM Tris-HCl, pH 7.5, 10 mM $MgCl_2$, and 10% glycerol solution at 4°C overnight to remove unincorporated chemicals. The concentrations of dye-labeled viruses were determined by quantitative Southern blotting.

5.5 *In vitro* complement-mediated lysis assays (IV)

5 x 10^4 lymphoma cells/well were plated in triplicate in 96 well plates with RPMI complemented with 10% heat-inactivated FBS, pre-incubated with PBS, 25µg/ml CD46 antibody (MEM-258, Serotec), or 25µg/ml Ad35 knob proteins. Eight hours later, 15µg/ml Rituximab was added to cells and incubated at room temperature for 30 minutes. NHS was added to a final dilution of 1:5 and cells were incubated at 37^{o}C for another 3 hours. Viable cells in each well were counted after trypan blue staining. Each sample was in triplicate and each well was counted four times. Three independent studies were performed.

5.6 Cell membrane protein preparation (V)

Total cellular membrane proteins were prepared as described earlier (Gaggar et al., 2007). Briefly, attached cells were detached with versene, washed 2 times with ice-cold PBS, cell pellets were then re-suspended in ice-cold homogenization buffer (20 mM Hepes, 1.5 mM $MgCl_2$, 5 mM KCl, 150 mM NaCl, 15% glycerol, 0.25 M sucrose, 0.1 mM EDTA, 2 mM β-mercaptoethanol, 1 mM PMSF). After disruption with a 3 ml syringe and 21G needle, the lysate was centrifuged at 400 x g for 15 minutes. The supernatant was diluted with 2 times volume of PBS and centrifuged at 35,000 rpm for 1 hour in a Beckman ultracentrifuge. The membrane protein pellet was resuspended in solubilization buffer (50 mM Hepes, 5 mM $MgCl_2$, 5 mM KCl, 150 mM NaCl, 15% glycerol, 0.25 M sucrose, 0.1 mM EDTA, 2 mM β-mercaptoethanol, 1 mM PMSF, 0.5% detergent. The use of Brij96V(Fluka, St Louis, MO) as a detergent was intrumental as

desmosomal proteins are highly insoluble.

5.7 Mass spectroscopy analysis of proteins (V)

The specific protein bands were cut from SDS-PAGE and digested with Trypsin Gold (Promega) according to manufacturer's protocol. The samples were processed on a Finnigan LCQ LC/MS (Finnigan) and data were processed using Sequest (M. Hackett, University of Washington).

5.8 Surface plasmon resonance (SPR) analyses (I, II, IV, V, VI)

All analyses were carried out on a BIAcore 3000 instrument. For biacore analysis of the recombinant knob-CD46 interaction, Ad35 knob and soluble CD46 peptide (sCD46-P), containing the knob interacting CD46 domains SCR-1 and SCR-2 were diluted to no less than 20 nM in 20 mM sodium acetate (pH 4). Ad35 knob protein was immobilized on CM5 chips and varying concentrations of sCD46-P were injected over the activated surface until the desired surface densities were achieved. Activated, coupled surfaces were then quenched of reactive sites with 1 M ethanolamine (pH 8) for 3-5 min. All data was collected at 1Hz using two replicate injections for each concentration of analyte. Flow rates during the experiment were maintained at 50 µl/min and HBSEP running buffer was supplemented with 0.1 mg/ml bovine serum albumin (BSA) to block the nonspecific binding. To completely remove remaining amounts of sCD46-P bound to the sensor chip surface, regenerations were performed by double 30 seconds injections of 20 mM sodium acetate solution (pH 4).

For biacore analysis of the DSG2 interaction, HBS-N (GE-Healthcare, Pittsburgh, PA) supplemented with 2 mM $CaCl_2$ was used as running buffer in all experiments at a flowrate of 5 ul min^{-1}. Immobilisation on CM4 sensorchip (BIAcore) was performed using DSG2 (Leinco Technology, Inc) at 0.1 mg ml^{-1} diluted in 10 mM sodium acetate buffer pH4.2 injected for 10 minutes on EDC-NHS activated flow-cell. A control flow-cell was activated by EDC-NHS and inactivated by ethanolamine. Different concentration of PtDd, BsDd, Ad3 fiber knobs were injected for 5 minutes followed by 3 minutes dissociation time and the signal was automatically subtracted from the background of the ethanolamine deactivated EDC-NHS flow cell. For the Ad

binding experiments, a similar protocol was used with the injection of wt Ad2, Ad3 and Ad5 at 5x 10^9 vp per ml.

6 Mouse strains (II, IV, V, VI)

CB-17/lcrCr1-scid-bgBR (CB17-SCID-beige) mice were purchased from Charles River Laboratories. CD46 transgenic C57Bl/6 mice line MCP8B (C57-CD46) were generously provided by Dr. Branka Horvat (INSERM, Paris, France) (Marie et al., 2002). (This line has been crossed into the C57Bl/6 background for 9 generations.) These mice express CD46 at levels similar to human cells. The transgene is a CD46 C1 isoform under the control of the ubiquitously active hydroxymethyl-glutaryl coenzyme A reductase (HMGR) promoter. In these mice CD46 protein expression was on non-lymphoid tissues as well as on activated T and B lymphocytes, macrophages, (Horvat et al., 1996) and on dendritic cells generated either from CD34+ bone marrow cells or from CD14+ peripheral blood monocytes (DiPaolo et al., 2006). All experiments involving animals were conducted in accordance with the institutional guidelines set forth by the University of Washington and were approved by the University Institutional Animal Care and Use Committee. All mice were housed in specific pathogen-free facilities.

7 Statistical analysis (I - VI)

All results are expressed as mean +/- SD. Statistical significance was evaluated using GraphPad Prism version 4.00c for Macintosh (GraphPad Software, San Diego, CA). Student`s T-test or ANOVA for multiple testing were applied when applicable. A p-value <0.05 was considered significant.

RESULTS AND DISCUSSION

1 Identification of CD46 binding sites within the Ad35 fiber knob (I).

In the past several years, gene transfer vectors based on species B Ads have shown promise for cell and gene therapy. Vectors derived from species B Ads or Ad5 vectors containing fibers from species B Ads efficiently transduce human cell types that are relatively refractory to infection with classical serotype Ad5 vectors. The most commonly used species B vectors contain Ad35 fibers (Ad35 or Ad5/F35), and therefore most studies on the interaction of species B Ads with CD46 have focused on Ad35. Ad35 binds through its trimeric fiber knob to CD46 with a high avidity (Shayakhmetov and Lieber, 2000; Tuve et al., 2006). While the interacting residues within CD46 have been localized to the two distal extracellular domains of CD46 (SCR1 and SCR2) (Fleischli et al., 2005; Gaggar et al., 2003a; Gaggar et al., 2005; Sakurai et al., 2006), the contact areas within the Ad35 knob have not been reported so far.

The structure of a CD46 interacting Ad knob (Ad11), which is similar overall to other Ad knobs, was recently published (Persson et al., 2007). Crystallization of recombinant Ad11 knob bound to CD46 domains SCR1 and SCR2 revealed three critical contact regions within the FG, HI, and IJ loops of the fiber knob. This model is supported by studies demonstrating that binding of Ad11 virus to CD46 can be abolished by introduction of a single aa substitution (Arg279Gln) within the Ad11 HI loop (Gustafsson et al., 2006). Although there is overlap in tropism between Ad11 and Ad35, Ad11 virus binds to CD46 with a higher avidity (Tuve et al., 2006), which implies that the mechanism of Ad11-CD46 interaction cannot necessarily be translated to Ad35.

1.1 Interaction of recombinant Ad35 fiber knob and CD46

Recombinant Ad35 knob containing an N-terminal 6-His tag was produced in *E.coli* and purified by affinity chromatography on Ni-agarose. The purified Ad35 knob formed trimers and only the trimeric form of Ad35 interacted with soluble CD46 (sCD46) (Figure 1A in study **I**).

We used SPR to study the affinity and stochiometry of interaction between recombinant Ad35 knob, and a peptide containing the knob interacting CD46 domains SCR1 and SCR2 (sCD46-P). Because preliminary experiments indicated that binding of Ad35 knob to the sensor surface containing immobilized sCD46-P was complex and could not be modeled by a simple 1:1

interaction scheme, we used surfaces with covalently attached Ad35 knob and injected varying concentrations of sCD46-P. The K_D of Ad35 knob to sCD46 was 15.55(5) nM (Figure 1B in study **I**). As the BiaCore instrument measures the mass of molecules bound to the sensor surface, we found the surface protein complex contains one molecule of soluble sCD46-P per monomer of Ad35 knob, that means a 1:1 interaction model.

1.2 Identification of the amino acid residues that are critical for CD46 binding

We generated a library of Ad35 knob mutants expressed in *E.coli*. We used mutagenic PCR (Cadwell and Joyce, 1992, 1994) in an approach that on average generated one to two aa mutations per knob. The Ad35 knob mutant library in XL-1 blue *E.coli* was plated on agar plates and knob expression was induced by IPTG. We used a two step colony blot protocol to simultaneously screen the library for knob trimerization and binding to sCD46. Notably, fiber knob trimerization is required for Ad binding to receptors (Hong and Engler, 1996) and analysis of trimerization allowed us to exclude mutations that reduce CD46 binding by causing major conformational changes within the Ad35 knob. Knob trimerization was assessed with the anti-6xHis-HRP antibody that recognizes only trimeric knob forms. Binding of CD46 was assessed by sCD46 and an anti-CD46 monoclonal antibody that does not interfere with the Ad35 knob-CD46 interaction. DNA from colonies that were positive for trimerization but negative for CD46 binding was sequenced. A first screening round of ~10,000 colonies revealed four aa residues (Phe242, Arg279, Ser282, Glu302) that abolished Ad35 knob binding to CD46 without affecting knob trimerization in colony assays. The identified residues were in areas that encompassed the 3 contact regions reported for the Ad11 knob. Further rounds of screening did not uncover other regions, indicating that all the detectable CD46 interacting areas had been found.

To assess the functional properties of mutants, knobs containing substitutions in positions 242, 279, 282 and 302 were purified. These mutations completely ablated binding to sCD46 as analyzed by Western blot and SPR. An example for mutant Arg279Cys is shown in Figure 3 in study **I**. As a more relevant functional assay, we used Ad35 knob mutants as competitors for attachment of Ad35 virus to HeLa cells, a cell line that expresses ~50,000 CD46 molecules per cell (Tuve et al., 2006). While 5ng of wt Ad35 knob almost completely inhibited Ad35 binding, Ad35 knobs with mutations Phe242Ser, Arg279Cys, Ser282Pro, and Glu302Val were not able to block Ad35 binding at the highest concentration tested (20ng). However, when the positively

charged Arg279 residue was substituted for a similar histidine, or the negatively charged Glu302 was substituted for negatively charged aspartate, the ability to block Ad35 binding was not completely ablated. In short, competition studies validated the functional importance of the Ad35 residues identified by library screening.

1.3 Ad35 fiber knob crystal structure and model of Ad35-CD46 interaction

To properly evaluate the residues identified by library screening, the Ad35 crystal structure was resolved by x-ray crystallography at 2.0 Å resolution, and the crystal structure for the Ad35 fiber knob was superimposed onto the Ad11-CD46 structure (Persson et al., 2007). Within the Ad11-CD46 structure, CD46 was shown to flex from its native bent conformation to a straightened rod like conformation. For binding of Ad35 to CD46, it is also likely that CD46 adopts a straightened conformation, however, the degree of flexing is impossible to predict accurately. For modeling the Ad35-CD46 interaction, we assumed that CD46 had the same conformation as in the Ad11-CD46 structure. Overall analysis of the Ad35 and Ad11 structures revealed that the FG loop of Ad35 gets closer to CD46 domain SCR1 than the FG loop of Ad11, while the IJ loop of Ad11 is 2 aa longer in length than the IJ loop of Ad35 allowing it to get closer to CD46 domain SCR2 (Figure 4 and 5 in study **I**).

Phe242 protrudes from the FG loop into the region between the FG and HI loops but is not in close enough proximity to directly interact with CD46 domain SCR1. However, the neighboring aa Asn243 and Thr246 likely form hydrogen (H) bonds with the carbonyl group of aa Tyr36 and the side chain of Tyr67 in SCR1 respectively. Furthermore, Phe242 likely stabilizes the proximity of the FG and HI loops to SCR1, by creating a region of hydrophobicity between the FG loop, HI loop and SCR1.. As with Arg 280 of Ad11, Arg279 in the Ad35 structure forms a salt bridge with Glu63 of SCR1, which is stabilized by docking of the hydrophobic portion of Arg279 against the Phe35 side chain of CD46. Ser282 in the Ad35 knob, which corresponds to aa Asn283 of Ad11, forms an H-bond with the carbonyl group of aa Tyr28 in SCR1. Glu302 of the Ad35 knob projects from the IJ loop into the space between the IJ and GH loops. It appears to stabilize the spatial proximity of the IJ and GH loops within the monomer by directly forming 2 H-bonds with Ser262 within the GH loop and one H-bond with Tyr259 in the GH loop.

Our model of Ad35-CD46 interaction differs from the model of Ad11-CD46 interaction in number of ways: *i*) The FG loop of the Ad35 knob is closer to CD46 than the Ad11 FG loop, *ii*) The IJ loop of Ad35 is shorter and does not get as close to CD46 as the Ad11 IJ loop, *iii*) We suggest a role for the GH loop, through interaction with Glu302, in stabilizing the interaction of the Ad35 IJ loop with CD46, *iv*) we have delineated the role of Phe242 in forming a 'hydrophobic sandwich' that stabilizes the FG and HI loops alongside SCR1 upon binding.

The existence of multiple contact residues, and the fact that the contact areas in the FG and HI loops are on opposite sides of the Ad35 monomer to the contact area in the IJ loop, implies that one CD46 unit binds between two Ad35 knob monomers (as described for the Ad11-CD46 interaction). This indicates that CD46-interacting species B Ads developed a different strategy to bind to their receptor than Ads that interact with CAR (Roelvink et al., 1999). For example, within the Ad5 knob the critical CAR binding residues cluster only in one area of the knob (Kirby et al., 2000; Roelvink et al., 1999).

2 In vitro and *in vivo* properties of Ad vectors with increased affinity to CD46 (II)

Because of the importance of species B Ads as a pathogen and application of species B-derived vectors for gene transfer, we studied the interaction between Ad35 and CD46 in more detail. Ad35 engages CD46 via residues in the C-terminal trimeric fiber knob domain (Gaggar et al., 2003a). Within CD46 the Ad35-interacting areas are located in the two distal extracellular domains of the receptor (Fleischli et al., 2005; Gaggar et al., 2005). In the previous section, we identified the aa residues within the Ad35 knob that mediate binding to CD46. In the present study we used the same expression library of Ad35 fiber knob with random mutations to screen for Ad35 knob mutants with increased binding to CD46 compared to wt Ad35 knob. Our goal was to construct Ad vectors with substantially increased affinity for CD46. The rational for such vectors comes from studies with phage antibody expression libraries (Vaughan et al., 1996), and more recently from studies with aptamers, protein-binding oligonucleotides (Shamah et al., 2008). The goal of phage and aptamer library screening is to identify variants with the highest affinity,

because in *in vitro* and *in vivo* studies with single-chain variable fragment (scFv) fragments and aptamers, higher affinity usually directly translates into more efficient binding to receptor-positive cells. Along this line, attempts were undertaken to incorporate high affinity ligands into measles virus (Hasegawa et al., 2007) and Ad vectors (Belousova et al., 2008; Campos et al., 2004; Zeng et al., 2008) in order to increase efficacy and specificity of target cell infection *in vivo* or to establish new receptor-ligand systems for the propagation of vectors.

2.1 Ad35 fiber knobs with increased affinity for CD46

We generated a library of Ad35 knob mutants expressed in *E. coli* strain M15. The expression from colonies was only allowed for 20 minutes after induction at room temperature. By using the Western blot with sCD46 approach described in 1.2., out of 10,000 colonies plated, twenty colonies with the most intense CD46 signals were picked and plasmid DNA was sequenced. 20% of colonies did not contain mutations. The knob sequences of the remaining colonies had single or combined substitutions of aa residues Asp207, Thr245, or Ile256 Recombinant mutant knob proteins were purified and their affinity to sCD46 was measured by SPR in comparison to wt Ad35 knob and Ad35 knob that contained a Arg279Cys substitution resulting in ablation of CD46 binding (Figure 1B in study **II**). The K_D (equilibrium dissociation constant) of wt knob was 14.64 nM, while the K_D for knob mutants with the single substitutions Asp207Gly, Thr245Ala, and Ile256Leu were 1.77, 7.64, and 10.96 nM, respectively. This translates into an 8.3, 1.9, and 1.3 fold higher affinities, compared to wt knob. The majority of identified knob mutants contained two or three of the above listed substitution. The highest affinity (0.63 nM; 23.2 fold higher than wtAd35 knob) had a knob mutant with a double Asp207Gly - Thr245Ala substitution. Two of the identified knobs with multiple mutations had substitutions Asn217Asp or Thr226Ala, however, when analyzed individually, these substitutions had no impact on knob affinity. The association kinetics was comparable for all knobs. However, the dissociation rate constants inversely correlated with the knob affinities. This indicates that knobs with higher affinity dissociate slower from CD46 than wt Ad35 knob.

In an attempt to understand the structural basis for increased affinity of our knob mutants to CD46, we superimposed the crystal structure of the Ad35 knob with that of CD46 (Persson et al., 2007). For the Asp207Gly mutant, the hydrophobic Ile13 residue of CD46 is the closest aa R group to Asp207, unlike the polar Asp residue, glycine is hydrophobic (lacking a side chain), so

an Asp207Gly substitution may enable the Ad35 DE loop to approach CD46 more closely near Ile13. Subsequently the HI loop would also get closer to CD46. For the Thr245Ala mutant, according to our original Ad35-CD46 binding model, the Ad35 Thr246 residue is important for binding and interacts with CD46 Tyr67. It seems Thr245Ala influences the loop conformation in this region and then may make the Thr246 to Tyr67 interaction stronger since the FG loop can move closer to CD46. For the Ile256Leu, Ad35 residue Ile256 is oriented towards the central core of the fiber trimer in the center of the G sheet, our model suggests that the methyl groups of Leu256 would be closer to Asn271 than those of Ile256, and the increased repulsion would likely push the G and H sheets further apart. How this affects Ad35-CD46 affinity is unclear, but it may be due to increased stability of the knob trimer.

2.2 Ad vectors containing Ad35 fiber knobs with increased affinity to CD46

Ad particles possess 12 fibers. Since one Ad35 fiber knob binds to three CD46 molecules at the same time one virus can potentially bind to a maximum of 36 CD46 molecules on a cell. We hypothesized that upon virus binding subsequent events such as clustering of receptor proteins and receptor-mediated signaling will be different between individual solubleAd35 knob molecules and corresponding knobs in the context of virions. In order to investigate this, we generated viruses containing Ad35 knobs with increased affinity to CD46. The coding sequences of Ad35 fibers, which are the CD46 interacting moiety within the Ad35 capsid, were transferred into Ad5 vectors to replace the corresponding Ad5 fiber sequence. We created three types of such chimeric vectors, Ad5/35, which contained the wt-Ad35 fiber, Ad5/35+, which contained the Asn217Asp, Thr245Pro, and Ile256Leu mutations resulting in a 3-fold higher affinity of fiber knob to CD46, and Ad5/35++, which contained the Asp207Gly, Thr245Ala substitutions, resulting in a 23.2 fold higher affinity. Ad5/35+ and Ad5/35++ genomes also contained additional XhoI and HindIII restriction sites, which allowed us to confirm the identity of virus preparation after amplification and purification in CsCl gradients by restriction endonuclease analysis of viral DNA. To measure the binding between purified Ad particles and CD46 by SPR, biotinylated virions were immobilized on Bioacore sensorchips and subsequently injected with sCD46 analyte. The affinities of Ad5/35+ and Ad5/35++ were 4.2x and 60x higher compared to the virus that contained the wtAd35 knob (Figure 3 in study **II**). While the association kinetics

were comparable for all three viruses, dissociation from sCD46 was slower for Ad5/35+ and Ad5/35++ viruses.

2.3 *In vitro* studies with Ad vectors with increased affinity to CD46

We tested whether higher knob affinities might translate into higher viral particle avidities and better vector transduction of cells (Figure 4 and 5 in study **II**). A set of CHO cell clones that expressed different densities of human CD46 (3,406; 5,221; 18,598; and 101,442 CD46 molecules per cell) (Anderson et al., 2004) were used. Transduction rates of CHO-CD46 cell clones with the Ad5/35 vector (measured based on mean GFP fluorescence) correlated with CD46 receptor density on clones. Disappointingly, when Ad5/35+ and Ad5/35++ were included into the studies, significantly higher transduction rates were not observed, regardless of the receptor density present on CHO-CD46 cells. CHO cells do not express surface integrins which are thought to be required for Ad5/35 infection (Murakami et al., 2007; Shayakhmetov D M, 2004). Furthermore, non-primate cells are refractory to infection with Ad5/35 (Shayakhmetov et al., 2000). We therefore performed further transduction studies on human cell lines of different tissue origins. No difference were seen in the transduction between Ad5/35, Ad5/35+, and Ad5/35++ HeLa cells, A549 cells and 293 cells. However, transduction of suspension cultures K562, MO7e, and Ramos was higher for Ad5/35+ and Ad5/35++, although the difference only reached significance ($p<0.05$) for Ad5/35+ and Ad5/35++ on MO7e cells.

Higher virion avidity might affect virus entry and intracellular trafficking. We did not see difference at attachment and internalization rate for these three viruses in MO7e cells. Intracellular trafficking of Ad5/35 and Ad5/35++ virions was studied using FITC-labeled anti-cathepsin B antibodies to visualize late endosomes (Figure 6 in study **II**). In agreement with earlier studies (Shayakhmetov et al., 2003), the vast majority of Ad5/35 particles co-localized with the endosomal marker at 1 hour post-infection, and there was no difference between Ad5/35 and Ad5/35++. However, when analyzed at 4 hours post-infection, more Ad5/35++ particles were still associated with endosomes inside the cytoplasm, whereas a large amount of Ad5/35 particles were found on the cell surface as free particles or associated with endosomal membranes. This is also in agreement with a previous report that Ad5/35 particles can be recycled back to the cell surface (Shayakhmetov et al., 2004; Shayakhmetov and Lieber, 2000). Apparently, the slower dissociation of Ad5/35++ from CD46 decreases this retrograde transport and allows more Ad

genomes to reach the nucleus, which might, in part, explain the higher transduction efficiencies of Ad5/35++ in MO7e cells.

2.4 Tumor targeting after intravenous vector injection

Ad5/35 vectors have shown promise for targeting of tumors because the majority of tumor types overexpress CD46 compared to normal tissue (Stone and Lieber, 2006). However, after i.v. injection, interaction of Ad5/35 vectors with $CD46^{high}$ tumors is affected by unspecific sequestration, involving high affinity interactions with soluble blood factors (Kalyuzhniy et al., 2008; Shayakhmetov et al., 2005; Waddington et al., 2008), blood cells (Lyons et al., 2006; Stone et al., 2007), and tissue macrophages (Worgall et al., 1997). This unspecific Ad sequestration and degradation affects the majority of intravenously injected viral particles and greatly reduces the efficiency of tumor cell transduction. We hypothesized that Ad5/35 vectors with increased affinity to CD46 would have an advantage in competing with non-CD46 mediated sequestration and demonstrate better tumor transduction after i.v. injection. To test this hypothesis, TC1-CD46 cells were injected into the portal vein of C57Bl/6-CD46tg mice to establish liver metastases. Three weeks after TC1-CD46 transplantation, tumor-bearing mice were intravenously injected with Ad5/35 and Ad5/35++ at dose of $5x10^9$ pfu per mouse and GFP expression was analyzed on tumor and organ sections 3 days later (Figure 8 in study **II**). Quantitation of GFP-positive tumor cells/mm^2 of consecutive liver sections (20 sections per mouse, 3 mice per virus) revealed a 6.1 (+/-1.8) fold higher transduction efficiency of TC1-CD46 metastases with Ad5/35++ compared to Ad5/35. Other than in tumors, GFP expressing cells were only found in individual cells in the liver parenchyma and the marginal zones of the spleen. Transduction of sparse normal cells in the liver and spleen had no side effects. No abnormal elevation in serum transaminases or changes in blood cell counts were observed in animals that were injected with Ad5/35 vectors. There was no significant difference in the number of GFP expressing cells between the two viruses in these tissues. This is not surprising as transduction of liver with Ad5/35 vectors is not mediated through CD46 but through interaction of Ad5 hexon with coagulation factor X and cellular HSPGs (Kalyuzhniy et al., 2008; Waddington et al., 2008). To better quantitate the number of GFP-expressing cells in this mouse model, microdissected tumors were digested by collagenase and versen. Cell suspensions were analyzed for CD46 and GFP using flow cytometry (Figure 8C in study **II**). In cell suspensions, transduced TC1-CD46 tumor cells appear as $CD46^{high}/GFP^{+}$ cells.

In mice injected with Ad5/35 and Ad5/35++, the percentage of GFP^+ cells in the $CD46^{high}$ cell fractions was 6.3% (+/-2.9%) and 23.9% (+/-9.5%), respectively. Taken together, our *in vivo* data demonstrated that Ad5/35++ is superior in transduction of $CD46^{high}$ liver metastases after i.v. vector administration. Notably, although metastases were dissected under a microscope, analyzed tumors still contained remnants of normal liver parenchyma. Normal hepatocytes can however be distinguished from tumor cells based on their lower CD46 expression.

3 Receptor usage of a newly emergent Ad14 (Ad14a) (III)

Recently, cases of severe respiratory illness in military and civilian populations have been associated with a new genomic variant of Ad14, designated Ad14a. The prototype Ad14, Ad14-de Wit, and Ad14a are identical in the fiber knob sequences except for a deletion of two amino-acids (Lys and Glu) at aa positions 251/252 found in Ad14a. This mutation is located within the F-G loop directly adjacent to the G-beta sheet. A comparison of Ad14a with other species B Ads revealed that 252Glu is conserved in species B serotypes. Furthermore, a 3D-model of Ad14a that we generated based on the published crystal structures of Ad3, Ad11, Ad16, and Ad35 (Durmort et al., 2001; Pache et al., 2008; Persson et al., 2007; Wang et al., 2007) indicated that the Lys/Glu deletion in Ad14a might change the structure of the FG loop and its proximity to the neighboring knob monomer. Taken these findings together, we speculated that the Lys/Glu mutation within Ad14a might change the fiber structure and thus the receptor usage of Ad14a, which in turn might account for the apparent higher virulence of Ad14a as compared the Ad14-de Wit.

To test this, we performed competition studies in 293 cells for virus attachment to investigate whether Ad14-de Wit and Ad14a use the same receptor(s) (Figure 2A in study **III**). We found that attachment of ^{3}H-Ad14-de Wit or ^{3}H-Ad14a was inhibited to the same degree by Ad14-de Wit and Ad14a. This suggests that Ad14-de Wit and Ad14a utilize the same receptor(s). This receptor is not CD46 because anti-CD46 antibodies that block interaction of Ad35 with CD46 (Tuve et al., 2006) did not compete for attachment of ^{3}H-Ad14-de Wit and ^{3}H-Ad14a. Furthermore, CD46-interacting serotype Ad35 did not affect the binding of ^{3}H-Ad14-de Wit. On

the other hand, pre-incubation of cells with Ad3, significantly reduced ^{3}H-Ad14-de Wit binding ($p<0.05$). Furthermore, attachment of ^{3}H-Ad3 was efficiently blocked by pre-incubation with Ad14-de Wit but not by pre-incubation with Ad35 virus or anti-CD46 antibodies as shown before (Tuve et al., 2006). Along this line, Ad14-de Wit and Ad3 did not block binding of the CD46-interacting ^{3}H-Ad35. In summary, these data show that Ad14-de Wit and Ad14a recognize the same receptor (which is not CD46) and that this receptor is also used by Ad3 (Tuve et al., 2008; Tuve et al., 2006). To study quantitative differences in Ad14-de Wit and Ad14a binding to test cells, we measured the avidity of both viruses as described previously using Scatchard blots (Figure 2C in study **III**). (Tuve et al., 2006). The K_a for Ad14-de Wit and Ad14a were $5.438x10^{9}M^{-1}$ and $9.062x10^{9}M^{-1}$, respectively. Therefore, Ad14a binds to 293 cells at a 1.67-fold higher affinity than Ad14-de Wit.

In our competition studies described above, we used complete virus particles. We then used the recombinant Ad14-de Wit and Ad14a knobs which were produced in *E.coli* as competitors in virus attachment studies. 0.4μg or 4μg knob proteins were used as competitors. Both Ad14-de Wit knob and Ad14a knob blocked attachment of Ad14-de Wit and Ad14a virus. In the presence of 0.4μg Ad14-de Wit and Ad14a knobs, Ad14-de Wit attachment was reduced by 65.1 and 68.3%, respectively. Ad14a attachment decreased 75.2 and 75.5% after Ad14-de Wit knob and Ad14a knob incubation, respectively. A 10-fold higher concentration of knobs (4μg) did not proportionally decrease Ad14-de Wit or Ad14a attachment. Notably, in previous studies with Ad5 and Ad35 viruses (Tuve et al., 2006), we found that the corresponding Ad5 and Ad35 knobs inhibited virus binding more than 95% at concentrations lower than 0.4 μg (Tuve et al., 2006).

We also tested how the higher affinity of Ad14a affects subsequent infection steps. For Ad5, and apparently also for species B Ads, following initial attachment, RGD motifs within the penton base interact with cellular integrins triggering endocytosis of Ad particles (Murakami et al., 2007; Wickham et al., 1993). To study Ad14-de Wit and Ad14a internalization, test cells were incubated ^{3}H-Ad14-de Wit or ^{3}H-Ad14a virus on ice to allow for attachment. Then, cells were moved to a 37^{o}C incubator for the indicated time periods. Cells were then washed with PBS and incubated with trypsin at 37^{o}C for 20 minutes to remove surface bound virus. The number of internalized viral particles was measured based on cell associated radioactivity. Our internalization study (Figure 4 in study **III**) did not reveal significant differences between Ad14-

de Wit and Ad14a. Taken together, our data indicate that the 251Lys/252Glu deletion in the Ad14a fiber and the 366Asp→Asn mutation in the Ad14a penton did not significantly influence the attachment and internalization of this virus. Most likely, differences in post-internalization steps or in the ability to elude the host immune response account for the higher virulence of Ad14a compared to Ad14-de Wit. Based on the findings of this study we group Ad14a into species B group 2, which so far consisted of Ad3, Ad7p and Ad14-de Wit.

4 A recombinant Ad35 fiber knob protein sensitizes lymphoma cells to rituximab therapy (IV)

Monoclonal antibodies (mAbs) have emerged as a class of novel oncology therapeutics. Rituximab is a humanized unconjugated IgG1 mAb against CD20 and has been used for the treatment of B-cell non-Hodgkins lymphoma (NHL), mantle cell lymphoma, hairy cell leukemia, chronic lymphocytic leukemia. However, resistance to rituximab treatment has also been found in many patients, this is partly due to the over-expression of membrane complement regulatory proteins, such as CD46, CD55, and CD59 (Fishelson et al., 2003; Hara et al., 1992a; Ong et al., 2006) on tumor cells. The trimeric structure of the Ad35 knob leads to a tight association with CD46 and cross-linking of several CD46 molecules on the membrane of cancer cells. Based on this we hypothesized that Ad35 fiber knobs can be used to block or remove CD46 and sensitize lymphoma cells to rituximab therapy. For our studies, we selected a Ad35 knob mutant (Ad35K++) which had a higher affinity (0.63 nM) to CD46 than did the natural Ad35 fiber knob (14.6 nM).

4.1 Removal of CD46 from cell surface by Ad35K++

Flow cytometry studies showed high and relatively uniform levels of CD46 on primary chronic lymphocytic leukemia (B-CLL) cells and test lymphoma cell lines. We first studied the effect of Ad35K++ on CD46 levels in Raji cells, a CD20-positive, human Burkitt's lymphoma cell line. ***i)*** Flow cytometry showed that incubation of Raji cells with Ad35K++ resulted in a 90% decrease of CD46 levels within 6 hours, after which surface CD46 was restored (Figure 1B in

study **IV**). The effect of the wt Ad35 fiber knob (Ad35K) was less pronounced. No decrease in CD46 levels was seen with an Ad35 knob that was ablated for CD46 binding (Ad35K-279) or with a monoclonal antibody specific to a CD46 epitope different from that of the anti-CD46 detection antibody. Together with a decrease of surface CD46, we also found less cell-bound Ad35K and Ad35K++ knob after 6 hours of incubation, indicating that CD46 and Ad35 knobs are taken up together (Figure 1C in study **IV**). ***ii)*** Immunofluorescence microscopy for CD46 and Ad35K++ knob further corroborated less surface CD46 in Ad35K++ treated cells compared to cells incubated with Ad35K-279 at 30 min and 60min after adding knob proteins. At 12 hours or 24 hours, cells treated with Ad35K++ demonstrated predominantly cytoplasmic CD46 staining, whereby it appeared that CD46 signals were less than before incubation, indicating degradation of internalized CD46-Ad35K++. CD46 reappeared on the cells surface by 48 hours. Internalized CD46 and Ad35K++ did not co-localize with the late endosomal marker cathepsin B. Instead both proteins co-stained with caveolin, an early endosomal marker at early time points. Taken together, this indicates that the internalized CD46-Ad35K++ complex is either directly released from early endosomes to the cytosol or sorted to a compartment different from late endosomes or lysosomes, where subsequent degradation occurs. Overtime, de novo produced CD46 reappears on the cell surface. ***iii)*** Previous studies have shown that transduction with Ad35-fiber containing Ad vectors directly correlates with the density of CD46 on the cell surface (Anderson et al., 2004). In transduction studies with a GFP-expressing Ad35 vector (Ad35-GFP) that uses CD46 for infection, we found that pre-incubation of Raji cells with Ad35K++ decreased GFP expression levels more than 1000-fold, compared to cells incubated with Ad35K-279. Note that the non-mutated Ad35K protein conferred less protection from Ad35-GFP infection.

Taken together, these studies show that Ad35K++ incubation of Raji cells results in transient removal of CD46 from the cell surface.

4.2 Incubation of lymphoma cells with Ad35K++ sensitizes them to rituximab-mediated complement-dependent cytolysis (CDC) *in vitro*

We then studied whether Ad35K++ incubation would render lymphoma cells more susceptible to CDC induced by rituximab. Initial experiments were done with Raji cells (Figure 2A in study **IV).** Incubation of Raji cells with rituximab followed by normal human serum (NHS), used as a source of complement, resulted in killing of about 70% of Raji cells within 3 hours. It is

noteworthy that the remaining viable Raji cells had CD20 levels that were about 50-fold lower than the mean CD20-fluorescence level of the control population (no rituximab or no NHS). To test whether the efficacy of rituximab-mediated CDC can be increased by Ad35K++-triggered internalization of CD46, we incubated Raji cells with Ad35K-279, Ad35K, and Ad35K++ for 8 hours. Ad35K and Ad35K++ increased rituximab/NHS-mediated cell killing by about 2 and 10 fold respectively, compared to rituximab/NHS alone. The sensitizing effect of Ad35K++ was seen at doses as low as 25ng/ml. Ad35K-279 had no effect on rituximab/NHS-mediated killing. Pre-incubation of Raji cells with anti-CD46 mAb in combination with rituximab/NHS was significantly less efficient than pre-incubation with Ad35K or Ad35K++ (anti-CD46mAb vs Ad35K: p=0.024). We speculate that this is due to the fact that an Ad35 fiber knob simultaneously binds to several CD46 molecules and that this cross-linking mediates internalization of the knob-CD46 complex. Another potential reason could that the affinity of Ad35 knobs to CD46 is higher than that of anti-CD46 antibodies, although we did not measure the latter. Incubation of Raji cells with CD46 ligands (anti-CD46mAb, Ad35K, or Ad35K++) together with NHS caused a ~30% decline in cell viability, most likely as a result of CDC when CD46 is blocked. To test the specificity of rituximab-mediated CDC of CD20-positive lymphoma cells, we used the humanized mAb daclizumab that binds to CD25, which is not expressed on Raji cells. There was no significant cell killing mediated by this antibody when combined with NHS.

To consolidate our findings on Raji cells, we performed studies with other CD20-positive cell lines, including BJAB (EBV-negative Burkitt's lymphoma), Farage (non-Hodgkin's B cell lymphoma), and Mino (Mantle cell lymphoma). In all cell lines tested we found a significant increase in rituximab/NHS-mediated cell killing when cells were pre-incubated with Ad35K++ (Figure 2B in study **IV)**. Furthermore, we used primary cells from B-CLL patients. Pre-incubation of B-CLL cells with Ad35K++ knob significantly increased the efficacy of rituximab/NHS treatment. Notably, the cell sample that was most resistant to Ad35K++/rituximab killing (CCL-3) had the lowest percentage of CD20-positive cells and the lowest CD20 levels. No cell killing was detected when normal human peripheral blood mononuclear cells were incubated with Ad35K++/rituximab/NHS.

In summary, the *in vitro* studies show that Ad35K++ pre-incubation of primary B-CLL cells and lymphoma cell lines increases the cytotoxity of rituximab.

4.3 Ad35K++ improves anti-tumor efficacy of rituximab *in vivo*

To establish a xenograft lymphoma model, we intravenously injected Raji cells into immunodeficient SCID/beige mice. At different time points after injection, mice were sacrificed and blood, spleen, lymph nodes, and bone marrow were analyzed for the presence of Raji cells by flow cytometry for human CD20 and immunofluorescence microscopy. HuCD20-positive Raji cells were predominantly found in the spleen and lymph nodes and were very sparse in the spleen. The percentage of huCD20-positive cells increased from 20(+/-4)% (bone marrow) and 5(+/-1.2)% (lymph nodes) at day 10 p.i. to 75(+/-6)% and 42(+/-8)% at day 14 p.i. At days 15 or 16 after Raji cell injection, mice developed hind leg paralysis (due to tumor growth inside the spinal cord), a symptom that we eventually used as an endpoint in Kaplan-Meyer survival studies. To better reflect the situation in end-stage cancer patients, we decided to test our therapy approach in a challenging model by starting the treatment only 2 days before the animals would reach the experimental endpoint. For therapy studies, 14 days after implantation of Raji cells, mice received either 50µg (2.5mg/kg) of Ad35K++ protein or 50µg of CD46-binding ablated Ad35K-279 protein (Figure 3B in study **IV)**. Ten hours later, either PBS or 50µg of rituximab was injected via the tail vein. One group of mice was sacrificed 12 hours later and the effect of Ad35K++, rituximab, and Ad35K++/rituximab on killing of Raji cells *in vivo* was measured based on the percentage of huCD20-positive cells in the bone marrow and lymph nodes. Compared to Ad35K-279-treated control mice, no significant therapeutic effect was observed when Ad35K++ or rituximab (at a dose of 2mg/kg) were injected alone. However, the combination of Ad35K++ and rituximab resulted in a significant decrease (>2-fold) in huCD20-positive cell ($p<0.03$). These findings were confirmed in survival studies (Figure 3D in study **IV)**. There was a remarkable increase in survival (by 3 days) when mice were treated with Ad35K++/rituximab compared to rituximab only or Ad35K-279 treatment (rituximab vs Ad35K++/rituximab: $p=0.0050$; Ad35K-279 vs Ad35K++/rituximab: $p=0.0016$) N=10. There was no difference in survival between the control (Ad35K-279) and Ad35K++ only groups. Rituximab at a dose of 2.5mg/kg alone did not exert a significant therapeutic effect *in vivo* (Ad35K-279 vs rituximab: $p=0.1289$), however a further increase to a dose of 12.5mg/kg resulted

in therapeutic efficacy. (Notably, doses from 2 to 25mg/kg of rituximab are used in clinical settings.) In an attempt to further increase the therapeutic efficacy of our approach, we applied a second cycle of Ad35K++/rituximab treatment 72 hours after the first injection of rituximab. Repeated injection of Ad35K++/rituximab increased the medium survival times to 24 days, compared to 16.5 days after treatment with rituximab alone.

We then tested our approach in a second tumor model using the human NHL cell line Farage (Figure 4 in study **IV)**. i.v. injection of $5x10^6$ cells into SCID/beige mice resulted in onset of morbidity/paralysis at day 23. At this time, Farage cells had massively infiltrated the bone marrow, mesenteric lymph nodes, and spleen as shown by immunofluorescence microscopy with anti-huCD20 antibodies. In these organs huCD20-positive cells displayed a predominantly nodular neoplastic growth pattern, which is characteristic for follicular NHL in humans. Treatment of mice was started at day 21 after injection of Farage cells. As seen with Raji cells, Ad35K++/rituximab treatment resulted in a significant reduction of huCD20-positive cells in all affected tissues compared to rituximab treatment alone ($p<0.05$ for Ad35K++/rituximab vs all other groups). The median survival times for PBS-, rituximab-, and Ad35K++/rituximab-treated mice were 25, 27, and 32 days, respectively. The difference between rituximab and Ad35K++/rituximab was significant ($p=0.04$) (N=10).

These studies suggest that Ad35K++ can improve the efficacy or rituximab therapy.

4.4 Safety and immunogenicity of intravenous Ad35K++ injection

Because in mice the homologue of CD46 is expressed only in the testis, transgenic mice that express huCD46 in a pattern and at levels similar to humans are a better model for safety studies. We intravenously injected the same dose of Ad35K++ that was used in the therapy studies into huCD46 transgenic, immunocompetent C57Bl/6 mice (strain MCP-8B) (Marie et al., 2002). Notably, immunodeficient mice that are transgenic for human CD46 are not available. Analyses of blood cell counts and other hematological parameters at 6 and 48 hours after Ad35K++ injection did not show abnormalities. At necropsy (day 14 p.i.), no pathological or histological changes were found in all organs analyzed (brain, lung, heart, liver, kidney, intestines, bone marrow, and testis).

To assess the potential immunogenicity of Ad35K++ and the possibility for repeated injection in settings without immuno-suppression, we measured Ad35K++ specific antibodies in serum of cancer patients (Figure 5 in study **IV)**. None of the 20 serum samples tested contained antibodies that reacted with either Ad35K or Ad35K++. On the other hand, 18 serum samples contained antibodies specific to Ad5 hexon, Ad5 fiber knob, and Ad5 penton. This outcome is not surprising. While the vast majority of humans have neutralizing antibodies against Ad5 virus, less than 10% of humans have neutralizing antibodies against Ad35 virus (Abbink et al., 2007), implying that Ad35K++ can be applied at least once in most humans. However, it is expected that injection of Ad35K++ will trigger the production of Ad35K++ antibodies in immunocompetent patients. In an attempt to assess whether anti-Ad35K++ antibodies affect Ad35K++-mediated sensitization to rituximab therapy, we injected Ad35K++ into huCD46 transgenic mice. We compared a standard vaccination scheme involving three subsequent subcutaneous Ad35K++ injections with i.v. injection of Ad35K++ used in our *in vivo* studies before. While we detected antibodies that reacted with Ad35K++ and, to a lesser degree, with Ad35K in mice that received Ad35K++ subcutaneously, no detectable antibodies were observed when Ad35K++ was given intravenously. This is probably due to inefficient uptake of Ad35K++ by antigen-presenting cells after i.v. injection. We also used the serum from vaccinated or naïve mice together with Ad35K++ in rituximab-mediated CDC assays. Regardless of the presence of anti-Ad35K++ antibodies, we found the same stimulating effect of Ad35K++ in cell killing. This might be due to the fact that the Ad35K++ interaction with CD46 is of very high affinity and cannot be disrupted by polyclonal anti-Ad35K++ antibodies that develop in Ad35K++ injected mice. The finding that Ad35K++ induced antibodies reacted less with Ad35K than with Ad35K++ was interesting and we speculated that small conformational changes within the fiber knob can lead to loss or decrease of immunogenicity. Based on this one could imagine that a set of different Ad35K mutants (with different epitopes) could be used for in multiple cycle treatment regimens.

Overall, our data in huCD46 transgenic mice indicate that i.v. injection of Ad35K++ is safe and that repeated Ad35K++ application can potentially have a therapeutic effect in patients that do not receive immunosuppressive chemotherapy.

5 Desmoglein 2 is a receptor for Ad3, 7, 11, and 14 (V)

We have suggested a new grouping of species B Ads based on their receptor usage (Tuve et al., 2006). Group 1 (Ad16, 21, 35, 50) nearly exclusively utilize CD46 as a receptor; Group 2 (Ad3, Ad7, 14, 14a) share a common, unidentified receptor/s, which is not CD46 and which was tentatively named receptor X; Group 3 (Ad11) preferentially interacts with CD46, but also utilizes receptor X if CD46 is blocked. Collectively, we refer to all receptor X-utilizing serotypes (Ad3, Ad7, Ad14, Ad14a and Ad11) as AdB-2/3. For initial studies on the identification of receptor X we focused on Ad3.

5.1 DSG2 is a receptor for AdB-2/3 viruses

Previous studies showed that Ad3 binds at nanomolar affinity to a high-density cellular receptor (Tuve et al., 2006). First we sought to identify the Ad3 capsid protein that mediates high-affinity binding to cells, which we would later use to search for the high-affinity receptor X. Notably, high-affinity binding of Ad5 to CAR and Ad35 binding to CD46, respectively, is mediated by the corresponding fiber knob (Leopold and Crystal, 2007). Our previous studies, however, revealed that a recombinant, timeric Ad3 knob could not completely block Ad3 virus binding even when very high concentrations were used, indicating that other or additional capsid moieties are involved in Ad3 binding (Tuve et al., 2008). Consequently, we utilized recombinant Ad3 dodecahedra composed of Ad3 penton bases (BsDd) or Ad3 penton bases and fibers (PtDd) (Fender et al., 1997) to compete for Ad3 binding. We found that PtDd but not BsDd blocked attachment of Ad3 to cells (Figure 1a in study **V**). PtDd also blocked binding of other AdB-2/3, e.g. Ad14, Ad14a, as well as Ad11, if CD46 is also blocked. PtDd did, however, not inhibit binding of Ad5 and only partially blocked Ad35 binding. Preincubation of cells with PtDd resulted in a better Ad3 binding inhibition than Ad3 knob mixed with BsDd. The ability of PtDd to compete with Ad3 was also confirmed in transduction studies, where PtDd efficiently blocked an Ad3 vector (Ad3-GFP) but not the transduction of an Ad35 vector (Ad35-GFP (that uses CD46 as a receptor). Ad3-GFP (Constructed in this study) and Ad35-GFP (Gao et al., 2003) are wt Ad3- and Ad35-based vectors containing a CMV-GFP expression cassette inserted into the E3 region.

To select an optimal cell line for receptor X identification, we compared Ad3 virus binding to several human and animal cell lines. Ad3 did not bind to rodent cells suggesting that receptor X was not expressed or not accessible to Ad3 in these cells. Of the 10 human cell lines initially tested (HeLa, K562, SKOV3, 293, HT29, SKHep1, Saos, Y79, Ramos), Ad3 binding was absent only on Ramos (human Burkitt's lymphoma) cells.

To identify Ad receptor candidates, HeLa cell membrane proteins were solubilized, separated on polyacrylamide gels, and blotted. Blots were hybridized with viral particles and binding was visualized with virus fiber knob specific antibodies. Specific gel bands were excised and analyzed by tandem mass-spectroscopy (MS/MS). First, we tested whether this assay can detect a known Ad receptor, CD46. When filters were incubated with CD46-targeting Ad5/35++ virions, a single band was found that matched CD46. Incubation of filters with Ad3 virions revealed two bands with molecular weights of 160 kDa and 90 kDa (Figure 1e in study **V**). In addition to these two bands, Ad3 PtDd also reacted with HeLa proteins in the range of 130 kDa. Both 160 and 90 kDa bands were absent in Ramos cells, i.e. cells that do not bind Ad3. The ~130 kDa PtDd-binding band appeared in both HeLa and Ramos cells suggesting that it is not an Ad3 virus receptor. MS/MS-analysis of the 160 kDa band identified 14 peptides matching human desmoglein 2 (DSG2) (Figure 1f in study **V**). IP/Western analyses of HeLa membrane proteins demonstrated that both the 160 and 90 kDa bands were recognized by DSG2-specific antibodies. This is in aggreement with previous Western blot studies showing that the 160 kDa band represents full size DSG2, and that the 90 kDa band is a DSG2 variant that lacks the intracellular domain, the transmembrane domain, and the juxtamembrane extracellular anchor domain (Kowalczyk et al., 1994; Nava et al., 2007).

BIAcore SPR studies with sensors containing immobilized recombinant human DSG2 demonstrated that Ad3, but not Ad2 or Ad5, virions interact with DSG2 (Figure 1g-i in study V). Recombinant PtDd but not BsDd particles bound to DSG2. The K_D of PtDd –DSG2 interaction was 2.5 nM. PtDd binding to immobilized DSG2 was specific as soluble DSG2 competed with it. SPR analysis of binding kinetics also showed that Ad3 fiber knob dissociates faster from DSG2, which suggests the existence of additional DSG2 binding site(s) within the fiber shaft and/or the requirement of fiber multimerization for high affinity binding to DSG2.

Loss- and gain-of-function studies were performed on cell lines to validate DSG2 as a critical receptor for AdB-2/3 binding/infection (Figure 2 and 3 in study **V)**. Recombinant DSG2 protein blocked the binding of Ad3 as well as other AdB2/3 Ads, i.e. Ad7, Ad14, Ad14a, and Ad11 to HeLa cells, but not the binding of Ad5 and Ad35. Ad3-GFP infection was efficiently inhibited by DSG2 protein but not by other structurally related members of the cadherin superfamily (desmoglein 1-DSG1 and desmocollin 1-DSC1) (Getsios et al., 2004). This study also showed that DSG2 protein had no effect on transduction by the CD46-targeting vector (Ad35-GFP). Significant inhibition of Ad3 attachment was observed with mAbs against extracellular domains 3 and 4. Transfection of HeLa cells with a pool of *DSG2*-specific siRNAs resulted in ~7-fold downregulation of surface DSG2 levels. Ad3 attachment was 3 fold lower in *DSG2*-siRNA treated HeLa cells compared to control siRNA-treated cells ($p<0.001$). GFP expression levels after infection with Ad3-GFP were 13.9-fold lower in *DSG2*-siRNA transfected cells than in control siRNA transfected cells. *DSG2*-specific siRNA did not affect transduction with the CAR-targeting vector Ad5-GFP. However, *DSG2*- siRNA transfection also decreased binding and transduction with the CD46-specific vectors Ad35-GFP and Ad5/35-GFP. *DSG2*-siRNA did not decrease CD46 levels in HeLa cells. At this point we cannot explain this phenomenon.

siRNA mediated DSG2 downregulation also decreased viral cytolysis and spread in cells that were infected at 100% confluence at an MOI of one Ad3-GFP pfu per cell (Figure 2f and2g in study **V**).

For gain-of-function studies, we selected a series of cell lines with different DSG2 expression levels and measured Ad3-GFP transduction. All cell lines that lacked DSG2 expression (lymphoma Ramos, Raji, Mino, and HH cells) were refractory to Ad3-GFP transduction but could be transduced by the CD46 targeting Ad5/35-GFP vector (because CD46 is expressed on these cells. DSG2-positive K562 cells, on the other hand, could be efficiently transduced with Ad3-GFP. About 70% of BJAB cells were DSG2 positive and, correspondingly, the percentage of GFP-positive cells reached a plateau at about 50%. To conclusively prove the critical role of DSG2 in Ad3 infection, we ectopically expressed DSG2 via lentivirus vector gene transfer in the histiocytic lymphoma cell line U937, which is refractory to Ad3-GFP transduction. Ectopic DSG2 expression in U937-DSG2 cells conferred efficient Ad3 attachment and transduction, whereas Ad35 attachment and Ad5/35-GFP transduction were unaffected in these cells.

These studies demonstrated that DSG2 is a crucial receptor for AdB-2/3 infection.

5.2 DSG2 localization in human cells (Figure 4 in study **V)**

As expected, we found DSG2 in cell membranes of normal epithelial tissues (foreskin and colon) and epithelial cancers (breast and ovarian cancer). Confocal immunofluorescence microscopy studies of polarized colon cancer T84 and CaCo-2 cells demonstrated colocalization of DSG2 and the intercellular junction protein Claudin 7. In stacked XZ image sections (or XY sections taken at different depth of the cell layer), DSG2 appears at the distal end of intercellular junctions. DSG2 also colocalized with the adherens junction protein E-cadherin in epithelial cells. Fifteen minutes after adding Cy3-labelled Ad3 to polarized cells, viral particles were detectable in association with junction-localized DSG2. Similar results were obtained with normal small airway epithelial cells incubated with PtDd for 15 min as shown by triple labeling of Cy5-PtDd, DSG2, and E-cadherin. PtDd signals were on cell membranes and in the cytoplasm, most likely reflecting internalized particles.

In contrast to polarized epithelial cell lines, in non-polarized cells, such as HeLa cells, intercellular junctions (i.e. membrane-localized Claudin 7 and E-cadherin signals) were absent. DSG2 and Ad3 were found dispersed over the cell surface.

These studies showed that the target for AdB-2/3, DSG2, is localized in epithelial junctions.

5.3 Ad3 interaction with DSG2 triggers EMT

Recently, we found that AdB-2/3 interaction with epithelial ovarian cancer cells triggered EMT. EMT is characterized by increased expression of mesenchymal markers, increased expression of extracellular matrix compounds, decreased expression of epithelial markers, altered location of transcription factors, and activation of kinases (Turley et al., 2008). Here, we attempted to prove that Ad3 interaction with DSG2 triggers EMT-like events. To avoid potential side effects of viral gene expression on cell morphology, the studies utilized ultraviolet light (UV)-inactivated Ad particles and recombinant Ad3 PtDd. Overall, the results with both types of particles were similar. Incubation of epithelial cancer cells with PtDd (Figure 5 in study **V**) or UV-inactivated Ad3 caused remodeling of junctions as reflected by the decrease in of membrane/junction-localized Claudin 7 or E-cadherin signals. Furthermore, after PtDd treatment

we found stronger immunofluorescence signals of the mesenchymal markers Vimentin and Lipocalin 2. To identify intracellular signaling pathways triggered by PtDd interaction with DSG2, we studied mRNA expression profiles. Twelve hours after incubation of polarized BT474 cells with PBS, BsDd, or PtDd, mRNA was analyzed using Affymetrix human ST gene arrays. We found that PtDd treatment resulted in >1.5-fold upregulation of 430 genes and >1.5-fold down-regulation of 352 genes when compared to PBS-treated cells. The list of altered genes was further processed by Pathway-Express software (Khatri et al., 2006). This computation suggested that PtDds mediated marked activation of a number of signaling pathways involved in EMT, including phosphatidylinositol, extracellular signal-regulated kinase 1 and 2(ERK1/2) (also known as mitogen-activated protein kinase (MAPK), Wnt, adherens junctions, focal adhesion, and regulation of actin cytoskeleton signaling pathways.

Western blot analysis using phosphorylation-specific antibodies showed that PtDd, but not BsDd, triggered the activation of PI3K and MAPK/ERK1/2, i.e. key kinases involved in EMT. Activation of these pathways was also triggered by DSG2-specific mAbs (6D8, and to a lesser degree 10D2, and 13B11) but not with mAbs directed against CD46. PtDd activation of pathways was mediated by DSG2, because MAPK/ERK1/2 and PI3K phosphorylation was decreased in cells transfected with *DSG2* siRNA but not in control siRNA treated cells. Finally, PtDd-triggered phosphorylation of kinases was absent when cells were pretreated with the ERK1/2 inhibitor UO126 or the PI3K inhibitor Wortmannin.

Taken together, our data suggest that Ad3 or Ad3PtDd binding to DSG2 triggers EMT in epithelial cells and thus allows for breaching the barrier for infection of epithelial tissues.

5.4 Ad3 and PtDd increase access to receptors that are trapped in intercellular junctions

To test whether Ad3 virion- or Ad3 PtDd-triggered EMT also results in opening of intercellular junctions, we studied barrier properties in monolayer of epithelial cells (Figure 6 in study **V)**. First we measured the flux of 4 kDa FITC-dextran through confluent polarized BT474 cells cultured in transwell chambers. We found that PtDd but not BsDd incubation significantly increased the permeability coefficient compared to PBS. We then tested whether Ad3 or PtDd-triggered EMT and transient junction-opening would increase access to proteins that are normally not accessible due to epithelial cell junctions. An example for such a junction-localized receptor

is CD46, the high-affinity receptor for Ad35 and Ad5/35 (Strauss et al., 2009a). We confirmed that a large number of CD46 molecules localizes to junctions of BT474 cells. PtDd pre-treatment significantly increased the attachment of ^{3}H-Ad35 to BT474 cells when compared to BsDd treatment. An enhancing effect of PtDd on transduction of CD46-targeting Ad vectors was also demonstrated *in vivo* in subcutaneous epithelial tumors. Intravenous injection of PtDd eight hours before application of Ad5/35-bGal increased viral transduction. Beta-galactosidase activity, measured in tumor lysates 3 days after Ad injection, was 2.3(+/-0.2)x10^5 rlu/µg protein, 2.7(+/-0.6)x10^5 rlu/µg, and 38(+/-3.5)x10^5 rlu/µg for mice that were mock-injected, BsDd-coinjected, and PtDd-coinjected, respectively.

In another line of experiments in breast cancer cell cultures, we found that Her2/*neu*, the receptor for the widely used monoclonal antibody Herceptin (trastuzumab) co-stained with the intercellular junction protein Claudin 7. This suggests that not all Her2/*neu* molecules are accessible to Herceptin. Incubation of the Her2/*neu*-positive breast cancer cell line BT474 with PtDd triggered relocalization of Her2/*neu* to the cell surface. To consolidate this observation, we tested whether Ad3 or Ad3PtDd would improve BT474 cell killing by Herceptin. In agreement with earlier studies (Bostrom et al., 2009), Herceptin caused death of approximately 25% of BT474 cells cells. Pre-incubation of BT474 cells with UV-inactivated Ad3 particles or PtDd increased Herceptin cytotoxicity by more than 2-fold. Incubation with UV-inactivated Ad5 particles or BsDd had no effect on Herceptin killing. In addition, Herceptin and PtDd/Herceptin had no cytotoxic effect on the Her2/*neu*-negative breast cancer cell line MDA-MB-231. The enhancing effect of PtDd and Ad3 on Herceptin killing of BT474 cells was mediated by DSG2, as downregulation of DSG2 in BT474 cells by *DSG2* siRNA abolished this effect. We also studied whether inhibition of key pathways involved in EMT affects the enhancing effect of PtDd on Herceptin cytotoxicity. These studies showed that inhibtion of PI3K by Wortmannin, as well as inhibition of MAPK/ERK by UO126 counteracted PtDd enhancement of Herceptin therapy. Importantly, i.v. injection of PtDd (2 mg/kg) into BT474-M1-tumor-bearing mice before Herceptin treatment resulted in elimination of tumors, an outcome that could not be achieved with Herceptin injection alone.

These studies have practical implications for the improvement of mAb therapy of cancer.

6 Multimerization of Ad3 fiber knob domains is required for efficient binding of virus to desmoglein 2 and subsequent opening of epithelial junctions (VI)

The protruding fiber is the moiety within the Ad capsid that mediates a high affinity binding to the primary attachment receptor. For CAR- and CD46-interacting Ads, the C-terminal homo-trimeric knob domain binds with high affinity to the receptor and soluble fiber knobs completely block infection. Studies of Ad5 showed that the main interaction between Ad5 and CAR involves one Ad5 fiber knob monomer and one CAR monomer, implying that one trimeric fiber knob binds to three CAR molecules (Kirby et al., 2000). The K_D of Ad5 fiber knob interaction with CAR is 20-25nM (Lortat-Jacob et al., 2001). Studies of Ad35 (Wang et al., 2007) and Ad11 (Persson et al., 2007) showed that one CD46 molecule binds between two Ad35 or Ad11 knob monomers. This creates a rigid complex between the trimeric knob and three CD46 units. Moreover, CD46 has a bent configuration, that upon interaction with Ad knob, becomes straightened, thereby allowing additional CD46 and knob domains to interact with each other to give a high-affinity interaction (Persson et al., 2007). Surface plasmon resonance (SPR) analyses of soluble CD46 and Ad35 knobs showed a K_D of ~15.35 nM. The specifics of Ad35 and Ad11 interaction with CD46 could also explain why CD46-interacting species B Ads are released more slowly from endosomes upon uptake into cells than Ad5 (Kalin et al., 2010).

In the previous study, we identified desmoglein 2 (DSG2) as the main receptor for a group of species B Ads, including Ad3. Ad3 virus binds to DSG2 with a nanomolar affinity (Tuve et al., 2006). However, in contrast to CAR- and CD46-binding Ads, trimeric Ad3 fiber knob was unable to completely block Ad3 virus binding, even when very high fiber knob concentrations were used, indicating that other or additional capsid moieties were involved in Ad3 binding (Tuve et al., 2008). Efficient blocking of Ad3 infection was achieved with recombinant Ad3 penton-dodecahedral particles (PtDds), consisting of 12 Ad3 fibers linked to penton bases (Norrby et al., 1967). Ad3 fiber and penton must be physically linked, because pre-incubation of cells with Ad3 fiber knobs mixed with penton bases did not block Ad3 binding to the degree seen with PtDds (Wang et al., 2011). These findings suggest that DSG2 interacting domain(s) within Ad3 are formed by the fiber or fiber/penton only in the spatial constellation that is present in viral particles, i.e. Ad3 virions or PtDds. SPR studies with recombinant PtDds showed a K_D of 2.5 nM. These studies also demonstrated that Ad3 fiber knob dissociated faster from DSG2 than PtDds do.

This again indicates that high affinity binding of Ad3 requires additional DSG2 binding site(s) within the fiber shaft, fiber multimerization, and/or a specific spatial constrain of fiber knobs.

6.1 Chimeric Ad5 vectors containing Ad3 fibers use DSG2 as a receptor

Our previous studies indicated that DSG2 interacting domain(s) within Ad3 are formed by the fiber or fiber/penton only in the spatial constellation that is present in viral particles, i.e. Ad3 virions or PtDds. To assess a potential role of Ad3 penton (which is present in PtDds) in binding to DSG2, we generated an Ad vector that contained Ad3 fibers (Ad5/3S-GFP), but had all other capsid proteins (including the penton) derived from Ad5. To evaluate whether the Ad3 fiber shaft had a cucial role in Ad3-DSG2 interaction, e.g. contained DSG2 additional binding sites, we also generated a chimeric Ad5/3 vector that had the Ad3 shaft substituted by the Ad5 shaft (Ad5/3L-GFP). Notably, while the Ad3 fiber shaft contains 6 shaft repeat motifs, the Ad5 shaft is longer and contains 22 shaft motifs. For comparison, we also used an Ad3-GFP vector constructed in previous study. We analyzed whether Ad5/3S-GFP and Ad5/3L-GFP vectors use DSG2 for infection (Figure 1 in study **VI**). Attachment of ^{3}H-labeled Ad vectors to HeLa cells was blocked by recombinant DSG2 protein to the same degree for Ad3-GFP, Ad5/3S-GFP, and Ad3/5L-GFP. As expected, recombinant DSG2 also blocked transduction of all three vectors as measured based on GFP intentsity 18 hours after infection of HeLa cells. PtDd, used as a competor for DSG2 interaction domains within the Ad virions, blocked Ad3-GFP, Ad5/3S-GFP, and Ad3/5L-GFP transduction to similar levels. To prove the crucial role of DSG2 in the infection of Ad3 and Ad5/3 vectors, we transfected HeLa cells with siRNA specific to DSG2 mRNA or control siRNA. DSG2 mRNA knockdown significantly decreased Ad3-GFP, Ad5/3S-GFP, and Ad3/5L-GFP transduction ($p<0.001$). Taken together, these studies show *i)* Ad5/3 vectors use DSG2 as a receptor. *ii)* the DSG2 interacting domains of Ad3 are located within the fiber. It appears that the Ad pentons (within PtDds or Ad5 and Ad3 virions) merely provides a scaffold for the correct spatial constellation of Ad3 fiber knobs for interaction with DSG2.

6.2 Crosslinking of Ad3 fiber knobs is required for efficient binding to DSG2

We then focused our attention on the Ad3 fiber (Figure 2 in study **VI**). We produced in *E. coli* a series of recombinant Ad3 fiber knob proteins, containing the fiber knob and increasing numbers of Ad3 shaft repeats (from one to six repeats). Western blot analyses using DSG2 or

antiAd3 fiber knob antibodies showed that all recombinant fiber knobs formed trimers. As observed previously (Wang et al., 2011), the Ad3 fiber knob plus one shaft domain did not bind DSG2 in Western blot analyses, indicating a potential steric influence of the shaft motif on the Ad3 knob conformation. However, when used in competition studies, all recombinant fiber knob proteins inhibited Ad3-GFP transduction significantly less than PtDds. We then attempted to test whether Ad3 fiber knob dimerization would increase DSG2 binding. Because all recombinant fiber knobs contained an N-terminal His tag,we mixed Ad3 fiber knobs with antibodies against the His tag to achieve their crosslinking (Figure 2F-H in study **VI**). When anti-His antibodies crosslinked fiber knobs were used as competitors, a significant inhibition of Ad3-GFP transduction (compared to fiber knobs mixed with control IgG) was observed, suggesting that dimers of Ad3 fiber knobs are required for DSG2 binding. This appeared to be a new Ad binding strategy unique to Ad3, because anti-His antibody crosslinking of the Ad35 fiber knobs had no effect on infection by the CD46-interacting vector Ad35-GFP.

6.3 Ad3 fiber knob dimers block Ad3 infection

Crosslinking with antibodies enhanced the blocking effect of Ad3 fiber knobs containing fewer shaft motifs than the wt Ad3 fiber knob. For a potential biotechnological application of Ad3 fiber knobs as junction openers, we focused our further studies on fiber knob variants with the minimum number of shaft motifs, i.e. S-5,6. Based on the finding that fiber knob cross-linking increased binding to DSG2, we generated dimers of S2/Kn by incorporating dimerization domains. To avoid the spontaneous fiber knob dimerization and potential formation of inclusion bodies during production in *E.coli*, we utilized a hetero-dimeric system consisting of E-coil and K-coil peptides, which interact with each other with high affinity (Litowski and Hodges, 2002). Two fiber knob variants containing five repeats of EVSALEK (K-coil) and KVSALKE (E-coil) respectively, a G/S rich-flexibility domain followed by two shaft motifs and the homotrimeric fiber knob domain were generated (Figure 3 in study **VI**). Ad3-K/S2/Kn and Ad3-E/S2/Kn were produced separately in *E.coli* and purified by affinity chromatography. For dimerization, both purified proteins were mixed at a 1:1 concentration ratio. The mixture of Ad3-K/S2/Kn and Ad3-E/S2/Kn blocked Ad3 infection as efficiently as PtDds. Interestingly, Ad3-K/S2/Kn alone had the same competing strength as the mixture of both peptides, while Ad3-E/S2/Kn alone only inefficiently blocked infection. This suggests that Ad3-K/S2/Kn is able to homodimerize, while

Ad3-E/S2/Kn is not. In support of this, we found that further crosslinking with anti-His antibodies increased the blocking effect of Ad3-E/S2/Kn ($p<0.05$) but not that of Ad3-K/S2/Kn.

6.4 Binding of a minimal dimeric Ad3 fiber knob protein to DSG2

We then attempted to produce the smallest Ad3 fiber knob dimer possible, containing the K-coil or E-coil dimerization domain, only one shaft motif, and the homotrimeric Ad3 fiber knob (Ad3-K/S/Kn and Ad3-E/S/Kn) (Figure 4 in study **VI**). Because of their smaller size, such proteins have potential advantages in egress from blood vessels, tissue penetration and, theoretically, also contain fewer immunogenic epitopes. Ad3-K/S/Kn and Ad3-E/S/Kn were produced in *E.coli* and purified by affinity chromatography. Analysis by polyacrylamid gel electrophoresis showed that the vast majority of Ad3-K/S/Kn and Ad3-E/S/Kn were present as trimers (~65-70kDa). Ad3-K/S/Kn alone and in combination with Ad3-E/S/Kn were analyzed by negative stain electron microscopy to assess their assembly status. Dimers of fiber knobs and aggregates thereof were found for both Ad3-K/S/Kn and Ad3-K/S/Kn+Ad3-E/S/Kn, but larger aggregates were less abundant in Ad3-K/S/Kn preparations. Both Ad3-K/S/Kn and Ad3-K/S/Kn+Ad3-E/S/Kn blocked Ad3 attachment to HeLa cells at a level comparable to PtDds. Pre-incubation of HeLa cells with Ad3-K/S/Kn and Ad3-K/S/Kn+Ad3-E/S/Kn did not affect Ad5 attachment. As expected, Ad3-K/S/Kn and Ad3-K/S/Kn+Ad3-E/S/Kn also efficiently inhibited Ad3 infection. A side-by-side comparison of the fiber knobs with two and one shaft motif did not reveal significant differences in their ability to block Ad3 infection.

6.5 SPR analysis of dimeric Ad3 fiber knob binding to DSG2

To study the interaction of Ad3-K/S/Kn and Ad3-K/S/Kn+Ad3-E/S/Kn with DSG2 in more detail, we performed surface plasmon resonance (SPR) studies (Figure 5 in study **VI**). We initially designed binding experiments, in which DSG2 molecules were allowed to bind to immobilized fiber knobs. For immobilization, fiber knobs were biotinylated and linked via streptavidin to sensorchips. Kinetics analyses showed that both Ad3-K/S/Kn and Ad3-K/S/Kn+Ad3-E/S/Kn similarly recognized DSG2 with a low dissociation at the end of injection. Clearly, the binding of soluble DSG2 to fibers only poorly mimics the physiological interaction between a cell surface and the virus. We therefore immobilized the DSG2 receptor at the sensorchip surface and injected Ad3-K/S/Kn and Ad3-K/S/Kn+Ad3-E/S/Kn, and, for comparison,

PtDd and (monomeric) Ad3 fiber knob at concentrations that give a similar SPR response. The outcome of these studies should depend on the valence of the fiber knobs. i.e. trimeric for Ad3 fiber knob (monomer), 2x trimeric for Ad3-K/S/Kn and Ad3-K/S/Kn+Ad3-E/S/Kn, 12x trimeric for PtDd). It is further complicated by the fact that within PtDd not all fibers can simultaneously interact with DSG2. While the association of the fiber knob dimers was similar, there were clear differences in the dissociation behavior. Ad3 fiber knob (monomer) dissociated faster than the other three ligands. Almost no dissociation was seen for PtDd and Ad3-K/S/Kn+Ad3-E/S/Kn. Ad3-K/S/Kn dissociation was between that of Ad3 fiber knob (monomer) and Ad3-K/S/Kn+Ad3-E/S/Kn. Although complex, these data clearly show that dimeric Ad3-K/S/Kn and Ad3-K/S/Kn+Ad3-E/S/Kn dissociate slower from DSG2 than does Ad3 fiber knob (monomer). This can be explained by an avidity mechanism, implying that Ad3-K/S/Kn and Ad3-K/S/Kn+Ad3-E/S/Kn bind to several DSG2 molecules; a mechanism that allows achieving an overall low dissociation rate and highly stable attachment. Notably, although it is possible that all dimers in Ad3-K/S/Kn+Ad3-E/S/Kn are formed by Ad3-K/S/Kn, differences in dissociation rates argue against it. Further studies are required to prove this in detail.

Interaction of Ad3 with several DSG2 molecules is supported by immunofluorescence analyses of epithelial cells. These studies, using Cy3-labelled Ad3 virions, suggest that one virion clusters several DSG2 proteins around itself. As outlined later, we hypothesize that this specific clustering of receptors has functional consequences with regards to triggering intracellular signaling and opening of epithelial junctions. Notably, previously we showed that PtDd binding to DSG2 triggers an epithelial-to-mesenchymal transition (EMT) in epithelial cells resulting in transient opening of intercellular junctions (Wang et al., 2011).

6.6 Multimeric DSG2 ligands (Ad3 virions, PtDds, Ad3-K/S/Kn) trigger opening of epithelial junctions

Epithelial cells maintain several intercellular junctions (tight junctions, adherens junctions, gap junctions, and desmosomes), a feature which is often conserved in epithelial cancers *in situ* and in cancer cell lines (Turley et al., 2008). Figure 6A in study **VI** shows confocal immunofluorescence microscopy images of polarized colon carcinoma T84 cells. Shown are the cells from the lateral side, i.e. stacked XZ-layers. In the upper panel, intercellular junctions are visible as long vertical streaks marked by the adhesion junction protein claudin 7. DSG2 (green)

is localized at the apical end of claudin 7 signals. The tight junction protein ZO-1 can be found further apical of DSG2 (lower panel). The latter is also visualized in XY images, which show a "chicken-wire" network of tight junctions marked by ZO-1 at the apical cell surface, whereas a section taken 1um deeper shows DSG2 staining (Figure 6B in study **VI**). Importantly, exposure of T84 cells to Ad3-K/S/Kn triggered partial dissolution of epithelial junctions, reflected in decreased staining for DSG2 and ZO-1, in comparison to untreated cells .

Opening of epithelial junctions be Ad3-K/S/Kn was further confirmed by electron microscopy (EM) studies. EM images of untreated epithelial cells show intact tight and desmosomal junctions as judged by the exclusion of the apically applied dye ruthenium red from basolateral space (Figure 6D in study **VI**). The dye appears as an electron-dense line along the cell membrane surface. Incubation of epithelial cells with Ad3-K/S/Kn resulted in leakage of ruthenium red deep into the lateral space within 1 hour of Ad3-K/S/Kn addition. Disassembly of desmosomes in Ad3-K/S/Kn treated cells is clearly visible in Figure 6E. In addition to Ad3-K/S/Kn, opening of epithelial junctions was observed in confocal immunofluorescence and EM studies also with Ad3 virions, PtDds, and Ad3-K/S/Kn+Ad3-E/S/Kn. Exposure of cells to Ad3 fiber knob (monomer) or Ad3-E/S/Kn, i.e. DSG2 ligands that are unable to multimerize, had no effect on epithelial junctions. These studies indicate that opening of epithelial junctions requires dimers or multimers of Ad3 fiber knobs.

In addition to leakage studies with ruthenium red, we used three functional assays to demonstrate opening of epithelial junctions by Ad3-K/S/Kn. *i)* Exposure of polarized epithelial cells to Ad3-K/S/Kn increased the transepithelial permeability within 30 minutes, as shown by ^{14}C-PEG-4000 transflux studies (Figure 7A in study **VI**). *ii)* Previous studies showed that in polarized breast cancer BT474-M1 cells, Her2/*neu*, the target for Herceptin/trastuzumab, is trapped in epithelial junctions, and that incubation of BT474-M1 cells with Ad3 PtDds increases access to Her2/*neu* and increases trastuzumab killing of cancer cells (Wang et al., 2011). Here we used this assay to study the effect of additional DSG2 ligands on trastuzumab cytotoxicity (Figure 7B in study **VI**).We found that Ad3-K/S/Kn significantly increased killing of BT474-M1 cells by trastuzumab. In contrast, DSG2 ligands that are not able to dimerize, i.e. Ad3-E/S/Kn and a series of anti-DSG2 antibodies, had significant effect on trastuzumab killing. *iii)* CAR, the receptor for Ad5, is localized in tight junctions of polarized T84 epithelial cells. (Coyne and Bergelson,

2005). This is shown by confocal immunofluorescence microscopy in T84 cells (Figure 7C and D in study **VI**). Incubation of these cells with Ad3-K/S/Kn greatly increased CAR staining, which now appeared along the lateral membranes and at the cells surface. We speculated that this is the result of disassembly of tight junctions and better accessibility of CAR to anti-CAR antibodies that were applied to the apical side of T84 cells. Another potential read-out for disruption of tight junctions and CAR accessibility is transduction with a CAR-targeting Ad vectors. Infection of polarized T84 cells with Ad5-GFP at an MOI of 250pfu/cell resulted in transduction of 8(+/-2)% of cells (based on GFP-positive cells counted 20 hours after infection) (Figure 7E in study **VI**). Ad5-GFP infection in the presence of Ad3-K/S/Kn yielded 38(+/-9)% of GFP positive cells. Ad3-GFP in the presence of dilution buffer or Ad3-K/S/Kn transduced 17(+/-6)% or 68(+/-17)% of T84 cells, respectively. This is in agreement with an earlier study, showing that Ad3 infects polarized epithelial cells more efficiently than Ad5 (Strauss et al., 2009b). This is most likely due to its ability to bind to DSG2 and trigger junction opening. Ad3-K/S/Kn increased Ad3-GFP transduction. We speculate that the relatively small size of the Ad3-K/S/Kn protein and its high concentration initially help reach more DSG2 receptors than can be targeted with Ad3 virions to open the tight junctions.

Overall, our functional studies show that Ad3-K/S/Kn can trigger opening of epithelial junctions, while ligands that are unable to multimerize have no effect on junctions. The small recombinant protein Ad3-K/S/Kn has potential as a co-therapeutic for mAbs.

SUMMARY AND CONCLUSIONS

Species B Ads are important human pathogens and have great potential as *in vitro* and *in vivo* gene transfer vectors. The goal of this thesis was to better understand virological and translational aspects of species B Ads. As outlined below, the specific aims outlined on page 38 have been accomplished.

Aim 1. Identify the CD46 binding sites within the Ad35 fiber knob. Studies with random mutant Ad35 fiber knob library identified four aa residues (Phe242, Arg279, Ser282, Glu302) that abolished Ad35 knob binding to CD46 without affecting knob trimerization. Crystal structure analysis revealed two main contact areas on the opposite sites of the fiber knob. This implies that one CD46 unit binds between two Ad35 knob monomers and indicates that CD46-interacting species B Ads developed a different strategy to bind to their receptor than Ads that interact with CAR. The specific configuration of Ad35 binding to CD46 could also explain why CD46 interacting species B Ads are released more slowly from endosomes upon uptake into cells than Ad5 (Shayakhmetov et al., 2003). The rigid binding of Ad35 fiber knob to CD46 is also important for our approach to sensitize tumor cells to mAb therapy (see Aim 4).

Aim 2. Study the in vitro and in vivo properties of Ad vectors with increased affinity to CD46. Gene transfer vectors containing Ad35 fibers have shown promise for cancer and stem cell gene therapy. We attempted to improve the *in vitro* and *in vivo* infection properties of these vectors by increasing their affinity to the Ad35 fiber receptor CD46. The rationale for such vectors comes from studies with phage antibody expression libraries and more recently from studies with aptamers, protein-binding oligonucleotides. The goal of phage and aptamer library screening is to identify variants with the highest affinity, because in *in vitro* and *in vivo* studies with single-chain variable fragment fragments and aptamers, higher affinity usually directly translates into more-efficient binding to receptor-positive cells. We constructed Ad vectors containing either the wt Ad35 fiber knob (Ad5/35) or Ad35 knob mutants with 4-fold- and 60-fold-higher affinity to CD46 (Ad5/35+ and Ad5/35++, respectively). In *in vitro* studies with cell lines, the higher affinities of Ad5/35+ and Ad5/35++ to CD46 did not translate into correspondingly higher transduction efficiencies, regardless of the CD46 receptor density present on cells. However, *in vivo*, in a mouse model with preestablished $CD46^{high}$ liver metastases, i.v. injection of Ad5/35++ resulted in more-efficient tumor cell transduction. We conclude that

Ad5/35 vectors with increased affinity to CD46 have an advantage in competing with non-CD46-mediated sequestration of vector particles after i.v. injection.

Aim 3. Study the receptor usage of a newly emergent Ad14a. A new genomic variant of Ad 14, designated Ad14a, has been recently associated with several outbreaks with fatal consequences. Compared to the Ad14 reference strain (de Wit), this new virus had a deletion of two aa residues in the fiber protein knob. We tested whether this mutation changed receptor usage of Ad14a compared to Ad14-de Wit. Competition studies with radio-labeled viruses revealed that both Ad14-de Wit and Ad14a used the same receptor X. Taken together, our data indicate that the 251Lys/252Glu deletion in the Ad14a fiber and the 366Asp→Asn mutation in the Ad14a penton did not significantly influence the attachment and internalization of this virus. Most likely, differences in post-internalization steps or in the ability to elude the host immune response account for the higher virulence of Ad14a compared to Ad14-de Wit. The identification of receptor X (see Aim 5) has great importance for understanding the pathogenesis of Ad14a infections and the development of anti-viral therapeutics.

Aim 4. Study whether a high affinity Ad35 fiber knob can enhance the anticancer efficacy of monoclonal antibodies. mAbs have emerged as a class of novel oncology therapeutics. Despite their commercial successes, each of these mAbs is only effective in a minority of patients. It is now recognized that one of the major impediments to their therapeutic efficacy is the overexpression of complement inhibitory proteins, e.g. CD46, on the cell surface of solid tumors and hematologic malignancies. To address the problem we capitalized on our earlier finding that Ad35 uses CD46 as a high-affinity attachment receptor. From an *E.coli* expression library of Ad35 fiber knob mutants, we selected a variant (Ad35K++) that had a higher affinity to CD46 than the natural Ad35 fiber knob. Ad35K++ is produced as a soluble protein in *E.coli* and is purified by affinity chromatography. Ad35K++ binding results in the transient removal of CD46 from the surface of lymphoma, leukemia, and other tumor cells, including breast and colon cancer cells, for approximately 72 hours post treatment. During this time period, tumor cells that are normally resistant to mAb therapy become susceptible and can be killed by complement dependent cytotoxicity. In *in vitro* studies, we demonstrated an enhancing effect of Ad35K++ for the following mAbs: rituximab/Rituxan (used for the treatment of B-cell non-Hodgkin's lymphoma), alemtuzumab/Campath (for chronic lymphocytic leukemia), trastuzumab/Herceptin

(for breast cancer), and certiximab/Erbitux for colon cancer) and ofatumumab/Arzerra (for lymphoma and CLL). Thus far, *in vivo* studies have been completed for the combination of Ad35K++ and the CD20-targeting mAb rituximab. In these studies, we demonstrated in two murine lymphoma models that rituximab plus Ad35K++ achieved superior anti-tumor effects and animal survival when compared to animals treated with rituximab alone. For example, sixty percent of mice injected with human lymphoma Raji cells were cured with Ad35K++ / rituximab treatment, while all mice treated with only rituximab died within 19 days after Raji cell transplantation. Based on these efficacy data we are currently planning to gather sufficient safety data in mice and non-human primates to submit an IND application for a phase I clinical trial for a combination therapy of Ad35K++ and rituximab in non-Hodgkin's lymphoma patients.

Aim 5. Identify the receptor for Ad3, Ad7, Ad11, and Ad14. We have identified desmoglein 2 (DSG2) - a calcium-binding transmembrane glycoprotein and component of the epithelial cell-cell adhesion structure -as the primary high-affinity receptor used by Ad3, Ad7, Ad11, and Ad14. Loss- and gain-of-function studies confirmed DSG-2 to be crucial for the binding, infection and spread of these serotypes. Further studies demonstrated that chimeric Ad5 vectors with Ad3 fibers also use DSG2 as a receptor. Murine DSG2 cannot be used as an AdB-2/3 receptor. Based on this finding we are currently generating mice that contain the human DSG2 locus and express DSG2 in a pattern and at levels similar to humans.

Aim 6. Study structural details of Ad3 virus interaction with DSG2. While Ad binding CAR and CD46 involves only a high affinity interaction between the fiber knob domain and the cellular receptor, we found that binding of Ad3 to DSG2 requires multimerization of the fiber knob domain. We therefore designed two recombinant Ad3 fiber knob domains containing dimerization domains. Both proteins can be can be produced in *E.coli* and purified by affinity chromatography. Upon mixing they dimerize (Ad3K-K dimer). Ad3K-K efficiently and specifically blocked Ad3 infection. Ad3K-K is a minimal Ad3-derived DSG2 ligand formed by two fiber knob domains. This protein, with a molecular weight of approximately 50 kDa, is produced in *E. coli* and can be easily purified. Ongoing crystal structure analyses are aimed towards the identification of aa residues that are involved in the interaction of Ad3K-K with DSG2. With regards to DSG2, we found that Ad3 binding involved the third and fourth extracellular domain of DSG2. Ad3K-K is used as a co-therapeutic in Aim 7.

Aim 7. Study the functional consequences of Ad3-DSG2 interaction. We also studied the consequences of adenoviral-DSG-2 interaction, following exposure to Ad3 virions or Ad3K-K, using epithelial cancer cell lines. Pathways involved in epithelial-to-mesenchymal transition were found to be activated, leading to transient intercellular junction opening. This finding has implications for Ad spread in epithelial tissues and for cancer therapy as intercellular junctions represent physical obstacles for access and intratumoral dissemination of anti-cancer therapeutics. We demonstrated that pre-incubation of cancer cell lines with Ad3K-K increased the cytotoxicity of trastuzumab and cetuximab - monoclonal antibodies which bind to the Her2/neu receptor and EGFR respectively. *In vivo*, in mice carrying Her2/neu-positive breast cancer xenografts, pre-injection of Ad3K-K significantly increased the therapeutic efficacy of trastuzumab.

In summary, these studies provide a basis for a better understanding of species B virus infection and pathology. The identification of DSG2 as a receptor has implication for the field of cancer virotherapy because Ad3-based vectors and Ad3-fiber containing Ad5 vectors are being used clinically. Finally the identification of two small species B Ad-derived proteins (Ad35K++ and Ad3K-K) is of importance for the improvement of cancer therapy with mAbs and our current efforts are focused on the clinical testing of these proteins.

ACKNOWLEDGEMENTS

This thesis would not be possible without the support of many to whom I am immensely grateful. I am deeply grateful to Prof. Akseli Hemminki for being my advisor on behalf of the University of Helsinki. I would like to thank Prof. Andre Lieber for supporting my work in his Lab at the University of Washington, for his guidance and wisdom, and for teaching me skills that apply far beyond the work in this thesis. I would also like to thank Dr.Lotta Kangasniemi for her mentoring.

I would like to acknowledge the whole, former and present colleagues from the Lieber Lab. Specifically, Dr. Dmitry Shayakhmetov, Dr. Daniel Stone, Dr. Zongyi Li, Dr. Sebastian Tuve and Dr. Robert Strauss.

Finally, I express my deepest gratitude to my family for their love and support.

REFERENCES

Abbink, P., Lemckert, A.A., Ewald, B.A., Lynch, D.M., Denholtz, M., Smits, S., Holterman, L., Damen, I., Vogels, R., Thorner, A.R., *et al.* (2007). Comparative seroprevalence and immunogenicity of six rare serotype recombinant adenovirus vaccine vectors from subgroups B and D. J Virol *81*, 4654-4663.

Abbod, M.F., Hamdy, F.C., Linkens, D.A., and Catto, J.W. (2009). Predictive modeling in cancer: where systems biology meets the stock market. Expert Rev Anticancer Ther *9*, 867-870.

Abrahamsen, K., Kong, H.L., Mastrangeli, A., Brough, D., Lizonova, A., Crystal, R.G., and Falck-Pedersen, E. (1997). Construction of an adenovirus type 7a E1A- vector. J Virol *71*, 8946-8951.

Adams, G.P., and Weiner, L.M. (2005). Monoclonal antibody therapy of cancer. Nat Biotechnol *23*, 1147-1157.

Alba, R., Bradshaw, A.C., Parker, A.L., Bhella, D., Waddington, S.N., Nicklin, S.A., van Rooijen, N., Custers, J., Goudsmit, J., Barouch, D.H., *et al.* (2009). Identification of coagulation factor (F)X binding sites on the adenovirus serotype 5 hexon: effect of mutagenesis on FX interactions and gene transfer. Blood 114, 965-971.

Anderson, B.D., Nakamura, T., Russell, S.J., and Peng, K.W. (2004). High CD46 receptor density determines preferential killing of tumor cells by oncolytic measles virus. Cancer Res *64*, 4919-4926.

Arthur, J.F., Butterfield, L.H., Roth, M.D., Bui, L.A., Kiertscher, S.M., Lau, R., Dubinett, S., Glaspy, J., McBride, W.H., and Economou, J.S. (1997). A comparison of gene transfer methods in human dendritic cells. Cancer Gene Ther *4*, 17-25.

Balamotis, M.A., Huang, K., and Mitani, K. (2004). Efficient delivery and stable gene expression in a hematopoietic cell line using a chimeric serotype 35 fiber pseudotyped helper-dependent adenoviral vector. Virology *324*, 229-237.

Barouch, D.H., Pau, M.G., Custers, J.H., Koudstaal, W., Kostense, S., Havenga, M.J., Truitt, D.M., Sumida, S.M., Kishko, M.G., Arthur, J.C., *et al.* (2004). Immunogenicity of recombinant adenovirus serotype 35 vaccine in the presence of pre-existing anti-Ad5 immunity. J Immunol *172*, 6290-6297.

Belin, M.T., and Boulanger, P. (1987). Processing of vimentin occurs during the early stages of adenovirus infection. J Virol *61*, 2559-2566.

Bellosillo, B., Villamor, N., Lopez-Guillermo, A., Marce, S., Esteve, J., Campo, E., Colomer, D., and Montserrat, E. (2001). Complement-mediated cell death induced by rituximab in B-cell lymphoproliferative disorders is mediated *in vitro* by a caspase-independent mechanism involving the generation of reactive oxygen species. Blood *98*, 2771-2777.

Belousova, N., Mikheeva, G., Gelovani, J., and Krasnykh, V. (2008). Modification of adenovirus capsid with a designed protein ligand yields a gene vector targeted to a major molecular marker of cancer. Journal of virology *82*, 630-637.

Bergelson, J.M., Cunningham, J.A., Droguett, G., Kurt-Jones, E.A., Krithivas, A., Hong, J.S., Horwitz, M.S., Crowell, R.L., and Finberg, R.W. (1997a). Isolation of a common receptor for Coxsackie B viruses and adenoviruses 2 and 5. Science *275*, 1320-1323.

Bergelson, J.M., Cunningham, J.A., Droguett, G., Kurt-Jones, E.A., Krithivas, A., Hong, J.S., Horwitz, M.S., Crowell, R.L., and Finberg, R.W. (1997b). Isolation of a common receptor for Coxsackie B viruses and adenoviruses 2 and 5. Science *275*, 1320-1323.

Beyer, I., Li, Z., Persson, J., Liu, Y., van Rensburg, R., Yumul, R., Zhang, X.B., Hung, M.C., and Lieber, A. (2011). Controlled Extracellular Matrix Degradation in Breast Cancer Tumors Improves Therapy by Trastuzumab. Mol Ther 19, 479-489.

Biedermann, K., Vogelsang, H., Becker, I., Plaschke, S., Siewert, J.R., Hofler, H., and Keller, G. (2005). Desmoglein 2 is expressed abnormally rather than mutated in familial and sporadic gastric cancer. J Pathol *207*, 199-206.

Bollard, C.M., Straathof, K.C., Huls, M.H., Leen, A., Lacuesta, K., Davis, A., Gottschalk, S., Brenner, M.K., Heslop, H.E., and Rooney, C.M. (2004). The generation and characterization of LMP2-specific CTLs for use as adoptive transfer from patients with relapsed EBV-positive Hodgkin disease. J Immunother *27*, 317-327.

Bostrom, J., Yu, S.F., Kan, D., Appleton, B.A., Lee, C.V., Billeci, K., Man, W., Peale, F., Ross, S., Wiesmann, C., *et al.* (2009). Variants of the antibody herceptin that interact with HER2 and VEGF at the antigen binding site. Science *323*, 1610-1614.

Cadwell, R.C., and Joyce, G.F. (1992). Randomization of genes by PCR mutagenesis. PCR Methods Appl *2*, 28-33.

Cadwell, R.C., and Joyce, G.F. (1994). Mutagenic PCR. PCR Methods Appl *3*, S136-140.

Campos, S.K., and Barry, M.A. (2007). Current advances and future challenges in Adenoviral vector biology and targeting. Curr Gene Ther *7*, 189-204.

Campos, S.K., Parrott, M.B., and Barry, M.A. (2004). Avidin-based targeting and purification of a protein IX-modified, metabolically biotinylated adenoviral vector. Mol Ther *9*, 942-954.

Chen, P., Tian, J., Kovesdi, I., and Bruder, J.T. (1998). Interaction of the adenovirus 14.7-kDa protein with FLICE inhibits Fas ligand-induced apoptosis. J Biol Chem *273*, 5815-5820.

Chen, P.H., Ornelles, D.A., and Shenk, T. (1993). The adenovirus L3 23-kilodalton proteinase cleaves the amino-terminal head domain from cytokeratin 18 and disrupts the cytokeratin network of HeLa cells. J Virol *67*, 3507-3514.

Cho, S.W., Oglesby, T.J., Hsi, B.L., Adams, E.M., and Atkinson, J.P. (1991). Characterization of three monoclonal antibodies to membrane co-factor protein (MCP) of the complement system and quantification of MCP by radioassay. Clin Exp Immunol *83*, 257-261.

Christiansen, J., and Rajasekaran, A.K. (2004). Biological impediments to monoclonal antibody-based cancer immunotherapy. Mol Cancer Ther *3*, 1493-1501.

Christiansen, J.J., and Rajasekaran, A.K. (2006). Reassessing epithelial to mesenchymal transition as a prerequisite for carcinoma invasion and metastasis. Cancer Res *66*, 8319-8326.

Cohen, C.J., Shieh, J.T., Pickles, R.J., Okegawa, T., Hsieh, J.T., and Bergelson, J.M. (2001). The coxsackievirus and adenovirus receptor is a transmembrane component of the tight junction. Proc Natl Acad Sci U S A *98*, 15191-15196.

Combredet, C., Labrousse, V., Mollet, L., Lorin, C., Delebecque, F., Hurtrel, B., McClure, H., Feinberg, M.B., Brahic, M., and Tangy, F. (2003). A molecularly cloned Schwarz strain of measles virus vaccine induces strong immune responses in macaques and transgenic mice. J Virol *77*, 11546-11554.

Coyne, C.B., and Bergelson, J.M. (2005). CAR: a virus receptor within the tight junction. Adv Drug Deliv Rev *57*, 869-882.

D'Ambrosio, E., Del Grosso, N., Chicca, A., and Midulla, M. (1982). Neutralizing antibodies against 33 human adenoviruses in normal children in Rome. J Hyg (Lond) *89*, 155-161.

de Jong, J.C., Osterhaus, A.D., Jones, M.S., and Harrach, B. (2008). Human adenovirus type 52: a type 41 in disguise? J Virol *82*, 3809; author reply 3809-3810.

Deckert, M., Kubar, J., and Bernard, A. (1992). CD58 and CD59 molecules exhibit potentializing effects in T cell adhesion and activation. J Immunol *148*, 672-677.

Di Gaetano, N., Cittera, E., Nota, R., Vecchi, A., Grieco, V., Scanziani, E., Botto, M., Introna, M., and Golay, J. (2003). Complement activation determines the therapeutic activity of rituximab *in vivo*. J Immunol *171*, 1581-1587.

Di Guilmi, A.M., Barge, A., Kitts, P., Gout, E., and Chroboczek, J. (1995). Human adenovirus serotype 3 (Ad3) and the Ad3 fiber protein bind to a 130-kDa membrane protein on HeLa cells. Virus Res *38*, 71-81.

DiPaolo, N., Ni, S., Gaggar, A., Strauss, R., Tuve, S., Li, Z.Y., Stone, D., Shayakhmetov, D., Kiviat, N., Toure, P., *et al.* (2006). Evaluation of adenovirus vectors containing serotype 35 fibers for vaccination. Mol Ther *13*, 756-765.

Dorig, R.E., Marcil, A., Chopra, A., and Richardson, C.D. (1993). The human CD46 molecule is a receptor for measles virus (Edmonston strain). Cell *75*, 295-305.

Duraiswamy, J., Bharadwaj, M., Tellam, J., Connolly, G., Cooper, L., Moss, D., Thomson, S., Yotnda, P., and Khanna, R. (2004). Induction of therapeutic T-cell responses to subdominant tumor-associated viral oncogene after immunization with replication-incompetent polyepitope adenovirus vaccine. Cancer Res *64*, 1483-1489.

Durmort, C., Stehlin, C., Schoehn, G., Mitraki, A., Drouet, E., Cusack, S., and Burmeister, W.P. (2001). Structure of the fiber head of Ad3, a non-CAR-binding serotype of adenovirus. Virology *285*, 302-312.

Escutenaire, S., Cerullo, V., Diaconu, I., Ahtiainen, L., Hannuksela, P., Oksanen, M., Haavisto, E., Karioja-Kallio, A., Holm, S.L., Kangasniemi, L., *et al.* (2011). *In vivo* and *in vitro* distribution of type 5 and fiber-modified oncolytic adenoviruses in human blood compartments. Ann Med *43*, 151-163.

Fender, P., Boussaid, A., Mezin, P., and Chroboczek, J. (2005). Synthesis, cellular localization, and quantification of penton-dodecahedron in serotype 3 adenovirus-infected cells. Virology *340*, 167-173.

Fender, P., Ruigrok, R.W., Gout, E., Buffet, S., and Chroboczek, J. (1997). Adenovirus dodecahedron, a new vector for human gene transfer. Nat Biotechnol *15*, 52-56.

Fessler, S.P., Wotkowicz, M.T., Mahanta, S.K., and Bamdad, C. (2009). MUC1* is a determinant of trastuzumab (Herceptin) resistance in breast cancer cells. Breast Cancer Res Treat *118*, 113-124.

Fishelson, Z., Donin, N., Zell, S., Schultz, S., and Kirschfink, M. (2003). Obstacles to cancer immunotherapy: expression of membrane complement regulatory proteins (mCRPs) in tumors. Mol Immunol *40*, 109-123.

Fleischli, C., Sirena, D., Lesage, G., Havenga, M.J., Cattaneo, R., Greber, U.F., and Hemmi, S. (2007). Species B adenovirus serotypes 3, 7, 11 and 35 share similar binding sites on the membrane cofactor protein CD46 receptor. J Gen Virol *88*, 2925-2934.

Fleischli, C., Verhaagh, S., Havenga, M., Sirena, D., Schaffner, W., Cattaneo, R., Greber, U.F., and Hemmi, S. (2005). The distal short consensus repeats 1 and 2 of the membrane cofactor protein CD46 and their distance from the cell membrane determine productive entry of species B adenovirus serotype 35. J Virol *79*, 10013-10022.

Fredman, J.N., and Engler, J.A. (1993). Adenovirus precursor to terminal protein interacts with the nuclear matrix *in vivo* and *in vitro*. J Virol *67*, 3384-3395.

Freimuth, P., Springer, K., Berard, C., Hainfeld, J., Bewley, M., and Flanagan, J. (1999). Coxsackievirus and adenovirus receptor amino-terminal immunoglobulin V-related domain binds adenovirus type 2 and fiber knob from adenovirus type 12. J Virol *73*, 1392-1398.

Furuse, M., Hirase, T., Itoh, M., Nagafuchi, A., Yonemura, S., and Tsukita, S. (1993). Occludin: a novel integral membrane protein localizing at tight junctions. J Cell Biol *123*, 1777-1788.

Gaggar, A., Shayakhmetov, D., and Lieber, A. (2003a). CD46 is a cellular receptor for group B adenoviruses. Nature Medicine *9*, 1408-1412.

Gaggar, A., Shayakhmetov, D., and Lieber, A. (2007). Identifying functional adenovirus-host interactions using tandem mass spectrometry. Methods Mol Med *131*, 141-155.

Gaggar, A., Shayakhmetov, D.M., and Lieber, A. (2003b). CD46 is a cellular receptor for group B adenoviruses. Nat Med *9*, 1408-1412.

Gaggar, A., Shayakhmetov, D.M., Liszewski, M.K., Atkinson, J.P., and Lieber, A. (2005). Localization of regions in CD46 that interact with adenovirus. J Virol *79*, 7503-7513.

Gao, W., Robbins, P.D., and Gambotto, A. (2003). Human adenovirus type 35: nucleotide sequence and vector development. Gene Ther *10*, 1941-1949.

Getsios, S., Huen, A.C., and Green, K.J. (2004). Working out the strength and flexibility of desmosomes. Nat Rev Mol Cell Biol *5*, 271-281.

Gill, D.B., Koomey, M., Cannon, J.G., and Atkinson, J.P. (2003). Down-regulation of CD46 by piliated Neisseria gonorrhoeae. J Exp Med *198*, 1313-1322.

Gill, D.B., Spitzer, D., Koomey, M., Heuser, J.E., and Atkinson, J.P. (2005). Release of host-derived membrane vesicles following pilus-mediated adhesion of Neisseria gonorrhoeae. Cell Microbiol *7*, 1672-1683.

Gimenez-Alejandre, M., Cascallo, M., Bayo-Puxan, N., and Alemany, R. (2008). Coagulation factors determine tumor transduction *in vivo*. Hum Gene Ther 19, 1415-1419.

Golay, J., Cittera, E., Di Gaetano, N., Manganini, M., Mosca, M., Nebuloni, M., van Rooijen, N., Vago, L., and Introna, M. (2006). The role of complement in the therapeutic activity of rituximab in a murine B lymphoma model homing in lymph nodes. Haematologica *91*, 176-183.

Goosney, D.L., and Nemerow, G.R. (2003). Adenovirus infection: taking the back roads to viral entry. Curr Biol *13*, R99-R100.

Goossens, P.H., Havenga, M.J., Pieterman, E., Lemckert, A.A., Breedveld, F.C., Bout, A., and Huizinga, T.W. (2001). Infection efficiency of type 5 adenoviral vectors in synovial tissue can be enhanced with a type 16 fiber. Arthritis Rheum *44*, 570-577.

Greber, U.F., Willetts, M., Webster, P., and Helenius, A. (1993). Stepwise dismantling of adenovirus 2 during entry into cells. Cell *75*, 477-486.

Gugala, Z., Olmsted-Davis, E.A., Gannon, F.H., Lindsey, R.W., and Davis, A.R. (2003). Osteoinduction by ex vivo adenovirus-mediated BMP2 delivery is independent of cell type. Gene Ther *10*, 1289-1296.

Guo, B., Ma, Z.W., Li, H., Xu, G.L., Zheng, P., Zhu, B., Wu, Y.Z., and Zou, Q. (2008). Mapping of binding epitopes of a human decay-accelerating factor monoclonal antibody capable of enhancing rituximab-mediated complement-dependent cytotoxicity. Clinical immunology 128, 155-163.

Gustafsson, D.J., Segerman, A., Lindman, K., Mei, Y.F., and Wadell, G. (2006). The Arg279Gln [corrected] substitution in the adenovirus type 11p (Ad11p) fiber knob abolishes EDTA-resistant binding to A549 and CHO-CD46 cells, converting the phenotype to that of Ad7p. J Virol *80*, 1897-1905.

Hamann, J., Stortelers, C., Kiss-Toth, E., Vogel, B., Eichler, W., and van Lier, R.A. (1998). Characterization of the CD55 (DAF)-binding site on the seven-span transmembrane receptor CD97. European journal of immunology *28*, 1701-1707.

Hanley, P.J., Cruz, C.R., Savoldo, B., Leen, A.M., Stanojevic, M., Khalil, M., Decker, W., Molldrem, J.J., Liu, H., Gee, A.P., *et al.* (2009). Functionally active virus-specific T cells that target CMV, adenovirus, and EBV can be expanded from naive T-cell populations in cord blood and will target a range of viral epitopes. Blood *114*, 1958-1967.

Hara, T., Kojima, A., Fukuda, H., Masaoka, T., Fukumori, Y., Matsumoto, M., and Seya, T. (1992a). Levels of complement regulatory proteins, CD35 (CR1), CD46 (MCP) and CD55 (DAF) in human haematological malignancies. Br J Haematol *82*, 368-373.

Hara, T., Kojima, A., Fukuda, H., Masaoka, T., Fukumori, Y., Matsumoto, M., and Seya, T. (1992b). Levels of complement regulatory proteins, CD35 (CR1), CD46 (MCP) and CD55 (DAF) in human haematological malignancies. Br J Haematol *82*, 368-373.

Harada, H., Iwatsuki, K., Ohtsuka, M., Han, G.W., and Kaneko, F. (1996). Abnormal desmoglein expression by squamous cell carcinoma cells. Acta Derm Venereol *76*, 417-420.

Harari, P.M., Allen, G.W., and Bonner, J.A. (2007). Biology of interactions: antiepidermal growth factor receptor agents. J Clin Oncol *25*, 4057-4065.

Harjunpaa, A., Junnikkala, S., and Meri, S. (2000). Rituximab (anti-CD20) therapy of B-cell lymphomas: direct complement killing is superior to cellular effector mechanisms. Scand J Immunol *51*, 634-641.

Hasegawa, K., Hu, C., Nakamura, T., Marks, J.D., Russell, S.J., and Peng, K.W. (2007). Affinity thresholds for membrane fusion triggering by viral glycoproteins. Journal of virology *81*, 13149-13157.

Havenga, M.J., Lemckert, A.A., Grimbergen, J.M., Vogels, R., Huisman, L.G., Valerio, D., Bout, A., and Quax, P.H. (2001). Improved adenovirus vectors for infection of cardiovascular tissues. J Virol *75*, 3335-3342.

Havenga, M.J., Lemckert, A.A., Ophorst, O.J., van Meijer, M., Germeraad, W.T., Grimbergen, J., van Den Doel, M.A., Vogels, R., van Deutekom, J., Janson, A.A., *et al.* (2002). Exploiting the

natural diversity in adenovirus tropism for therapy and prevention of disease. J Virol *76*, 4612-4620.

Heemskerk, B., Veltrop-Duits, L.A., van Vreeswijk, T., ten Dam, M.M., Heidt, S., Toes, R.E., van Tol, M.J., and Schilham, M.W. (2003). Extensive cross-reactivity of CD4+ adenovirus-specific T cells: implications for immunotherapy and gene therapy. J Virol *77*, 6562-6566.

Hemminki, O., Bauerschmitz, G., Hemmi, S., Kanerva, A., Cerullo, V., Pesonen, S., and Hemminki, A. (2010). Preclinical and clinical data with a fully serotype 3 oncolytic adenovirus Ad3-hTERT-E1A in the treatment of advanced solid tumors. . Molecular Therapy *18*, S74.

Hemminki, O., Bauerschmitz, G., Hemmi, S., Lavilla-Alonso, S., Diaconu, I., Guse, K., Koski, A., Desmond, R.A., Lappalainen, M., Kanerva, A., *et al.* (2011). Oncolytic adenovirus based on serotype 3. Cancer Gene Ther *18*, 288-296.

Hierholzer, J.C., Atuk, N.O., and Gwaltney, J.M., Jr. (1975). New human adenovirus isolated from a renal transplant recipient: description and characterization of candiate adenovirus type 34. J Clin Microbiol *1*, 366-376.

Hong, J.S., and Engler, J.A. (1996). Domains required for assembly of adenovirus type 2 fiber trimers. J Virol *70*, 7071-7078.

Horvat, B., Rivailler, P., Varior-Krishnan, G., Cardoso, A., Gerlier, D., and Rabourdin-Combe, C. (1996). Transgenic mice expressing human measles virus (MV) receptor CD46 provide cells exhibiting different permissivities to MV infections. J Virol *70*, 6673-6681.

Hsu, E.C., Dorig, R.E., Sarangi, F., Marcil, A., Iorio, C., and Richardson, C.D. (1997). Artificial mutations and natural variations in the CD46 molecules from human and monkey cells define regions important for measles virus binding. J Virol *71*, 6144-6154.

Johansson, L., Rytkonen, A., Bergman, P., Albiger, B., Kallstrom, H., Hokfelt, T., Agerberth, B., Cattaneo, R., and Jonsson, A.B. (2003). CD46 in meningococcal disease. Science *301*, 373-375.

Kalin, S., Amstutz, B., Gastaldelli, M., Wolfrum, N., Boucke, K., Havenga, M., DiGennaro, F., Liska, N., Hemmi, S., and Greber, U.F. (2010). Macropinocytotic uptake and infection of human epithelial cells with species B2 adenovirus type 35. J Virol *84*, 5336-5350.

Kalyuzhniy, O., Di Paolo, N.C., Silvestry, M., Hofherr, S.E., Barry, M.A., Stewart, P.L., and Shayakhmetov, D.M. (2008). Adenovirus serotype 5 hexon is critical for virus infection of hepatocytes *in vivo*. Proc Natl Acad Sci U S A *105*, 5483-5488.

Kanerva, A., Mikheeva, G.V., Krasnykh, V., Coolidge, C.J., Lam, J.T., Mahasreshti, P.J., Barker, S.D., Straughn, M., Barnes, M.N., Alvarez, R.D., *et al.* (2002a). Targeting adenovirus to the serotype 3 receptor increases gene transfer efficiency to ovarian cancer cells. Clin Cancer Res *8*, 275-280.

Kanerva, A., Wang, M., Bauerschmitz, G.J., Lam, J.T., Desmond, R.A., Bhoola, S.M., Barnes, M.N., Alvarez, R.D., Siegal, G.P., Curiel, D.T., *et al.* (2002b). Gene transfer to ovarian cancer versus normal tissues with fiber-modified adenoviruses. Mol Ther *5*, 695-704.

Kangasniemi, L., Kiviluoto, T., Kanerva, A., Raki, M., Ranki, T., Sarkioja, M., Wu, H., Marini, F., Hockerstedt, K., Isoniemi, H., *et al.* (2006). Infectivity-enhanced adenoviruses deliver efficacy in clinical samples and orthotopic models of disseminated gastric cancer. Clin Cancer Res *12*, 3137-3144.

Kemper, C., Leung, M., Stephensen, C.B., Pinkert, C.A., Liszewski, M.K., Cattaneo, R., and Atkinson, J.P. (2001). Membrane cofactor protein (MCP; CD46) expression in transgenic mice. Clin Exp Immunol *124*, 180-189.

Khatri, P., Desai, V., Tarca, A.L., Sellamuthu, S., Wildman, D.E., Romero, R., and Draghici, S. (2006). New Onto-Tools: Promoter-Express, nsSNPCounter and Onto-Translate. Nucleic Acids Res *34*, W626-631.

Kinugasa, N., Higashi, T., Nouso, K., Nakatsukasa, H., Kobayashi, Y., Ishizaki, M., Toshikuni, N., Yoshida, K., Uematsu, S., and Tsuji, T. (1999a). Expression of membrane cofactor protein (MCP, CD46) in human liver diseases. Br J Cancer *80*, 1820-1825.

Kinugasa, N., Higashi, T., Nouso, K., Nakatsukasa, H., Kobayashi, Y., Ishizaki, M., Toshikuni, N., Yoshida, K., Uematsu, S., and Tsuji, T. (1999b). Expression of membrane cofactor protein (MCP, CD46) in human liver diseases. Br J Cancer *80*, 1820-1825.

Kirby, I., Davison, E., Beavil, A.J., Soh, C.P., Wickham, T.J., Roelvink, P.W., Kovesdi, I., Sutton, B.J., and Santis, G. (2000). Identification of contact residues and definition of the CAR-binding site of adenovirus type 5 fiber protein. J Virol *74*, 2804-2813.

Knaan-Shanzer, S., Van Der Velde, I., Havenga, M.J., Lemckert, A.A., De Vries, A.A., and Valerio, D. (2001). Highly efficient targeted transduction of undifferentiated human hematopoietic cells by adenoviral vectors displaying fiber knobs of subgroup B. Hum Gene Ther *12*, 1989-2005.

Knippertz, I., Hesse, A., Schunder, T., Kampgen, E., Brenner, M.K., Schuler, G., Steinkasserer, A., and Nettelbeck, D.M. (2009). Generation of human dendritic cells that simultaneously secrete IL-12 and have migratory capacity by adenoviral gene transfer of hCD40L in combination with IFN-gamma. J Immunother *32*, 524-538.

Koeser, J., Troyanovsky, S.M., Grund, C., and Franke, W.W. (2003). De novo formation of desmosomes in cultured cells upon transfection of genes encoding specific desmosomal components. Exp Cell Res *285*, 114-130.

Koski, A., Kangasniemi, L., Escutenaire, S., Pesonen, S., Cerullo, V., Diaconu, I., Nokisalmi, P., Raki, M., Rajecki, M., Guse, K., *et al.* (2010). Treatment of Cancer Patients With a Serotype 5/3 Chimeric Oncolytic Adenovirus Expressing GMCSF. Mol Ther 18, 1874-1884.

Kostense, S., Koudstaal, W., Sprangers, M., Weverling, G.J., Penders, G., Helmus, N., Vogels, R., Bakker, M., Berkhout, B., Havenga, M., *et al.* (2004). Adenovirus types 5 and 35 seroprevalence in AIDS risk groups supports type 35 as a vaccine vector. Aids *18*, 1213-1216.

Kowalczyk, A.P., Stappenbeck, T.S., Parry, D.A., Palka, H.L., Virata, M.L., Bornslaeger, E.A., Nilles, L.A., and Green, K.J. (1994). Structure and function of desmosomal transmembrane core and plaque molecules. Biophys Chem *50*, 97-112.

Krasnykh, V.N., Mikheeva, G.V., Douglas, J.T., and Curiel, D.T. (1996). Generation of recombinant adenovirus vectors with modified fibers for altering viral tropism. J Virol *70*, 6839-6846.

Leen, A.M., Christin, A., Myers, G.D., Liu, H., Cruz, C.R., Hanley, P.J., Kennedy-Nasser, A.A., Leung, K.S., Gee, A.P., Krance, R.A., *et al.* (2009). Cytotoxic T lymphocyte therapy with donor T cells prevents and treats adenovirus and Epstein-Barr virus infections after haploidentical and matched unrelated stem cell transplantation. Blood *114*, 4283-4292.

Leen, A.M., Myers, G.D., Sili, U., Huls, M.H., Weiss, H., Leung, K.S., Carrum, G., Krance, R.A., Chang, C.C., Molldrem, J.J., *et al.* (2006). Monoculture-derived T lymphocytes specific for multiple viruses expand and produce clinically relevant effects in immunocompromised individuals. Nat Med *12*, 1160-1166.

Leopold, P.L., and Crystal, R.G. (2007). Intracellular trafficking of adenovirus: many means to many ends. Adv Drug Deliv Rev *59*, 810-821.

Leopold, P.L., Kreitzer, G., Miyazawa, N., Rempel, S., Pfister, K.K., Rodriguez-Boulan, E., and Crystal, R.G. (2000). Dynein- and microtubule-mediated translocation of adenovirus serotype 5 occurs after endosomal lysis. Hum Gene Ther *11*, 151-165.

Leppard, K.N. (1997). E4 gene function in adenovirus, adenovirus vector and adeno-associated virus infections. J Gen Virol *78 (Pt 9)*, 2131-2138.

Lesniak, D., Xu, Y., Deschenes, J., Lai, R., Thoms, J., Murray, D., Gosh, S., Mackey, J.R., Sabri, S., and Abdulkarim, B. (2009). Beta1-integrin circumvents the antiproliferative effects of trastuzumab in human epidermal growth factor receptor-2-positive breast cancer. Cancer Res *69*, 8620-8628.

Li, Y., Pong, R.C., Bergelson, J.M., Hall, M.C., Sagalowsky, A.I., Tseng, C.P., Wang, Z., and Hsieh, J.T. (1999). Loss of adenoviral receptor expression in human bladder cancer cells: a potential impact on the efficacy of gene therapy. Cancer Res *59*, 325-330.

Li, Z.Y., Ni, S., Yang, X., Kiviat, N., and Lieber, A. (2004). Xenograft models for liver metastasis: Relationship between tumor morphology and adenovirus vector transduction. Mol Ther *9*, 650-657.

Liszewski, M.K., Farries, T.C., Lublin, D.M., Rooney, I.A., and Atkinson, J.P. (1996). Control of the complement system. Adv Immunol *61*, 201-283.

Litowski, J.R., and Hodges, R.S. (2002). Designing heterodimeric two-stranded alpha-helical coiled-coils. Effects of hydrophobicity and alpha-helical propensity on protein folding, stability, and specificity. J Biol Chem *277*, 37272-37279.

Lortat-Jacob, H., Chouin, E., Cusack, S., and van Raaij, M.J. (2001). Kinetic analysis of adenovirus fiber binding to its receptor reveals an avidity mechanism for trimeric receptor-ligand interactions. J Biol Chem *276*, 9009-9015.

Louie, J.K., Kajon, A.E., Holodniy, M., Guardia-LaBar, L., Lee, B., Petru, A.M., Hacker, J.K., and Schnurr, D.P. (2008). Severe pneumonia due to adenovirus serotype 14: a new respiratory threat? Clin Infect Dis *46*, 421-425.

Lyons, M., Onion, D., Green, N.K., Aslan, K., Rajaratnam, R., Bazan-Peregrino, M., Phipps, S., Hale, S., Mautner, V., Seymour, L.W., *et al.* (2006). Adenovirus type 5 interactions with human blood cells may compromise systemic delivery. Mol Ther *14*, 118-128.

Madara, J.L. (1998). Regulation of the movement of solutes across tight junctions. Annu Rev Physiol *60*, 143-159.

Madjd, Z., Durrant, L.G., Pinder, S.E., Ellis, I.O., Ronan, J., Lewis, S., Rushmere, N.K., and Spendlove, I. (2005). Do poor-prognosis breast tumours express membrane cofactor proteins (CD46)? Cancer Immunol Immunother *54*, 149-156.

Mallam, J.N., Hurwitz, M.Y., Mahoney, T., Chevez-Barrios, P., and Hurwitz, R.L. (2004). Efficient gene transfer into retinal cells using adenoviral vectors: dependence on receptor expression. Invest Ophthalmol Vis Sci *45*, 1680-1687.

Manchester, M., Smith, K.A., Eto, D.S., Perkin, H.B., and Torbett, B.E. (2002). Targeting and hematopoietic suppression of human CD34+ cells by measles virus. J Virol *76*, 6636-6642.

Marie, J.C., Astier, A.L., Rivailler, P., Rabourdin-Combe, C., Wild, T.F., and Horvat, B. (2002). Linking innate and acquired immunity: divergent role of CD46 cytoplasmic domains in T cell induced inflammation. Nat Immunol *3*, 659-666.

Marttila, M., Persson, D., Gustafsson, D., Liszewski, M.K., Atkinson, J.P., Wadell, G., and Arnberg, N. (2005). CD46 is a cellular receptor for all species B adenoviruses except types 3 and 7. J Virol *79*, 14429-14436.

Mei, Y.F., Lindman, K., and Wadell, G. (1998). Two closely related adenovirus genome types with kidney or respiratory tract tropism differ in their binding to epithelial cells of various origins. Virology *240*, 254-266.

Mei, Y.F., Skog, J., Lindman, K., and Wadell, G. (2003). Comparative analysis of the genome organization of human adenovirus 11, a member of the human adenovirus species B, and the commonly used human adenovirus 5 vector, a member of species C. J Gen Virol *84*, 2061-2071.

Metzgar, D., Osuna, M., Kajon, A.E., Hawksworth, A.W., Irvine, M., and Russell, K.L. (2007). Abrupt emergence of diverse species B adenoviruses at US military recruit training centers. J Infect Dis *196*, 1465-1473.

Micklethwaite, K.P., Savoldo, B., Hanley, P.J., Leen, A.M., Demmler-Harrison, G.J., Cooper, L.J., Liu, H., Gee, A.P., Shpall, E.J., Rooney, C.M., *et al.* (2010). Derivation of human T lymphocytes from cord blood and peripheral blood with antiviral and antileukemic specificity from a single culture as protection against infection and relapse after stem cell transplantation. Blood *115*, 2695-2703.

Miller, C.R., Buchsbaum, D.J., Reynolds, P.N., Douglas, J.T., Gillespie, G.Y., Mayo, M.S., Raben, D., and Curiel, D.T. (1998). Differential susceptibility of primary and established human glioma cells to adenovirus infection: targeting via the epidermal growth factor receptor achieves fiber receptor-independent gene transfer. Cancer Res *58*, 5738-5748.

Murakami, S., Sakurai, F., Kawabata, K., Okada, N., Fujita, T., Yamamoto, A., Hayakawa, T., and Mizuguchi, H. (2007). Interaction of penton base Arg-Gly-Asp motifs with integrins is crucial for adenovirus serotype 35 vector transduction in human hematopoietic cells. Gene Ther *14*, 1525-1533.

Murray, K.P., Mathure, S., Kaul, R., Khan, S., Carson, L.F., Twiggs, L.B., Martens, M.G., and Kaul, A. (2000a). Expression of complement regulatory proteins-CD 35, CD 46, CD 55, and CD 59-in benign and malignant endometrial tissue. Gynecol Oncol *76*, 176-182.

Murray, K.P., Mathure, S., Kaul, R., Khan, S., Carson, L.F., Twiggs, L.B., Martens, M.G., and Kaul, A. (2000b). Expression of complement regulatory proteins-CD 35, CD 46, CD 55, and CD 59-in benign and malignant endometrial tissue. Gynecol Oncol *76*, 176-182.

Nan, X., Peng, B., Hahn, T.W., Richardson, E., Lizonova, A., Kovesdi, I., and Robert-Guroff, M. (2003). Development of an Ad7 cosmid system and generation of an Ad7deltaE1deltaE3HIV(MN) env/rev recombinant virus. Gene Ther *10*, 326-336.

Nava, P., Laukoetter, M.G., Hopkins, A.M., Laur, O., Gerner-Smidt, K., Green, K.J., Parkos, C.A., and Nusrat, A. (2007). Desmoglein-2: a novel regulator of apoptosis in the intestinal epithelium. Mol Biol Cell *18*, 4565-4578.

Neering, S.J., Hardy, S.F., Minamoto, D., Spratt, S.K., and Jordan, C.T. (1996). Transduction of primitive human hematopoietic cells with recombinant adenovirus vectors. Blood *88*, 1147-1155.

Ni, S., Bernt, K., Gaggar, A., Li, Z.Y., Kiem, H.P., and Lieber, A. (2005). Evaluation of biodistribution and safety of adenovirus vectors containing group B fibers after intravenous injection into baboons. Hum Gene Ther *16*, 664-677.

Ni, S., Gaggar, A., Di Paolo, N., Li, Z.Y., Liu, Y., Strauss, R., Sova, P., Morihara, J., Feng, Q., Kiviat, N., *et al.* (2006). Evaluation of adenovirus vectors containing serotype 35 fibers for tumor targeting. Cancer Gene Ther *13*, 1072-1081.

Nilsson, M., Karlsson, S., and Fan, X. (2004a). Functionally distinct subpopulations of cord blood CD34+ cells are transduced by adenoviral vectors with serotype 5 or 35 tropism. Mol Ther *9*, 377-388.

Nilsson, M., Ljungberg, J., Richter, J., Kiefer, T., Magnusson, M., Lieber, A., Widegren, B., Karlsson, S., and Fan, X. (2004b). Development of an adenoviral vector system with adenovirus serotype 35 tropism; efficient transient gene transfer into primary malignant hematopoietic cells. J Gene Med *6*, 631-641.

Norrby, E., Nyberg, B., Skaaret, P., and Lengyel, A. (1967). Separation and characterization of soluble adenovirus type 9 components. J Virol *1*, 1101-1108.

Nwanegbo, E., Vardas, E., Gao, W., Whittle, H., Sun, H., Rowe, D., Robbins, P.D., and Gambotto, A. (2004). Prevalence of neutralizing antibodies to adenoviral serotypes 5 and 35 in the adult populations of The Gambia, South Africa, and the United States. Clin Diagn Lab Immunol *11*, 351-357.

Okegawa, T., Li, Y., Pong, R.C., Bergelson, J.M., Zhou, J., and Hsieh, J.T. (2000). The dual impact of coxsackie and adenovirus receptor expression on human prostate cancer gene therapy. Cancer Res *60*, 5031-5036.

Oliveras-Ferraros, C., Vazquez-Martin, A., Cufi, S., Queralt, B., Baez, L., Guardeno, R., Hernandez-Yague, X., Martin-Castillo, B., Brunet, J., and Menendez, J.A. (2011). Stem cell property epithelial-to-mesenchymal transition is a core transcriptional network for predicting cetuximab (Erbitux) efficacy in KRAS wild-type tumor cells. J Cell Biochem *112*, 10-29.

Olmsted-Davis, E.A., Gugala, Z., Gannon, F.H., Yotnda, P., McAlhany, R.E., Lindsey, R.W., and Davis, A.R. (2002). Use of a chimeric adenovirus vector enhances BMP2 production and bone formation. Hum Gene Ther *13*, 1337-1347.

Ong, H.T., Timm, M.M., Greipp, P.R., Witzig, T.E., Dispenzieri, A., Russell, S.J., and Peng, K.W. (2006). Oncolytic measles virus targets high CD46 expression on multiple myeloma cells. Exp Hematol *34*, 713-720.

Ophorst, O.J., Kostense, S., Goudsmit, J., De Swart, R.L., Verhaagh, S., Zakhartchouk, A., Van Meijer, M., Sprangers, M., Van Amerongen, G., Yuksel, S., *et al.* (2004). An adenoviral type 5 vector carrying a type 35 fiber as a vaccine vehicle: DC targeting, cross neutralization, and immunogenicity. Vaccine *22*, 3035-3044.

Ostapchuk, P., and Hearing, P. (2001). Pseudopackaging of adenovirus type 5 genomes into capsids containing the hexon proteins of adenovirus serotypes B, D, or E. J Virol *75*, 45-51.

Pache, L., Venkataraman, S., Reddy, V.S., and Nemerow, G.R. (2008). Structural variations in species B adenovirus fibers impact CD46 association. J Virol *82*, 7923-7931.

Persson, B.D., Muller, S., Reiter, D.M., Schmitt, B.B., Marttila, M., Sumowski, C.V., Schweizer, S., Scheu, U., Ochsenfeld, C., Arnberg, N., *et al.* (2009). An arginine switch in the species B

adenovirus knob determines high-affinity engagement of the cellular receptor CD46. J Virol 83, 673-686.

Persson, B.D., Reiter, D.M., Marttila, M., Mei, Y.F., Casasnovas, J.M., Arnberg, N., and Stehle, T. (2007). Adenovirus type 11 binding alters the conformation of its receptor CD46. Nat Struct Mol Biol *14*, 164-166.

Pesonen, S., Nokisalmi, P., Escutenaire, S., Sarkioja, M., Raki, M., Cerullo, V., Kangasniemi, L., Laasonen, L., Ribacka, C., Guse, K., *et al.* (2010). Prolonged systemic circulation of chimeric oncolytic adenovirus Ad5/3-Cox2L-D24 in patients with metastatic and refractory solid tumors. Gene Ther *17*, 892-904.

Purcell, D.F., Russell, S.M., Deacon, N.J., Brown, M.A., Hooker, D.J., and McKenzie, I.F. (1991). Alternatively spliced RNAs encode several isoforms of CD46 (MCP), a regulator of complement activation. Immunogenetics *33*, 335-344.

Rea, D., Havenga, M.J., van Den Assem, M., Sutmuller, R.P., Lemckert, A., Hoeben, R.C., Bout, A., Melief, C.J., and Offringa, R. (2001). Highly efficient transduction of human monocyte-derived dendritic cells with subgroup B fiber-modified adenovirus vectors enhances transgene-encoded antigen presentation to cytotoxic T cells. J Immunol *166*, 5236-5244.

Reff, M.E., Carner, K., Chambers, K.S., Chinn, P.C., Leonard, J.E., Raab, R., Newman, R.A., Hanna, N., and Anderson, D.R. (1994). Depletion of B cells *in vivo* by a chimeric mouse human monoclonal antibody to CD20. Blood *83*, 435-445.

Roelvink, P.W., Lizonova, A., Lee, J.G., Li, Y., Bergelson, J.M., Finberg, R.W., Brough, D.E., Kovesdi, I., and Wickham, T.J. (1998). The coxsackievirus-adenovirus receptor protein can function as a cellular attachment protein for adenovirus serotypes from subgroups A, C, D, E, and F. J Virol *72*, 7909-7915.

Roelvink, P.W., Mi Lee, G., Einfeld, D.A., Kovesdi, I., and Wickham, T.J. (1999). Identification of a conserved receptor-binding site on the fiber proteins of CAR-recognizing adenoviridae. Science *286*, 1568-1571.

Rowe, W.P., Huebner, R.J., Gilmore, L.K., Parrott, R.H., and Ward, T.G. (1953). Isolation of a cytopathogenic agent from human adenoids undergoing spontaneous degeneration in tissue culture. Proc Soc Exp Biol Med *84*, 570-573.

Rushmere, N.K., Knowlden, J.M., Gee, J.M., Harper, M.E., Robertson, J.F., Morgan, B.P., and Nicholson, R.I. (2004). Analysis of the level of mRNA expression of the membrane regulators of complement, CD59, CD55 and CD46, in breast cancer. International journal of cancer *108*, 930-936.

Russell, S. (2004). CD46: a complement regulator and pathogen receptor that mediates links between innate and acquired immune function. Tissue Antigens *64*, 111-118.

Saitoh-Inagawa, W., Tanaka, K., Uchio, E., Itoh, N., Ohno, S., and Aoki, K. (2001). Genome typing of adenovirus type 34 isolated in two cases of conjunctivitis in Sapporo, Japan. J Clin Microbiol *39*, 4187-4189.

Sakurai, F., Akitomo, K., Kawabata, K., Hayakawa, T., and Mizuguchi, H. (2007). Downregulation of human CD46 by adenovirus serotype 35 vectors. Gene Ther *14*, 912-919.

Sakurai, F., Mizuguchi, H., and Hayakawa, T. (2003a). Efficient gene transfer into human CD34+ cells by an adenovirus type 35 vector. Gene Ther *10*, 1041-1048.

Sakurai, F., Mizuguchi, H., Yamaguchi, T., and Hayakawa, T. (2003b). Characterization of *in vitro* and *in vivo* gene transfer properties of adenovirus serotype 35 vector. Mol Ther *8*, 813-821.

Sakurai, F., Murakami, S., Kawabata, K., Okada, N., Yamamoto, A., Seya, T., Hayakawa, T., and Mizuguchi, H. (2006). The short consensus repeats 1 and 2, not the cytoplasmic domain, of human CD46 are crucial for infection of subgroup B adenovirus serotype 35. J Control Release *113*, 271-278.

Santoro, F., Kennedy, P.E., Locatelli, G., Malnati, M.S., Berger, E.A., and Lusso, P. (1999). CD46 is a cellular receptor for human herpesvirus 6. Cell *99*, 817-827.

Sawada, H., Aoki, K., Kawana, R., Matsumoto, I., Shinagawa, M., Guo, D.F., and Fajardo, R.V. (1987). Molecular epidemiology of adenoviral conjunctivitis in Sapporo, Japan, and Manila, the Philippines. Jpn J Ophthalmol *31*, 538-546.

Schmitt, C.J., Franke, W.W., Goerdt, S., Falkowska-Hansen, B., Rickelt, S., and Peitsch, W.K. (2007). Homo- and heterotypic cell contacts in malignant melanoma cells and desmoglein 2 as a novel solitary surface glycoprotein. J Invest Dermatol *127*, 2191-2206.

Segerman, A., Arnberg, N., Erikson, A., Lindman, K., and Wadell, G. (2003a). There are two different species B adenovirus receptors: sBAR, common to species B1 and B2 adenoviruses, and sB2AR, exclusively used by species B2 adenoviruses. J Virol *77*, 1157-1162.

Segerman, A., Atkinson, J.P., Marttila, M., Dennerquist, V., Wadell, G., and Arnberg, N. (2003b). Adenovirus type 11 uses CD46 as a cellular receptor. J Virol *77*, 9183-9191.

Segerman, A., Mei, Y.F., and Wadell, G. (2000). Adenovirus types 11p and 35p show high binding efficiencies for committed hematopoietic cell lines and are infective to these cell lines. J Virol *74*, 1457-1467.

Seshidhar Reddy, P., Ganesh, S., Limbach, M.P., Brann, T., Pinkstaff, A., Kaloss, M., Kaleko, M., and Connelly, S. (2003). Development of adenovirus serotype 35 as a gene transfer vector. Virology *311*, 384-393.

Shamah, S.M., Healy, J.M., and Cload, S.T. (2008). Complex target SELEX. Accounts of chemical research *41*, 130-138.

Shayakhmetov D M, A.E., Z-Y Li, A Lieber (2005). Deletion of penton RGD motifs affects the efficiency of both the internalization and the endosome escape of viral particles containing adenovirus serotype 5 or 35 fiber knobs. J Virol *79*, 1053-1061.

Shayakhmetov, D.M., Carlson, C.A., Stecher, H., Li, Q., Stamatoyannopoulos, G., and Lieber, A. (2002a). A high-capacity, capsid-modified hybrid adenovirus/adeno-associated virus vector for stable transduction of human hematopoietic cells. J Virol *76*, 1135-1143.

Shayakhmetov, D.M., Gaggar, A., Ni, S., Li, Z.Y., and Lieber, A. (2005). Adenovirus binding to blood factors results in liver cell infection and hepatotoxicity. J Virol *79*, 7478-7491.

Shayakhmetov, D.M., Li, Z.Y., Gaggar, A., Gharwan, H., Ternovoi, V., Sandig, V., and Lieber, A. (2004). Genome size and structure determine efficiency of postinternalization steps and gene transfer of capsid-modified adenovirus vectors in a cell-type-specific manner. J Virol *78*, 10009-10022.

Shayakhmetov, D.M., Li, Z.Y., Ni, S., and Lieber, A. (2002b). Targeting of adenovirus vectors to tumor cells does not enable efficient transduction of breast cancer metastases. Cancer Res *62*, 1063-1068.

Shayakhmetov, D.M., Li, Z.Y., Ternovoi, V., Gaggar, A., Gharwan, H., and Lieber, A. (2003). The interaction between the fiber knob domain and the cellular attachment receptor determines the intracellular trafficking route of adenoviruses. J Virol *77*, 3712-3723.

Shayakhmetov, D.M., and Lieber, A. (2000). Dependence of adenovirus infectivity on length of the fiber shaft domain. J Virol *74*, 10274-10286.

Shayakhmetov, D.M., Papayannopoulou, T., Stamatoyannopoulos, G., and Lieber, A. (2000). Efficient gene transfer into human CD34(+) cells by a retargeted adenovirus vector. J Virol *74*, 2567-2583.

Shenk, T. (1996). Adenoviridea. In Fields Virology, B.N. Fields, Knipe, D.M., Howley, P.M., ed. (Philadelphia, Lippincott-Raven Publisher), pp. 2111-2148.

Shields, A.F., Hackman, R.C., Fife, K.H., Corey, L., and Meyers, J.D. (1985). Adenovirus infections in patients undergoing bone-marrow transplantation. N Engl J Med *312*, 529-533.

Shindo, K., Kitayama, T., Ura, T., Matsuya, F., Kusaba, Y., Kanetake, H., and Saito, Y. (1986). Acute hemorrhagic cystitis caused by adenovirus type 11 after renal transplantation. Urol Int *41*, 152-155.

Short, J.J., Pereboev, A.V., Kawakami, Y., Vasu, C., Holterman, M.J., and Curiel, D.T. (2004). Adenovirus serotype 3 utilizes CD80 (B7.1) and CD86 (B7.2) as cellular attachment receptors. Virology *322*, 349-359.

Short, J.J., Vasu, C., Holterman, M.J., Curiel, D.T., and Pereboev, A. (2006). Members of adenovirus species B utilize CD80 and CD86 as cellular attachment receptors. Virus Res *122*, 144-153.

Sirena, D., Lilienfeld, B., Eisenhut, M., Kalin, S., Boucke, K., Beerli, R.R., Vogt, L., Ruedl, C., Bachmann, M.F., Greber, U.F., *et al.* (2004). The human membrane cofactor CD46 is a receptor for species B adenovirus serotype 3. J Virol *78*, 4454-4462.

Skog, J., Edlund, K., Widegren, B., Salford, L.G., Wadell, G., and Mei, Y.F. (2004). Efficient internalization into low-passage glioma cell lines using adenoviruses other than type 5: an approach for improvement of gene delivery to brain tumours. J Gen Virol *85*, 2627-2638.

Skog, J., Mei, Y.F., and Wadell, G. (2002). Human adenovirus serotypes 4p and 11p are efficiently expressed in cell lines of neural tumour origin. J Gen Virol *83*, 1299-1309.

Slager, E.H., Borghi, M., van der Minne, C.E., Aarnoudse, C.A., Havenga, M.J., Schrier, P.I., Osanto, S., and Griffioen, M. (2003). CD4+ Th2 cell recognition of HLA-DR-restricted epitopes derived from CAMEL: a tumor antigen translated in an alternative open reading frame. J Immunol *170*, 1490-1497.

Slager, E.H., van der Minne, C.E., Goudsmit, J., van Oers, J.M., Kostense, S., Havenga, M.J., Osanto, S., and Griffioen, M. (2004). Induction of CAMEL/NY-ESO-ORF2-specific CD8+ T cells upon stimulation with dendritic cells infected with a modified Ad5 vector expressing a chimeric Ad5/35 fiber. Cancer Gene Ther *11*, 227-236.

Smith, C.A., Woodruff, L.S., Rooney, C., and Kitchingman, G.R. (1998). Extensive cross-reactivity of adenovirus-specific cytotoxic T cells. Hum Gene Ther *9*, 1419-1427.

Stecher, H., Shayakhmetov, D.M., Stamatoyannopoulos, G., and Lieber, A. (2001). A capsid-modified adenovirus vector devoid of all viral genes: assessment of transduction and toxicity in human hematopoietic cells. Mol Ther *4*, 36-44.

Stevenson, S.C., Rollence, M., White, B., Weaver, L., and McClelland, A. (1995). Human adenovirus serotypes 3 and 5 bind to two different cellular receptors via the fiber head domain. J Virol *69*, 2850-2857.

Stone, D., David, A., Bolognani, F., Lowenstein, P.R., and Castro, M.G. (2000). Viral vectors for gene delivery and gene therapy within the endocrine system. J Endocrinol *164*, 103-118.

Stone, D., di Paolo, N.C., and Lieber, A. (2006). Development of group B adenoviruses as gene transfer vectors. Biotechnol Genet Eng Rev *22*, 101-123.

Stone, D., Furthmann, A., Sandig, V., and Lieber, A. (2003). The complete nucleotide sequence, genome organization, and origin of human adenovirus type 11. Virology *309*, 152-165.

Stone, D., and Lieber, A. (2006). New serotypes of adenoviral vectors. Curr Opin Mol Ther *8*, 423-431.

Stone, D., Liu, Y., Shayakhmetov, D., Li, Z.Y., Ni, S., and Lieber, A. (2007). Adenovirus-platelet interaction in blood causes virus sequestration to the reticuloendothelial system of the liver. J Virol *81*, 4866-4871.

Strauss, R., Li, Z.Y., Liu, Y., Beyer, I., Persson, J., Sova, P., Moller, T., Pesonen, S., Hemminki, A., Hamerlik, P., *et al.* (2011). Analysis of epithelial and mesenchymal markers in ovarian cancer reveals phenotypic heterogeneity and plasticity. PLoS One *6*, e16186.

Strauss, R., and Lieber, A. (2009). Anatomical and physical barriers to tumor targeting with oncolytic adenoviruses *in vivo*. Curr Opin Mol Ther *11*, 513-522.

Strauss, R., Sova, P., Liu, Y., Li, Z.-Y., Tuve, S., Pritchard, D., Brinkkoetter, P., Moller, T., Wildner, O., Pesonen, S., *et al.* (2009a). Epithelial phenotype of ovarian cancer mediates resistance to oncolytic adenoviruses. Cancer Research *15*, 5115-5125.

Strauss, R., Sova, P., Liu, Y., Li, Z.Y., Tuve, S., Pritchard, D., Brinkkoetter, P., Moller, T., Wildner, O., Pesonen, S., *et al.* (2009b). Epithelial phenotype confers resistance of ovarian cancer cells to oncolytic adenoviruses. Cancer Res *69*, 5115-5125.

Studeny, M., Marini, F.C., Champlin, R.E., Zompetta, C., Fidler, I.J., and Andreeff, M. (2002). Bone marrow-derived mesenchymal stem cells as vehicles for interferon-beta delivery into tumors. Cancer Res *62*, 3603-3608.

Su, E.J., Stevenson, S.C., Rollence, M., Marshall-Neff, J., and Liau, G. (2001). A genetically modified adenoviral vector exhibits enhanced gene transfer of human smooth muscle cells. J Vasc Res *38*, 471-478.

Surowiak, P., Materna, V., Maciejczyk, A., Kaplenko, I., Spaczynski, M., Dietel, M., Lage, H., and Zabel, M. (2006). CD46 expression is indicative of shorter revival-free survival for ovarian cancer patients. Anticancer research *26*, 4943-4948.

Svensson, U. (1985). Role of vesicles during adenovirus 2 internalization into HeLa cells. J Virol *55*, 442-449.

Thiery, J.P., and Sleeman, J.P. (2006). Complex networks orchestrate epithelial-mesenchymal transitions. Nat Rev Mol Cell Biol *7*, 131-142.

Thorsteinsson, L., O'Dowd, G.M., Harrington, P.M., and Johnson, P.M. (1998). The complement regulatory proteins CD46 and CD59, but not CD55, are highly expressed by glandular epithelium of human breast and colorectal tumour tissues. Apmis *106*, 869-878.

Trojan, L., Schaaf, A., Steidler, A., Haak, M., Thalmann, G., Knoll, T., Gretz, N., Alken, P., and Michel, M.S. (2005). Identification of metastasis-associated genes in prostate cancer by genetic profiling of human prostate cancer cell lines. Anticancer Res *25*, 183-191.

Turksen, K., and Troy, T.C. (2004). Barriers built on claudins. J Cell Sci *117*, 2435-2447.

Turley, E.A., Veiseh, M., Radisky, D.C., and Bissell, M.J. (2008). Mechanisms of Disease: epithelial-mesenchymal transition-does cellular plasticity fuel neoplastic progression? Nat Clin Pract Oncol 5, 280-290.

Tuve, S., Wang, H., Jacobs, J.D., Yumul, R.C., Smith, D.F., and Lieber, A. (2008). Role of cellular heparan sulfate proteoglycans in infection of human adenovirus serotype 3 and 35. PLoS Pathog *4*, e1000189.

Tuve, S., Wang, H., Ware, C., Liu, Y., Gaggar, A., Bernt, K., Shayakhmetov, D., Li, Z., Strauss, R., Stone, D., *et al.* (2006). A new group B adenovirus receptor is expressed at high levels on human stem and tumor cells. J Virol *80*, 12109-12120.

van der Kolk, L.E., Grillo-Lopez, A.J., Baars, J.W., Hack, C.E., and van Oers, M.H. (2001). Complement activation plays a key role in the side-effects of rituximab treatment. British journal of haematology *115*, 807-811.

van Raaij, M.J., Chouin, E., van der Zandt, H., Bergelson, J.M., and Cusack, S. (2000). Dimeric structure of the coxsackievirus and adenovirus receptor D1 domain at 1.7 A resolution. Structure *8*, 1147-1155.

Varela, J.C., Atkinson, C., Woolson, R., Keane, T.E., and Tomlinson, S. (2008). Upregulated expression of complement inhibitory proteins on bladder cancer cells and anti-MUC1 antibody immune selection. International journal of cancer 15, 1357-1363.

Vaughan, T.J., Williams, A.J., Pritchard, K., Osbourn, J.K., Pope, A.R., Earnshaw, J.C., McCafferty, J., Hodits, R.A., Wilton, J., and Johnson, K.S. (1996). Human antibodies with sub-nanomolar affinities isolated from a large non-immunized phage display library. Nature biotechnology *14*, 309-314.

Vogels, R., Zuijdgeest, D., van Rijnsoever, R., Hartkoorn, E., Damen, I., de Bethune, M.P., Kostense, S., Penders, G., Helmus, N., Koudstaal, W., *et al.* (2003). Replication-deficient human adenovirus type 35 vectors for gene transfer and vaccination: efficient human cell infection and bypass of preexisting adenovirus immunity. J Virol *77*, 8263-8271.

Von Seggern, D.J., Aguilar, E., Kinder, K., Fleck, S.K., Gonzalez Armas, J.C., Stevenson, S.C., Ghazal, P., Nemerow, G.R., and Friedlander, M. (2003). *In vivo* transduction of photoreceptors or ciliary body by intravitreal injection of pseudotyped adenoviral vectors. Mol Ther *7*, 27-34.

Waddington, S.N., McVey, J.H., Bhella, D., Parker, A.L., Barker, K., Atoda, H., Pink, R., Buckley, S.M.K., Custers, J., Morita, T., *et al.* (2008). A critical role for the adenovirus serotype 5 hexon in liver gene transfer. Hum gene ther 19,409.

Walters, R.W., Freimuth, P., Moninger, T.O., Ganske, I., Zabner, J., and Welsh, M.J. (2002). Adenovirus fiber disrupts CAR-mediated intercellular adhesion allowing virus escape. Cell *110*, 789-799.

Walters, R.W., Grunst, T., Bergelson, J.M., Finberg, R.W., Welsh, M.J., and Zabner, J. (1999). Basolateral localization of fiber receptors limits adenovirus infection from the apical surface of airway epithelia. J Biol Chem *274*, 10219-10226.

Wang, H., Li, Z.Y., Liu, Y., Persson, J., Beyer, I., Moller, T., Koyuncu, D., Drescher, M.R., Strauss, R., Zhang, X.B., *et al.* (2011). Desmoglein 2 is a receptor for adenovirus serotypes 3, 7, 11 and 14. Nat Med *17*, 96-104.

Wang, H., Liaw, Y.C., Stone, D., Kalyuzhniy, O., Amiraslanov, I., Tuve, S., Verlinde, C.L., Shayakhmetov, D., Stehle, T., Roffler, S., *et al.* (2007). Identification of CD46 binding sites within the adenovirus serotype 35 fiber knob. J Virol *81*, 12785-12792.

Watanabe, T., Kuszynski, C., Ino, K., Heimann, D.G., Shepard, H.M., Yasui, Y., Maneval, D.C., and Talmadge, J.E. (1996). Gene transfer into human bone marrow hematopoietic cells mediated by adenovirus vectors. Blood *87*, 5032-5039.

Wheeler, D.L., Dunn, E.F., and Harari, P.M. (2010). Understanding resistance to EGFR inhibitors-impact on future treatment strategies. Nat Rev Clin Oncol *7*, 493-507.

Wickham, T.J., Mathias, P., Cheresh, D.A., and Nemerow, G.R. (1993). Integrins alpha v beta 3 and alpha v beta 5 promote adenovirus internalization but not virus attachment. Cell *73*, 309-319.

Wold, W.S., Doronin, K., Toth, K., Kuppuswamy, M., Lichtenstein, D.L., and Tollefson, A.E. (1999). Immune responses to adenoviruses: viral evasion mechanisms and their implications for the clinic. Curr Opin Immunol *11*, 380-386.

Worgall, S., Wolff, G., Falck-Pedersen, E., and Crystal, R.G. (1997). Innate immune mechanisms dominate elimination of adenoviral vectors following *in vivo* administration. Hum Gene Ther *8*, 37-44.

Wu, E., Trauger, S.A., Pache, L., Mullen, T.M., von Seggern, D.J., Siuzdak, G., and Nemerow, G.R. (2004). Membrane cofactor protein is a receptor for adenoviruses associated with epidemic keratoconjunctivitis. J Virol *78*, 3897-3905.

Wu, H., Dmitriev, I., Kashentseva, E., Seki, T., Wang, M., and Curiel, D.T. (2002). Construction and characterization of adenovirus serotype 5 packaged by serotype 3 hexon. J Virol *76*, 12775-12782.

Yamamoto, M., and Curiel, D.T. (2010). Current issues and future directions of oncolytic adenoviruses. Mol Ther *18*, 243-250.

Yotnda, P., Onishi, H., Heslop, H.E., Shayakhmetov, D., Lieber, A., Brenner, M., and Davis, A. (2001). Efficient infection of primitive hematopoietic stem cells by modified adenovirus. Gene Ther *8*, 930-937.

Zell, S., Geis, N., Rutz, R., Schultz, S., Giese, T., and Kirschfink, M. (2007). Down-regulation of CD55 and CD46 expression by anti-sense phosphorothioate oligonucleotides (S-ODNs)

sensitizes tumour cells to complement attack. Clinical and experimental immunology *150*, 576-584.

Zeng, Y., Pinard, M., Jaime, J., Bourget, L., Uyen Le, P., O'Connor-McCourt, M.D., Gilbert, R., and Massie, B. (2008). A ligand-pseudoreceptor system based on de novo designed peptides for the generation of adenoviral vectors with altered tropism. The journal of gene medicine *10*, 355-367.

Zhang, L.Q., Mei, Y.F., and Wadell, G. (2003). Human adenovirus serotypes 4 and 11 show higher binding affinity and infectivity for endothelial and carcinoma cell lines than serotype 5. J Gen Virol *84*, 687-695.

Ziller, F., Macor, P., Bulla, R., Sblattero, D., Marzari, R., and Tedesco, F. (2005). Controlling complement resistance in cancer by using human monoclonal antibodies that neutralize complement-regulatory proteins CD55 and CD59. European journal of immunology *35*, 2175-2183.